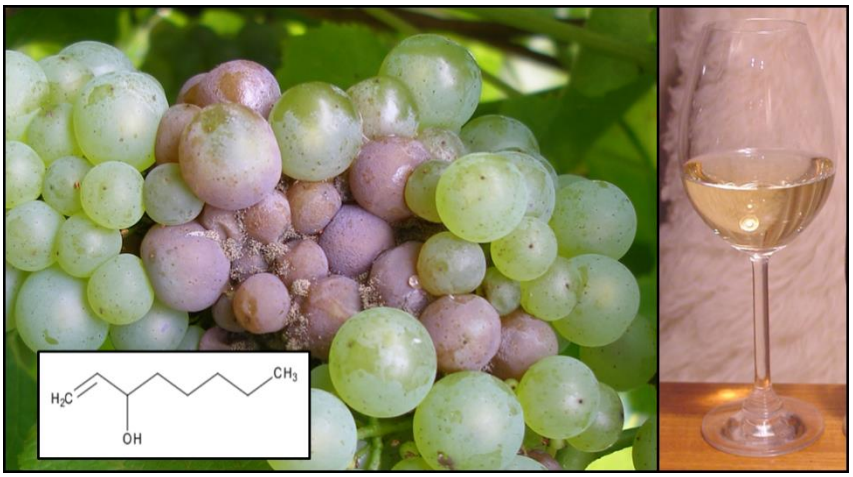
Australian Government
Wine Australia

National Wine & Grape Industry Centre
Charles Sturt University

Determination of thresholds for bunch rot contamination of grapes and techniques to ameliorate associated fungal taints



FINAL REPORT TO WINE AUSTRALIA

Project Number: **CSU 1301**

Principal Investigator: **Christopher C Steel**

Research Organisation: **NWGIC / CSU**

Date: **24th July 2018**

Project CSU 13-01: Determination of thresholds for bunch rot contamination of grapes and techniques to ameliorate associated fungal taints

Chief Investigator:
Prof Christopher C Steel

Institution:
National Wine and Grape Industry Centre
Charles Sturt University
Lock Bag 588
Wagga Wagga
New South Wales 2678

Citing this report
This report may be cited as Steel CC et al. (2018) Determination of thresholds for bunch rot contamination of grapes and techniques to ameliorate associated fungal taints, CSU13-01. Charles Sturt University, Wagga Wagga, NSW 100 pp

Copyright Statement:

Copyright © Charles Sturt University 2018

All rights reserved. Apart from any use permitted under the Copyright Act 1968, no part of this report may be reproduced by any process without written permission from Charles Sturt University.

Disclaimer:

The document may be of assistance to you. This document was prepared by the author in good faith on the basis of available information. The author, the National Wine and Grape Industry Centre and Charles Sturt University cannot guarantee completeness or accuracy of any data, descriptions or conclusions based on information provided by others.

The document is made available on the understanding that the author, the National Wine and Grape Industry Centre and Charles Sturt University accept no responsibility for any person acting on, or relying on, or upon any opinion, advice, representation, statement of information, whether expressed or implied in the document, and disclaim all liability for any loss, damage, cost or expense incurred or arising by reason of any person using or relying on the information contained in the document or by reason of error, omission, defect or mis-statement (whether such error, omission or mis-statement is caused by or arises from negligence, lack of care or otherwise).

The product trade names in this publication are supplied on the understanding that no preference between equivalent products is intended and that the inclusion of a product does not imply endorsement by the National Wine and Grape Industry Centre or Charles Sturt University over any other equivalent product from another manufacturer.

Table of Contents: Page

1. Abstract 1

2. Executive summary 2

3. Background 4

4. Project Aims and Performance targets 6

5. Methods 9

5.1 Fungal isolates, field sites, berry inoculation methods and wine making procedures 9

5.2 Establishment of an ATR FTIR method for grape analysis 16

5.3 GC/MS Analysis of laboratory-inoculated grape berries and wine 22

5.4 Methods for the analysis of field-infected bunch samples and threshold investigations 26

6. Results 31

6.1 ATR FTIR spectroscopy to discriminate fungal mycelium and grape berries inoculated with either *Aspergillus niger, A. carbonarius*, *Botrytis cinerea* or *Penicillium expansum.* 31

6.2 Analysis of laboratory-inoculated berries and bunches 39

6.3 Analysis of wines made from laboratory-inoculated grapes 54

6.4 Thresholds for Botrytis grey mould contamination of wine grapes 64

7. Outcomes / Conclusions 74

8. Recommendations 78

Appendix 1: Communication 80

Appendix 2: Intellectual property 81

Appendix 3: References 81

Appendix 4: Staff 86

Appendix 5: Supplementary Material 87

Appendix 5.1 - Supplementary Tables 87

Appendix 5.2 - Supplementary Figures 94

1. Abstract:

This project investigated measures of bunch rot contamination of wine grapes. Attenuated Total Reflectance Fourier Transform Infrared Spectroscopy (ATR FTIR) successfully discriminated individual grape berries inoculated with the different types of fungi (*Aspergillus* spp., *Botrytis cinerea* and *Penicillium expansum*) responsible for bunch rots. Each of the fungi investigated produced a different suite of secondary compounds, some of which were implicated in deleterious effects on wine quality. Based on the ergosterol content of fungal cultures, thresholds for Botrytis contamination of grapes was estimated to be between 0.3 and 1.0 g dry weight of fungus per kg wet weight of grapes.

2. Executive Summary:

Bunch rot of grapes causes economic losses to grape and wine industries worldwide. The causative agents are phytopathogenic filamentous fungi. *Botrytis cinerea* (responsible for grey mould) is the principal fungal species associated with rotting grapes close to harvest. Other fungal organisms include species of Aspergillus, Cladosporium, Penicillium and Rhizopus. These other fungi are often opportunistic pathogens, infecting plant tissues when the host is compromised (e.g. when the berry skin is damaged). The impact these other fungi have on grape and wine quality is different from the impacts of *B. cinerea*.

This work focused on four fungal species associated with bunch rots, *B. cinerea, Aspergillus carbonarius, A. niger* and *Penicillium expansum*. The studies involved detached inoculated individual grape berries, detached inoculated whole bunches and naturally infected commercially-grown bunch samples. The work examined a single wine grape cultivar, Chardonnay. Using a combination of techniques in plant pathology, analytical chemistry and sensory science, the aims of this work were to more fully characterise the impacts bunch rotting fungi have on grape and wine quality.

Attenuated Total Reflectance Fourier Transform Infrared Spectroscopy (ATR FTIR) in conjunction with chemometric modelling and machine learning algorithms, was successfully applied to objectively differentiate *Aspergillus carbonarius, A. niger*, *Botrytis cinerea* or *Pencillium expansum* fungal mycelium and mature wine-grape berries (*Vitis vinifera,* cultivar Chardonnay) infected with either of these bunch rot pathogens. The differentiation of *B. cinerea* infected grape berries from those infected with either *Aspergillus* or *Penicillium* species shows promise as a tool for the rapid detection of the pathogens when grapes are received at the winery for processing.

An untargeted metabolomics approach was used to classify volatile compounds produced in grapes infected with either *Aspergillus carbonarius, A. niger*, *Botrytis cinerea* or *Pencillium expansum*. Juice obtained from these grapes was subjected to GC/MS analysis. PLS-DA of the normalised summed mass ions across the chromatograms indicated sample classification according to pathogen. Compounds identified from those mass ion matrices that were responsible for classification included 1,5-dimethylnaphthalene and several unidentified sesquiterpenes that were relatively higher in *B. cinerea* infected samples. *A. niger* and *A. carbonarius* samples were higher in 2-carboxymethyl-3-hexylmaleic acid anhydride, while *P. expansum* samples were higher in *γ*-nonalactone and *m*-cresol. The differentiation of wines made from the different bunch rotting fungi was not as clear as for grape juice, suggesting that the compounds responsible for discriminating grape juices were lost during fermentation.

Grapes were sourced from a commercial vineyard and based on visual observations were sorted into one of five levels of *Botrytis cinerea* (grey mould) severity. Measurement of the fungal sterol, ergosterol, allowed more accurate quantification of the fungal biomass present in the batches of grapes. Based on this technique the amount of fungal biomass was determined and ranged from 0.07 to 5.16 g dry weight of fungus per kg wet weight of grapes for the five levels of grey mould severity. The five batches of grapes with the five different levels of grey mould severity were made into wine, the grape juice and finished wine were analysed by GC/MS and 1-octen-3-ol, 1-octen-3-one and 3-octanone, key volatile organic compounds associated with fungal contamination, were quantified. The finished wines were also subjected to sensory discrimination testing to determine the infection rate required to produce a significant difference in comparison to the control.. Volatile organic compounds associated with fungal taints in wine diminished during the wine making process, but were still above the sensory perception thresholds in wine made from grapes with the higher levels of grey mould contamination. The findings suggest that the threshold for Botrytis contamination in Chardonnay grapes is between 0.35 and 1.00 g dry weight of fungus per kg wet weight of grapes, equating to a range from 1-2 berries in the bunch to 10% of the bunch affected with Botrytis.

During the project a collaborative working relationship was established with researchers at the University of Cádiz, Spain. This facilitated the identification of some of the hitherto unknown compounds found in grape berries in response to fungal infection. It is anticipated that this collaboration will be on-going.

Findings from the work have been communicated to the wine industry and the broader scientific community via presentations at grape grower and wine maker meetings, international scientific conferences, on-line and printed extension publications and peer-reviewed scientific manuscripts.

The project has provided grape growers and wine makers with a better understanding of how fungal rots affect wine quality. While thresholds for bunch rot contamination still require some fine tuning, and studies have to be conducted on additional grape varieties, these improvements in objective measures of wine quality will allow decisions to be made around harvesting fruit that is affected with fungal bunch rots.

3. Background:

Grapevines are susceptible to attack by a range of plant pathogens, disease of the mature bunches are termed bunch rots. A number of different fungi are involved in bunch rots of grapes and the incidence and severity of the different types is driven by climatic influences and other viticultural factors. The most common fungal organism associated with grape berry rots is *Botrytis cinerea*, responsible for grey mould (Elad, et al. 2004). Other fungi associated with bunch rot of grapes include species of *Aspergillus* and *Penicillium* (Rousseaux, et al. 2014) and fungi associated with sub-tropical climates such as *Greeneria uvicola* and species of *Colletotrichum* (Steel, et al. 2013).

Bunch rot occurrence and type is seasonally dependant and this variability is largely driven by climatic factors. Management of bunch rot diseases relies on a combination of cultural practices (e.g. canopy management, appropriate choice of grape variety) and chemical control. Failure of fungicide sprays to control bunch rots is not uncommon due to poor bunch rot detection, fungicide resistance and lack of product registration. Management frequently fails in seasons when rain falls close to harvest. In such seasons growers and wine makers have to decide when, or even if, to harvest.

Determining the amount of bunch rot present in a vineyard or grape bunch is difficult. Monitoring the vineyard by visual assessments is subjective and prone to operator error, particularly with grey mould when the rot can be hidden within the interior of the bunch. Aside from these visual assessments (Hill, et al. 2014,Steel, et al. 2007), techniques to detect bunch rots include molecular methods involving PCR amplification (Diguta, et al. 2016,Saito, et al. 2013,Samuelian, et al. 2011), fungal antigen detection (Dewey and Meyer 2004) and laccase assays (Grassin and Dobourdieu 1989,Quijada-Morin, et al. 2018). All of these methods have their limitations, be it applicability for a field or winery situation or an inability to discriminate between bunch rot types.

The impact of grey mould infection of grapes on wine quality has been studied by a number of authors, in many cases the amount of fungal rot present has not been fully quantified. Fruit may have been sorted in to either grey-mould affected or apparently healthy grapes with little if any quantification as to the actual amount of fungal growth present (Pinar, et al. 2017). While these studies provide a valuable insight into the effects of Botrytis on wine quality, they are often of limited value when it comes to setting thresholds for grape growers and winemakers. Reported thresholds for bunch rot tolerance vary and those studies that have been conducted have not correlated this with levels of fungal taints (Ky, et al. 2012,Meunier and Steel 2009).

Spectroscopic measurements (NIR) have been investigated for determination of powdery mildew infection of grapes, but the technique was found to have insufficient sensitivity for applications in the wine industry (Scott 2012). ATR FTIR is an alternative technique that involves the collection of infrared

spectra of samples using reflectance spectroscopy. ATR FTIR has been investigated for other applications in viticulture (Schmidtke, et al. 2012).

Aside from affecting grape yields, bunch rots all impact on grape and wine quality. Detrimental effects to wine quality arise from metabolic activities that lead to changes in the chemical composition of the berry with consequences for potential downgrading of fruit and even fruit rejection at the winery. Limited techniques are currently available in wineries to rectify fungal faults found in wine made from bunch rot-affected grapes. Despite some recent advances, techniques to ameliorate fungal taints in wine are lacking, and the studies that have been conducted have not necessarily included aspects of wine production or sensory analysis (Behr, et al. 2013).

A pilot study (Steel 2014) which formed the basis of the current study examined a number of techniques for the detection and potential differentiation of bunch rot type. Using Chardonnay grapes, this pilot project investigated measuring chitin and the fungal sterol, ergosterol as an indicator of fungal biomass in grapevine tissues. The project also investigated the potential use of ATR FTIR to differentiate berries infected with different fungal species associated with the rotting of grapes. GC/MS analysis of grape juice from berries infected with different bunch rot fungi revealed some of the volatile organic compounds (VOC) produced by these fungi during infection of plant tissues.

Building on the aforementioned pilot study, the objectives of the current project were to develop improved methods of bunch rot detection and to more clearly establish how much bunch rot can be tolerated in a batch of grapes before fruit has to be downgraded or rejected. Coupled with this, the project sought to more fully understand the impact bunch rots of grape have on grape and wine quality and potential techniques that could be applied in a winery setting to ameliorate fungal faults. To achieve these aims the project utilised a combination of detached berries and bunches as well as naturally occurring field samples of bunch rot affected grapes from commercial vineyards. A limiting factor in the work was the seasonal variability in bunch rot occurrence in vineyards, a factor that is largely driven by the climate. To overcome this limitation, experiments were conducted on laboratory-inoculated grapes as well as field samples.

4. Project Aims and Performance targets:

The objectives of this project were to develop improved methods of bunch rot detection and discrimination, to establish clearer guidelines for thresholds for bunch rot contamination of wine grapes and to evaluate potential techniques to ameliorate fungal faults arising in wine as a result of bunch rot contamination. To achieve these aims the following outputs and performance targets were identified in the original project application. Some adjustments to the original target dates for completion were necessary due to unexpected changes in project staffing.

June 2014 to June 2015[1]

Output	Target Date	Activities
Staff appointed	31/08/2014	Post-doctoral scientist appointed
Knowledge developed regarding the impact at least one bunch rot pathogen (other than Botrytis) has on the off flavours / taints present in grapes.	30/11/2014	Berry samples collected as part of GWRDC project NWG1201 analysed by GC/MS and data analysed.
Field material collected and scored using a visual scale 0-4 and divided into (a) apparently healthy (b) Botrytis affected (c) Either Aspergillus or Penicillium affected	31/03/2015	Bunch rot affected fruit sourced from commercial vineyards, and hand harvested based on visually different levels of bunch rots. Fungal bunch rots identified from field samples using conventional plating out techniques.
Wine made from grapes with known levels of bunch rot infection.	31/05/2015	Grapes harvested from bunch rot affected vineyards made into wine. Fining trials commence.

[1]Funding commenced 31st May 2014

July 2015 to June 2016[2]

Output	Target Date	Activities
Validation of previously developed objective measures of bunch rots.	31/08/2015	Data analysed for grapes and wine from the 2014-15 growing season.
Season 1: Identification of thresholds for bunch rot contamination of grapes based on detrimental impacts on the sensorial properties of corresponding wine.	30/11/2015	Wine made with a quantified level of bunch rot contamination from the 2014 -15 growing season (Season 1) analysed by a sensory panel.
Data analysed on the impact bunch rots have on wine quality and potential use of remedial procedures to rectify wine faults.	31/01/2016	Wine made from grapes with known levels of bunch rot infection from the 2014 -15 season analysed by GC/MS and sensory evaluation. A range of fining agents utilised at various stages of wine production for fungal taint amelioration.
Field material for the second year of the project collected and scored using a visual scale 0-4 and divided into (a) apparently healthy (b) Botrytis affected (c) Either Aspergillus or Penicillium affected	31/03/2015	Bunch rot affected fruit sourced from commercial vineyards, and hand harvested based on visually different levels of bunch rots. Fungal bunch rots identified from field samples using conventional plating out techniques.
Additional wines made from grapes from the second year of the trial with known levels of bunch rot infection.	31/05/2016	Grapes harvested from bunch rot affected vineyards, analysed for degree of infection and made into wine

[2]Outputs were delayed due to the resignation of the post-doctoral scientist, Dr Lachlan Schwarz (March 2016) and the time required to find a replacement scientist, Dr Claudia Schueuermann. The project was granted an extension to 31st December 2017.

July 2016 to June 2017[3]

Output	Target Date	Activities
Further validation of objective measures of bunch rot assessment	31/08/2016	Data analysed for grapes and wine from the 2015-16 growing season (Season 2).
Season 2: Identification of thresholds for bunch rot contamination of grapes against detrimental impacts on sensorial properties of corresponding wine.	30/11/2016	Wine made with a quantified level of bunch rot contamination from the 2015 -16 growing season analysed by a scientific sensory panel and the wine analysed for off flavours using GC/MS
Knowledge on the impacts that bunch rot diseases have on wine taints and quality captured in the scientific literature.	31/12/2016	One or more scientific papers submitted to international peer-reviewed journals for publication.
Knowledge on the objective measures of wine quality in relation to fungal rots captured in the scientific literature.	30/06/2017	One or more scientific papers submitted to international peer-reviewed journals for publication.
Industry more fully understands the impact fungal rots have on wine quality and how to help ameliorate fungal taints.	30/06/2017	One or more wine industry articles produced on the applied outcomes of the research.

[3]Outputs were further delayed due to the resignation of Dr Claudia Schueuermann in July 2017. The project was granted a further extension until 30th June 2018.

5. Methods

5.1 Fungal isolates, field sites, berry inoculation methods and wine making procedures

5.1.1 Source of fungal isolates and maintenance of cultures

Botrytis cinerea and *Penicillium expansum* were isolated from commercially grown wine grape berries (*Vitis vinifera* L.) from the Hunter Valley (NSW, Australia). Fungal isolation involved transferring conidia from the berry surface of infected tissue berries to potato dextrose agar (PDA) plates and incubation at 25 °C in darkness for 4 days. Single spore isolations were sub-cultured to PDA plates and incubated at 25 °C in darkness for 7 days. Isolates of *Aspergillus carbonarius* (FFR 5690) and *Aspergillus niger* (FFR 5575) were obtained from the CSIRO culture collection (North Ryde, NSW, Australia). All cultures were stored on PDA slants at 4 °C and maintained in the National Wine and Grape Industry Centre (NWGIC, NSW, Australia) culture collection.

Fungal isolates were grown on potato dextrose agar (PDA) plates and incubated at 27 °C, under a 12 hour light/dark photoperiod in a Thermoline incubator (TRIL-396-1SD, Osram light source 36W/865, Lumilux fluorescent tubes) until spores developed. Spores were washed from the plates using 4 mL sterile distilled water, and were then counted using a haemocytometer. Spore concentrations were adjusted to approximately 10^6 spores per mL using sterile pure water.

5.1.2 Field sites for bunch and berry collection.

For laboratory inoculated grape berries and bunches, *Vitis vinifera* cv Chardonnay grapes were handpicked from disease-free vineyards in the MIA and Gundagai regions of NSW. During the term of this research project, the vineyards selected were free of any bunch rots or other vine diseases at harvest.

Bunches naturally-infected with bunch rots were collected from commercial vineyards located in the Hunter Valley (NSW) and Orange (NSW).

5.1.3 Individual berry inoculation

Disease-free *V. vinifera* (cultivar Chardonnay) grape berries were collected at maturity (12.5 – 14 Baumé) from either the Charles Sturt University vineyard in Wagga Wagga (NSW, Australia), from vineyards in Tumbarumba (NSW, Australia) or from Griffith (NSW, Australia). These berries were

surface sterilised and then inoculated with a spore suspension of one of the following fungal isolates, *Botrytis cinerea, Aspergillus niger, Aspergillus carbonarius* or *Penicillium expansum*. Individual berries were removed from the bunches by cutting the pedicel to ensure that the brush remained intact, and surface sterilised by dipping in a solution of sodium hypochlorite (1% v/v, plus 0.05% v/v Tween 20®, 2 min) followed by three successive washings in sterile distilled water. Berries were placed into the wells of a microtitre plate (24 well, flat-bottom, Iwaki Microplates) and inoculated by placing a 10 µL drop of spore suspension (10^6 spores/mL in sterile distilled water) onto the apex of the berry surface without wounding the berry (Steel, et al. 2011), (figure 1). Control berries were inoculated with 10 µL of sterile distilled water. Each replicate consisted of 24 individual berries and there were three replicates per treatment. Twenty millilitres of sterile distilled water were added to the base of each plate, surrounding the wells, giving a 100% relative humidity. Lids were placed on the microtitre plates, sealed with cling film and incubated at 25 °C. Each replicate consisted of one microtitre plate containing 24 berries. After 7 days of incubation, the berries were homogenized and the juice stored at -20 °C until measurement.

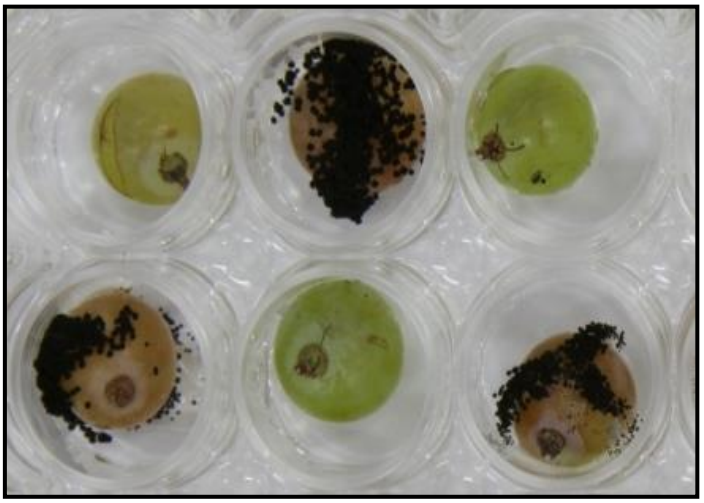


Figure 1: Section of a 24-well Iwaki plate containing chardonnay berries inoculated with *Aspergillus carbonarius* (FFR 5690). Plate was incubated at 25 ^{o}C for five days under a light (12hr) / dark (12hr) cycle. Berries represent different levels of infection.

5.1.4 Whole bunch inoculation and wine making procedure for laboratory-infected grapes

Healthy *Vitis vinifera* (cv Chardonnay) grape bunches (20 ˚Brix) were collected in February 2015, 2016 and February 2017 from a Chardonnay vineyard in Gundagai, NSW. The vineyard was free of any visible signs of vine diseases at the time of harvest. Any berries with visible signs of physical damage, such as sunburn were removed from bunches prior to use.

Whole bunches were dipped in a plastic tub (25 L volume) containing sodium hypochlorite (1.0 % v/v, plus 0.05 % v/v Tween 80®, 2 mins). Bunches were then rinsed three times with distilled water prior to use. Ten berries per bunch were wounded by puncturing once with a sterile syringe. Whole bunches were then dipped in a beaker containing 500 mL of a fungal spore suspension (i.e. either *Botrytis cinerea, Aspergillus niger, Aspergillus carbonarius* or *Penicillium expansum*), such that the entire bunch was exposed to the inoculum. Control bunches were treated in the same manner with the exception that they were dipped in a beaker with an equivalent volume of sterile distilled water. Inoculated grape bunches were either sealed individually in plastic zip-lock bags (2015 growing season) or placed onto wire racks at the base of a 20 L sealable plastic box in order that the berries were not in contact with the box surfaces (2016 growing season). One hundred millilitres of sterile water were added to the base of each box in order to provide 100 % relative humidity (2016 growing season only). The individual bags or boxes were then sealed and the grapes incubated at 23 °C for 7 days.

Diseased bunches from the 2015 growing season were separated into triplicate 0.3 kg & 0.6 kg batches for each fungal treatment, which were subsequently mixed with 29.7 & 29.4 kg of health Chardonnay grape bunches in order to simulate 1 % & 2 % infection. The mixture was immediately de-stemmed, crushed and pressed. Brix, TA and pH measurements were taken and recorded as described below. Every inoculated sample batch was treated separately (starting with control) and the equipment was cleaned and hosed-down with water between treatments and replicates to prevent cross-contamination. All batches were processed within 1 h. Sub-samples of the resulting juices were collected in 50 mL sterile falcon tubes and stored at -20 °C until analysis.

This process was repeated for the 2016 growing season with the following modification. The fully infected diseased bunches were separated into triplicate 3 kg batches for each fungal treatment. The fully infected 3 kg batches were then mixed with 27 kg of healthy/uninfected Chardonnay grape bunches (resulting in 10 % infected bunches). Sampling and wine production was performed as stated above.

5.1.5 Collection of field-infected bunches with visible signs of grey mould (*Botrytis cinerea*) from the Hunter Valley, NSW in the 2016 growing season

Chardonnay grape bunches affected with different levels of grey mould were sourced from a vineyard in the Hunter Valley, NSW. Fruit was harvested on 19th January 2016 and sorted into one of five levels of grey mould contamination (approximately 8 kg each) based on a visual assessment. These five levels equated with the following visible symptoms of grey mould; 0 = no visible signs of bunch rot, 1 = one or two berries in the bunch with bunch rots, 2 = one tenth to one quarter of the bunch with rot, 3 = one quarter to a half of the bunch with rot and a score of 4 = greater than half of the bunch affected with rot (Figure 2). After harvesting the fruit was chilled to 4 °C overnight and then transported to the Charles Sturt University Experimental Winery, Wagga Wagga NSW. A sample of each batch of fruit was selected to confirm the absence of bunch rots other than *B. cinerea*. This involved random sampling of individual berries that were surface sterilised which were then plated on to Dichloran Rose Bengal Agar plates supplemented with chloramphenicol, 20 µg / mL (DRBC). DRBC plates were incubated at 25 °C for up to one week. Resulting colonies were subcultured to PDA, incubated at 25 C for a further period of time until fungal cultures had sporulated. While a number of yeasts and filamentous fungi were isolated (data not shown), other than *B. cinerea*, none of these were associated with plant pathogens responsible for causing bunch rot diseases of grapes. The grapes were then vinified as described below.

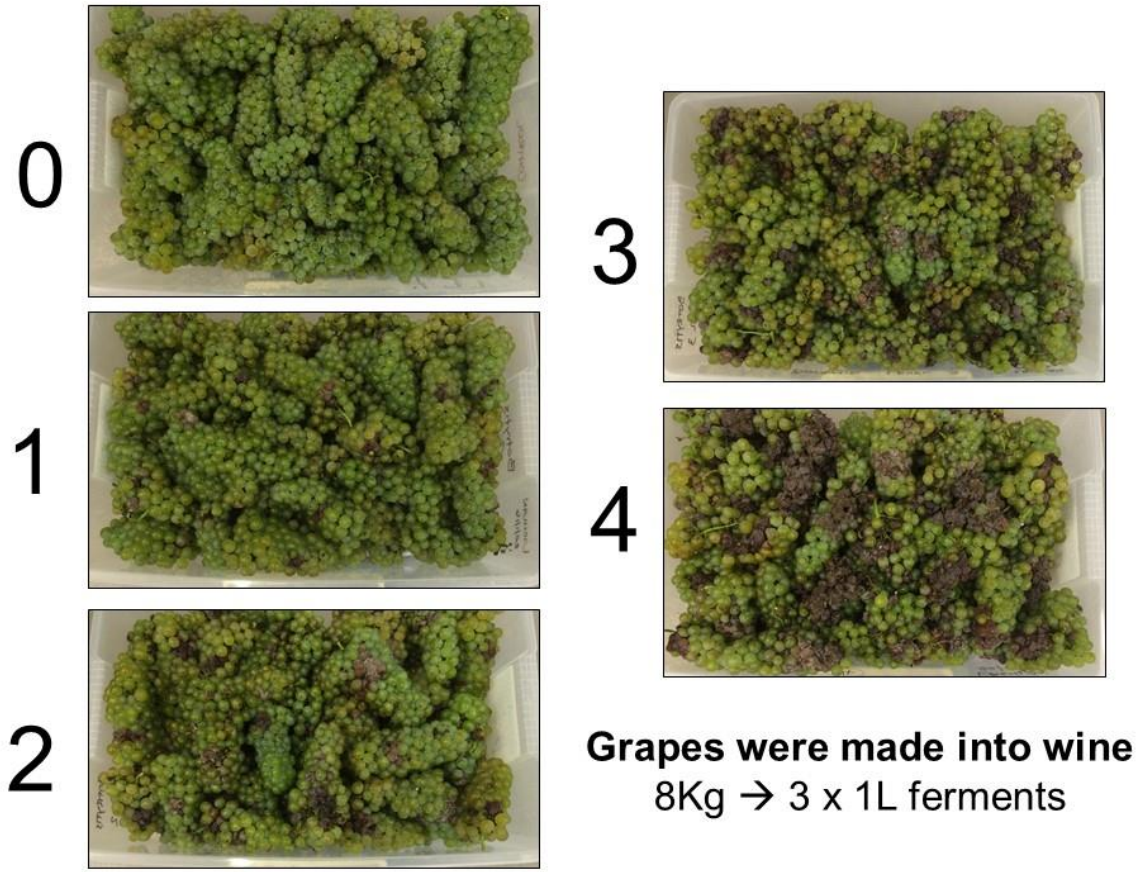


Figure 2: Botrytis affected grape bunches were hand harvested and sorted into one of five categories of severity. 0 = no visible signs of bunch rot, 1 = one or two berries in the bunch with bunch rots, 2 = one tenth to one quarter of the bunch with rot, 3 = one quarter to a half of the bunch with rot and a score of 4 = greater than half of the bunch affected with rot

5.1.6 Collection of field-infected bunches with visible signs of grey mould (*Botrytis cinerea*) from Orange, NSW in the 2017 growing season

The 2016 /17 growing season was relatively dry in NSW and most vineyards were bunch-rot free. Despite this Chardonnay bunches were hand-picked from a vineyard in Orange, NSW on 22nd March 2017 and sorted in to one of two batches, clean (i.e. apparently bunch rot free) and a low level of grey mould infection. Based on a visual inspection the grey mould affected fruit was assessed as having a disease severity score of 0 or 1 using the numerical scale described in the section above dealing with the 2016 Hunter Valley field trial. There were three replicates, each of approximately 10 kg of fruit for the two treatments. The harvested fruit was transported to the Charles Sturt University Experimental Winery, Wagga Wagga NSW and chilled to 4 °C overnight. The following day each fruit batch (0 and 1) were homogenised and sub samples were analysed for ergosterol to determine the fungal biomass (three replicates each), the grapes and sub-samples of resulting juice were taken for GC/MS analysis as described below.

5.1.7 Wine making procedure for field-infected bunches with visible signs of grey mould (*Botrytis cinerea*) in the 2016 and 2017 growing seasons

Treatments were divided into triplicates of approximately 2.5kg each and crushed/destemmed. Must samples were collected in 50 mL sterile falcon tubes and homogenised using an UltraTurrax® T25 and stored at -20 °C until ergosterol analysis. The must was pressed up to 1 bar using a small hydraulic basket press and the resultant juice collected in sterilised 1L Schott bottles. 50mL juice samples were also collected in sterile falcon tubes and kept at -20 °C until volatile and organic acid analysis. The pH of all treatments was measured using a Metrohm Fully Automated 59 Place Titrando System (Herisau, Switzerland). As the pH for all samples was found to be less than 3.10, acidity was not adjusted. Total Soluble Solids (TSS) expressed as °Brix was measured using an Anton Paar DMA 35N portable density meter (Graz, Austria). Potassium metabisulfite (50 mg L^{-1}) was added to the juice prior to chilling for 24 hours at approximately 6°C to allow for clarification by cold settling. Juice was then racked off the gross lees into another sterilised 1L Schott bottle and allowed to warm to room temperature. Juice was inoculated with 250 mg/L of Lalvin EC-1118 (Lallemand). All fermentations were maintained at 15 ± 1 °C and temperature and TSS monitored daily. When the residual sugar levels were measured at less than 0.5 g L^{-1}, the wine was decanted from the yeast lees into another sterilised Schott bottle and 100 mg L^{-1} potassium metabisulfite was added to ensure 0.5–0.8 mg L^{-1} of molecular SO_2. In order to help minimise oxidation, dry ice was added to the ullage of each bottle and placed onto a refrigerated cool room of approximately 4°C to allow settling of remaining solid material. After 5 days the wines

were sufficiently clear to decant into a 250 mL Schott bottle to be used for sensory testing and plastic falcon tubes for chemical analyses.

The pH and titratable acidity (TA), determined by sodium hydroxide titration to the end point pH of 8.2, were measured with a Metrohm Fully Automated 59 Place Titrando System (Herisau, Switzerland). Total Soluble Solids (TSS) expressed as °Brix was measured using an Anton Paar DMA 35N portable density meter (Graz, Austria). Aldehyde, gluconic acid, glycerol and acetic acid were analysed with Thermo Fisher Scientific enzymatic kits (Waltham, MA), with testing performed on an Arena Discrete Analyzer (Thermo Fisher Scientific). Alcohol content was determined using an Anton Paar Alcoholyser (Graz, Austria).

5.1.8 Sensory analysis of wines made from field-infected grapes

The wines vinified from the infected grapes were compared to the wine made from the apparently healthy grapes using a series of triangle tests in order to determine the presence of any perceptible sensorial difference. Due to the small volumes of wine available, triangle tests were first utilised to verify that treatment replicates were not different. As no differences were detected (results not shown) all replicates were used for subsequent testing. The panel was composed of 15 judges (4 females and 11 males, 25–55 years of age). The wine samples (30 mL) were presented at room temperature (20 °C), in black tulip-shaped glasses, covered with glass Petri dishes and coded with random three-digit codes. Each judge performed the four triangle tests in one session. Eight judges received the infected wine treatments as the odd sample while seven received the control wine as the odd sample. The order of presentation of each set of samples was also randomised. The judges were asked to identify the odd sample in each set. The statistical significance of the results of the triangle test was determined using published statistical tables (Roessler, et al. 1978).

5.1.9 Fining Trials

Chardonnay wines prepared from bunches with a known amount of diseased fruit (up to 2 % by weight) were treated with fining agents at two dosages as follows; Polyvinylpolypyrrolidone (PVPP) at 500 and 1000 ppm, carbon at 300 and 500 ppm and Isinglass at 20 and 50 ppm. Sensory analysis was conducted as described above following fining agent treatment.

5.2 Establishment of an ATR FTIR method for grape analysis

ATR FTIR analysis was performed on freeze-dried fungal mycelium and inoculated individual berries (detached from the bunch). In further work inoculated bunches and must, sampled during wine making were also analysed by ATR FTIR.

5.2.1 Preparation of material for ATR FTIR analysis

Cultures for the preparation of the freeze-dried mycelium were prepared as described above, except the fungi were cultured on synthetic grape juice (SGJ) medium (Belli, et al. 2004) rather than PDB. Eight replicate 25 mL aliquots of SGJ in 100 mL conical flasks were inoculated with 50 µL of a fungal spore suspension, prepared as described above. Cultures were incubated at 20 °C with agitation (90 rpm) for a period of 7 days, after which they were mechanically homogenised, separated into 5 mL aliquots, lyophilized and stored at -20 °C. Individual berries and whole bunches were inoculated with one of the fungal species used in this study as described above.

Attenuated Total Reflectance Fourier Transform Infrared Spectroscopy (ATR FTIR) analysis was performed using an Alpha–P Bruker ATR FTIR Spectrophotometer running OPUS 7.0 software (Bruker Optics, Ettlingen, Germany). Scans of homogenised fungal mycelium homogenate on a Diamond ATR crystal were acquired at 60 °C for each of the triplicate samples. Each sample was dried on the thermostated scanning surface for a period of 5 minutes prior to scan acquisition and repeated a total of five times, each with fresh mycelium homogenate. Background scans against air were performed every five samples. Data was converted to ascii format at a resolution of 1.4 cm^{-1} and imported into Matlab version R2012a (The Mathworks, Natick, Natick, MA, USA) and converted to absorbance to correct for differences in sample penetration of the beam at different wavelengths. Exploratory data analysis of the 'fingerprint' region between 375 – 1850 cm^{-1} was conducted *via* a principal components analysis on the standard normal variates scaled and mean centred data with sample scores and variable loadings presented in figures 3 and 4 respectively.

Thawed homogenates (10 µL) from both control un-inoculated berries and berries infected with either *A. carbonarius, A. niger, B. cinerea* or *P. expansum* were analysed on a Diamond ATR crystal. For berry infection studies the initial method development involved analysis of a representative sample of an infected berry juice at three temperatures, room temperature (~ 20 °C), 40 and 60 °C with drying times ranging from 0 - 20 minutes on the diamond crystal prior to acquisition (Appendix 5.2 - Supplementary Figure S1). Subsequent spectral analyses were performed on all juice samples at 60 °C with 10 µL samples allowed to concentrate on the crystal surface for 5 minutes prior to acquisition. Each sample was measured once with ATR spectra averaged over 64 scans for the spectral region spanning 375-

4000 cm^{-1} at a resolution of 4 cm^{-1}. A background scan against air was conducted approximately every 10 samples.

Thawed homogenates of must, prepared using up to 2 % (w/w) of bunches infected with either *A. carbonarius, A. niger, B. cinerea* or *P. expansum*, were analysed on a Diamond ATR crystal. Spectral analyses were conducted at 60 °C using 10 µL samples and 5 min drying time on the crystal surface prior to acquisition. Each sample was measured once with ATR spectra averaged over 64 scans for the spectral region spanning 375-4000 cm^{-1} at a resolution of 4 cm^{-1}. A background scan against air was conducted approximately every 10 samples.

ATR data was converted to absorbance to correct for differences in sample penetration of the beam at different wavelengths. Spectra from all samples and the 95% confidence interval (CI) for absorbance was plotted to identify regions of interesting variation (Figure 3). A principal component analysis (PCA) of the standard normal variates (SNV) scaled and mean centred data between the regions 375 – 1850 cm^{-1} was conducted using the singular value decomposition (SVD) algorithm with principal components (PC) 1-2 and plotted to identify specific sample groupings based on pathogen and sampling time (Data not shown). Inspection of the sample scores for date and pathogen revealed a cluster of ten samples in the data set, scanned sequentially, that were largely separate from the remaining samples (Appendix 5.2 - Supplementary Figure S2). This group of samples appeared to be separate due to a poor background scan prior to the analysis of the ten samples. For the purposes of cluster analysis and development of predictive modelling based upon pathogen, different models were constructed with these samples retained and excluded. As the models with excluded samples did not have greater predictive quality, the results are presented below for models with all samples retained and this serves as an indirect indicator of the robustness of the modelling.

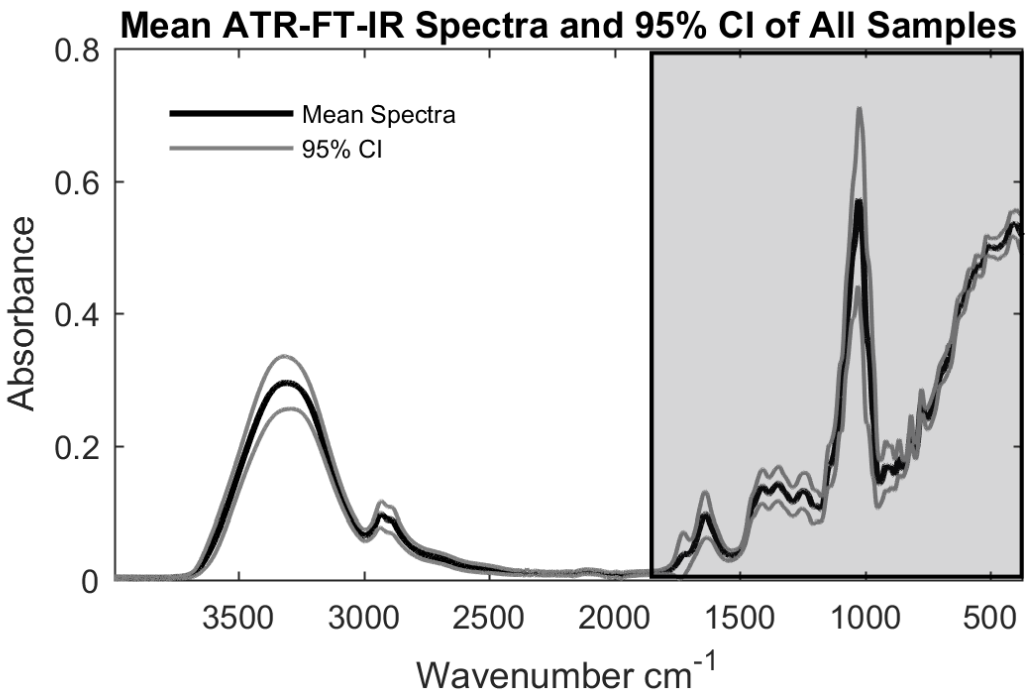


Figure 3. Mean ATR FTIR spectra of samples from berry infection studies. The shaded area was used for exploratory data analysis and predictive modelling of pathogen class.

5.2.2 Development of predictive models of pathogen in berry homogenates analysed by ATR FTIR

Prior to the development of predictive models, juice samples from infected berries with various pathogens were randomly assigned to either a training or independent test set such that the distribution of samples was approximately similar. The distribution of samples is shown in Table 1.

Predictive models of class based upon the pathogen were constructed using the classification modelling algorithms: Soft Independent Modelling of Class Analogy (SIMCA); Support Vector Classification (SVR), K-Nearest Neighbour (KNN) and a machine learning classification approach Random Forest which comprises an ensemble of decision trees constructed with the bagging method using the raw data. SIMCA, SVR and KNN models were constructed on the infrared spectra between 375-1850 cm^{-1} using SNV and mean centred data in the PLS Toolbox version 7.8 (Eigenvector Research, Manson, WA, USA) and random forest ensembles on the same spectral region using the raw data using Matlab version 7.14 Statistical Toolbox. Individual class models for SIMCA were constructed using principal components analysis retaining between three to six principal components (PCs) for each class, i.e. control or infected berry pathogen. The number of retained PCs was determined by cross validation within each class training set, inspection of the data variance explained for each PC, and the size of the eigenvalues associated with each PC (Table 2). The SVR, KNN and Random Forest models were cross validated using a 10 fold data split of the training data set with inspection of the cross

validated model predictive acuity to prevent overfitting (Appendix 5.1 - Supplementary Tables S1 and S2). The predictive acuity of each final model was assessed using the independent test data set (Table 1) and model comparisons for KNN, SVM, SIMCA and Random Forest models are presented as Receiver Operating Characteristic (ROC) curves that illustrate False Positive versus True Positive class predictions. As multiclass classifier models were developed, the sample probability for true class assignment was corrected by subtracting the maximum probability for incorrect classification prior to constructing ROC curves, which are illustrated in Figure 4.

For the purposes of comparing predictive acuity of each of the models for pathogen class, confusion matrices were determined using the following calculations of predicted class for the independent test set samples:

True Positive Rate: proportion of positive class correctly identified (Sensitivity) = TP/(TP + FN) False Positive Rate: proportion of negative class incorrectly classified as positive = FP/(FP + TN) True Negative rate: proportion of negative class that were correctly identified (Specificity) = TN/(TN + FP)

False negative Rate: proportion of positive class that were incorrectly classified as negative = FN/(FN + TP) Misclassification Error: proportion of samples incorrectly classified = 1 – accuracy = (FP + FN)/(TP + TN + FP + FN) Precision: = TP/(TP + FP) Accuracy (F_1 Score) = 2*TP/(2*TP + FP + FN) Area Under Curve (AUC) integrated from Receiver Operator Curves of the independent data set.

Table 1: Infected berry juice sample allocation to training and independent test data sets used for model development and testing.

Pathogen/Treatment	Identity	Training Set		Independent Test Set		TOTAL	
		Number Samples	Percent	Number Samples	Percent	Number Samples	Percent
Aspergillus carbonarius	Asc	22	19.3	8	21.6	30	20.0
Aspergillus niger	Asn	23	20.2	7	18.9	30	20.0
Botrytis cinerea	Bot	23	20.2	8	21.6	30	20.0
Penicillium expansum	Pen	23	20.2	7	18.9	30	20.0
Control	Con	23	20.2	7	18.9	30	20.0
TOTAL		114	100.0	37	100.0	150	100.0

Table 2: SIMCA PCA model data for each pathogen class

Pathogen Class	Number of Principal Components for Class	Percentage of Sample Data Variance Modelled
Aspergillus carbonarius (Asn)	5	97.4
Aspergillus niger (Asn)	5	97.5
Botrytis cinerea (Bot)	4	98.1
Penicillium expansum (Pen)	3	95.8
Control (Con)	5	97.2

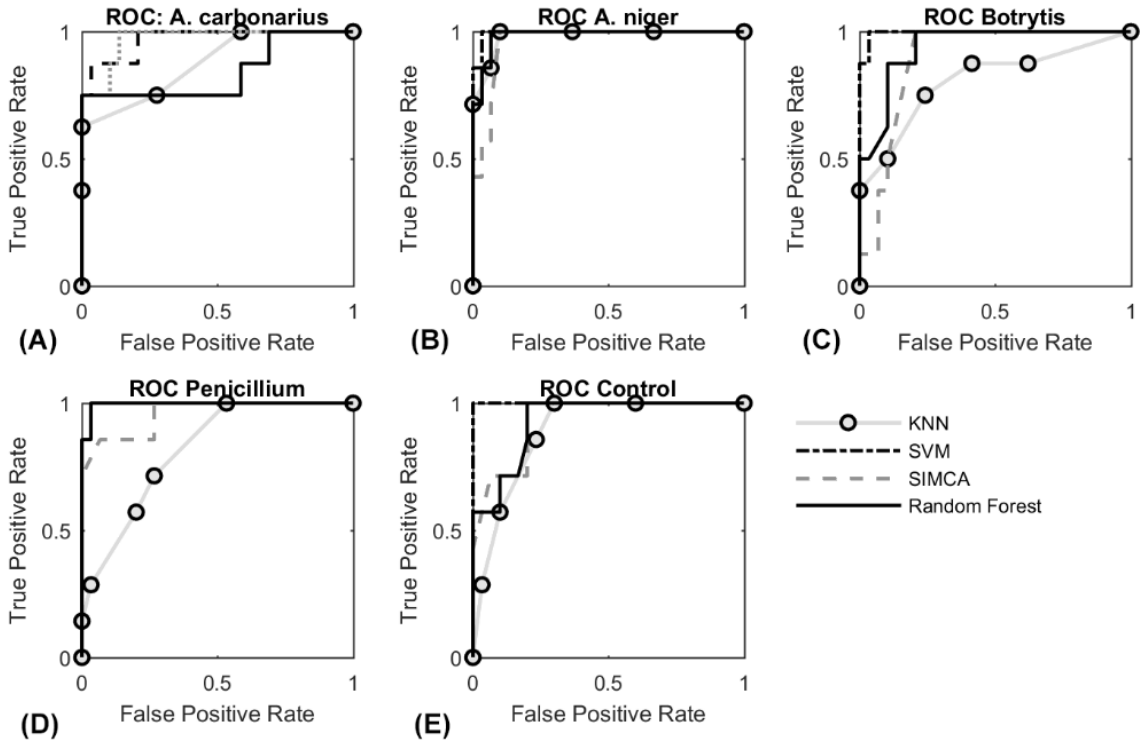


Figure 4: Receiver Operating Characteristic (ROC) Curves for bunch rot pathogen prediction and differentiation from control (un-inoculated) berries using four classifying models. Displayed are ROC curves for (A) *Aspergillus carbonarius*; (B) *Aspergillus niger*; (C) *Botrytis cinerea;* (D) *Penicillium expansum* and (E) control samples.

5.3 GC/MS Analysis of laboratory-inoculated grape berries and wine

5.3.1 SPME-GC/MS analysis of grape juice and wine

Samples were analysed in randomised order. For each sample, 3 g sodium chloride was weighed into a 20 mL headspace glass vial (Agilent Technologies, VIC, Australia), followed by 2.5 mL juice sample and 7.5 mL pure water. Before sealing with a Teflon screw cap, 50 µL of internal standard solution (containing 33.4 µg/L methyl isobutyl ketone, and 15.4 µg/L geosmin-d_3 in ethanol) was added to each vial. The vials were vortexed for 10 sec before analysis. To ensure reproducibility of the analytical method, an approach for analysis within and between vintage was adopted as previously described (Rebière, et al. 2010); the SPME fibre was conditioned before sample analysis using two water blanks and two random grape juices. A Gerstel Multipurpose Sampler (MPS2XL, Gerstel Inc., MD, USA) with automated SPME capability and a Peltier sample cooler tray was connected to an Agilent 7890A gas chromatograph, which was interfaced to an Agilent 5975C triple axis mass selective detector (Agilent Technologies Ltd., PA, USA). The column used for separation of compounds was a DB-Waxetr column (60 m x 250 µm inner diameter x 0.25 µm film thickness; Agilent Technologies Ltd., PA, USA). Sample vials were placed into the Peltier sample cooler (10 °C). Vials were subsequently transferred into the heated (65 °C) agitator stirrer (MPS2XL, Gerstel Inc., MD, USA), where they were incubated for 2 min before insertion of the SPME fibre (Supelco, 50/30 µm DVB/CAR/PDMS). Sample headspaces were extracted onto the SPME fibre for 64 min under agitation at 250 rpm. Injection of the SPME fibre into an ultra-inert straight SPME liner (0.75 mm, Agilent Technologies Inc., PA, USA) was performed at an inlet temperature of 260 °C in split-less mode for 1 min. The fibre was then baked for 10 min at 270 °C in a second injector. The helium carrier gas flow rate was 3 mL/min. The initial GC oven temperature was 40 °C, which was held for 3 min before heating at 5 °C/min until 115 °C; increased at 3 °C/min until 166 °C; then increased at 10 °C/min until 210 °C was reached. The final temperature was held for 15 min, resulting in a total run time of 54.4 min. After a solvent delay of 3 min, the mass detector recorded a range between mass ion ratios (*m/z*) 50 and 550 (at a frequency of about 3 Hz). The data was acquired using the Enhanced MSD Chemstation software (version E.02.00.493, Agilent Technologies Inc., PA, USA) and exported as three-dimensional data (.CDF) for data analysis.

5.3.2 Data processing

The data (.CDF) was imported into Matlab (version R.2016a, The Mathworks Inc., MI, USA) using the iCDF program available at www.models.life.ku.dk/icdf. Data processing proceeded in accordance with previously published methods for GC/MS data (Berna, et al. 2009). The sum of each *m/z* intensity

across the entire chromatogram was calculated and then normalised to the geometric mean of the internal standards (peak areas of prevalent *m/z* 58 for methyl isobutyl ketone and *m/z* 115 for geosmin-*d3*) for each sample replicate. Due to the calculation of this mass spectral intensity across the chromatogram, the *m/z* are no longer dependent on retention time and, hence, alignment is not required. *M/z* higher than 300 and siloxane related *m/z*, including 73, 75, 76, 110, 133, 147, 165, 177-180, 182, 189, 193-195, 197, 205, 207-214, 218-219, 223-231, 233-242, 245-255 and 257-260 were excluded from the analysis as they were due to SPME fibre breakdown products. The resulting matrix of *m/z* intensities was inspected for sample groupings using Principal Component Analysis (PCA) (Appendix 5.2 - Supplementary Figures S1-S3). For the subsequent supervised classification analysis, Partial Least Squares-Discriminant Analysis (PLS-DA) was used. Pre-processing for the PLS-DA models was done by applying a logarithm to the base 10, mean centring and variance scaling using the Pareto standardisation. Orthogonal signal correction (OSC) to remove structured but uncorrelated information was applied prior to PLS-DA analysis (PLS_toolbox, v. 8.1.1, Eigenvector Research, Inc., WA, USA). The data of each experiment (15 samples per experiment) was organised into five classes of three replicates each (control, *B. cinerea*, *A. niger*, *A. carbonarius* and *P. expansum*). Selection of the number of latent variables for each model was considered by inspection of the eigenvalues and variance captured for the X-block (Appendix 5.1 Supplementary Tables S3-5). To evaluate the efficacy of the models to predict fungal classes from the *m/z* data matrix, cross validation using 'leave-one-out' as re-sampling methodology was used. To determine overall model robustness and the appropriate numbers of orthogonal components, PLSDA models were validated using a cross validation approach (Westerhuis, et al. 2008) followed by Monte Carlo random permutations of the data labels under the null hypothesis (i.e. no predictive acuity). Q^2 and the area under the receiver operator curves (AUROC) were used to assess the overall model robustness derived from 1000 permuted data repetitions and were compared to the true model values to obtain the P values of model acuity (Szymańska, et al. 2012). This approach allows an empirical estimation of the P value by determining the proportion of test statistics from random models equal to or higher than the true model. Results of permutation testing (Q^2 and AUROC) for each data set are presented in the supplementary data (Appendix 5.2 Supplementary Figures S4-6). For the purposes of determining the appropriate numbers of orthogonal components permutation testing was performed with increasing numbers of orthogonal components extracted (zero to three) from the models with R^2Y used to determine the appropriate numbers and the most parsimonious model selected. Orthogonalisation was applied only to the 2016 bunch data set and results of permutation testing are presented in Appendix 5.1 Supplementary Table S6).

To identify the *m/z* with high discriminatory value for each pathogen class in a given model, three measures of importance were considered. Selection of discriminatory *m/z* was based upon those with selectivity ratios (SR) ranked in the 85^{th} percentile with variable importance to projection (VIP) values greater than one (Krakowska, et al. 2016) and were highly correlated with at least two other *m/*z determined by inspection of cross correlation coefficients. These three measures of importance were considered together to accommodate varying data structure and influence upon the predictive acuity for SR and VIP measures (Farrés, et al. 2015) and high cross correlations for *m/*z triplets could be reasonably expected for high quality mass spectra for eluting compounds in the chromatogram. SR and VIP scores were determined for each model using published methods (Farrés, et al. 2015) and are shown in the supplementary data (Appendix 5.1 Supplementary Tables S7-S9). Cross correlations of the normalised summed *m/z* data were determined in Matlab (data not shown). Having identified triplets of *m/z* with high discriminatory value, a putative peak table comprising integrated areas and elution times was constructed from extracted ion chromatograms at the retention times where all three ions were apparent. Peak areas for compounds were integrated using the main *m/*z for all samples within the respective model and values below a threshold of 1000 were set to zero. To identify the statistically significant peak areas thereof, multivariate analysis of variance (MANOVA) was conducted on the peak areas (normalised to peak area of the geometric mean of the internal standards). A post hoc test (Tukey, honest significant difference, HSD) was done for mean separation. An additional measure, the effect size, was calculated using the partial Eta-Squared, η_p^2 (SPSS Statistics, v. 20, IBM, IL, USA). Effect size values range between 0-1 and the closer the value to one, the higher the effect or discrimination size of the variable. η_p^2 is one of the most widely used measures of effect size, it provides added information to significance testing of ANOVA and it is defined as the ratio of the sum of squares (SS) of the effect (SS_E) to the sum of the effect and the residuals ($SS_E + SS_R$) (Lakens 2013).

Retention indices (RI) of the detected significant peak areas were calculated based on an alkane series (C8-C40), measured using the GC/MS method described above, according to the equation of van den Dool and Kratz (Van den Dool and Kratz 1963). Compounds were identified by comparing their RI and EI-MS spectra against authentic standards and the NIST2011 GC-MS metabolite (NIST, MD, USA) and the Massfinder4 Terpenoid (Dr. Hochmuth Scientific Consulting, Germany) database (a), or by comparing their RI and EI-MS against the above databases and peer-reviewed scientific literature (b).

5.3.3 SPME-GCQTOF analysis

Accurate masses were determined using an analogous method to the above but with detection by a quadrupole time-of-flight (QTOF) mass spectrometer. A GC 7890A gas chromatograph and a QTOF

7200 accurate mass spectrometer (Agilent Technologies Ltd., PA, USA) were fitted with a Shimadzu auto-sampler AOC-5000Plus (Shimadzu Scientific Instruments, MD, USA). A mass range from *m/z* 50-500 was recorded in the electron ionisation mode at 70 eV. The TOF mass analyser was operating in the 2-GHz resolution mode and a daily MS calibration was conducted using perfluorotributylamine (PFTBA). Further GC/QTOF conditions were analogous to the GC/MS method above, including the measurement of an alkane series for RI calculation and intensity checks as well as the use of the internal standards.

5.4 Methods for the analysis of field-infected bunch samples and threshold investigations

5.4.1 Extraction of fungal and plant material for ergosterol analysis

Fungal biomass based on ergosterol equivalents was conducted using a modification of the method described by (Porep, et al. 2014). *B. cinerea* was grown on PDA plates at 25 °C until such time that the cultures had formed spores. The spores were harvested from the plate using a volume of sterile distilled water and the spore concentration counted using a heamocytomer and adjusted with sterile distilled water to 10^6 spores per mL. A 100 µL volume of the spore suspension corresponding to 10^5 spores was then aseptically added to 100 mL of PDB in a 250 mL conical flask. The cultures (five replicates) were incubated with agitation at 25 °C for seven days using a rotary shaking incubator (Ratek OM25), after which the resulting mycelium was harvested by filtration, washed with two successive volumes of sterile distilled water, frozen overnight at – 20 °C and then freeze-dried.

The dry weight of the freeze-dried mycelium was recorded, and ground in liquid nitrogen using a mortar & pestle. The dried mycelium powder was stored in a desiccator until analysis. Approximately 50 mg of dried fungal biomass was accurately weighed, the weight recorded and transferred to a 250 mL round bottom flask. Deionized water (50 mL), (HPLC grade) (75 mL) and ethanol (HPLC grade) (50 mL) were added to the flask and the contents mixed. Once mixed 10 g of KOH pellets were added to the flask. The flask contents were refluxed for 30 mins using a Star fish apparatus that allowed five flasks to be refluxed simultaneously. After cooling to ambient temperature the flask contents were filtered through Whatman #1 filter paper. The flask was rinsed twice with methanol (25 mL) to wash the filter paper. The filtrate was transferred to a 250 mL separating funnel and the contents extracted twice with *n*-hexane (50 mL). The upper organic phase (*n*-hexane layer) was collected and the extraction repeated with a further volume of n-hexane (50 mL). The *n*-hexane extracts were combined and dried using anhydrous sodium sulfate (Na_2SO_4) overnight. The extracts were filtered (Whatman #1) to remove any sodium sulfate, and the filter paper rinsed with *n*-hexane (5 mL). The *n*-hexane was removed under reduced pressure by rotary evaporation and taken to dryness. The extract was re-constituted in 5 mL methanol (HPLC grade, 5 mL) and dissolution assisted with ultra-sonication. The extracts were stored in a sealed container under a N_2 atmosphere at 4 °C for later HPLC analysis.

5.4.2 Quantification of the ergosterol content of fungal cultures by reverse phase HPLC

The ergosterol content of extracts was quantified using a Waters 600 HPLC, using a C18 column (150 x 4.6 mm, 5 µm particle size) with C18 guard column in place. The mobile phase consisted of 95% v/v HPLC grade methanol and 5% v/v reverse osmosis water that was pumped isocratically at a

flow rate of 0.8 mL/min. Ergosterol was detected at 282 nm using a UV/Vis detector. External calibration was achieved with a series of diluted ergosterol standards (200, 20, 4, 1 and 0.04 mg /L) in HPLC grade methanol stored in the dark. Fungal biomass was determined using the following equation:

Fungal biomass (g/kg) = BCF x ERG

Where BCF (fungal biomass conversion factor) = the reciprocal of the average ergosterol content in mg/g dry mycelia; and ERG = ergosterol concentration in mg/kg.

5.4.3 Estimation of fungal biomass in infected grapevine tissues

Grape berries or bunches were extracted using organic solvents as described above for the extraction of freeze dried mycelium, except the fresh material was extracted without lyophilisation.

Fungal biomass in infected grape bunches was estimated using the equation Fungal biomass (g/kg) = BCF x ERG as described above. The wet weight of the grape material to be analysed was recorded and then the tissue homogenised. Ergosterol was extracted by saponification and the ergosterol content of the extract quantified using the HPLC method as described above. The fungal biomass of infected tissues was expressed as g dry weight of fungus per kg wet weight of grapes.

5.4.4 Measures of basic wine composition

The pH and titratable acidity (TA), determined by sodium hydroxide titration to the end point pH of 8.2, were measured with a Metrohm Fully Automated 59 Place Titrando System (Herisau, Switzerland). Total Soluble Solids (TSS) expressed as °Brix was measured using an Anton Paar DMA 35N portable density meter (Graz, Austria). Aldehyde, gluconic acid, glycerol and acetic acid were analysed with Thermo Fisher Scientific enzymatic kits (Waltham, MA), with testing performed on an Arena Discrete Analyzer (Thermo Fisher Scientific). Alcohol content was determined using an Anton Paar Alcoholyser (Graz, Austria).

5.4.5 SPME-GC/MS analysis of juice and wine

Samples were analysed in randomised order. For each sample, 3 g sodium chloride was weighed into a 20 mL headspace glass vial (Agilent Technologies, VIC, Australia), a volume of 2.5 mL juice sample and 7.5 mL pure water was added. In the case of wine samples, a volume of 2 mL wine and 8 mL pure water were added. Before sealing with a Teflon screw cap, 50 µL of internal standard solution (containing 33.4 µg/L methyl isobutyl ketone, 15.4 µg/L geosmin-*d3* and 28.8 µg/L 2-octanol in ethanol) was added to each vial. The vials were vortexed for 10 s before analysis.

The targeted compounds 3-octanone, 1-octen-3-one and 1-octen-3-ol were quantified by external calibration in a synthetic grape juice medium (for grape juice matrix) and in a base Chardonnay wine (for wine matrix) that were prepared into headspace vials analogous to the above method including sodium chloride, internal standard solution and the respective volume of pure water.

A Gerstel Multipurpose Sampler (MPS2XL, Gerstel Inc., MD, USA) with automated SPME capability and a Peltier sample cooler tray was connected to an Agilent 7890A gas chromatograph, which was interfaced to an Agilent 5975C triple axis mass selective detector (Agilent Technologies Ltd., PA, USA). The column used for separation of compounds was a DB-Waxetr column (60 m x 250 µm inner diameter x 0.25 µm film thickness; Agilent Technologies Ltd., PA, USA). Sample vials were placed into the Peltier sample cooler (10 °C). Vials were subsequently transferred into the heated (65 °C) agitator stirrer (MPS2XL, Gerstel Inc., MD, USA), where they were incubated for 2 min before insertion of the SPME fibre (50/30 µm DVB/CAR/PDMS, Stableflex 23Ga, Supelco, PA, USA) for headspace extraction of volatile organic compounds (VOCs). Sample headspaces were extracted onto the SPME fibre for 64 min under agitation at 250 rpm. Injection of the SPME fibre into an ultra-inert straight SPME liner (0.75 mm, Agilent Technologies Inc., PA, USA) was done at an inlet temperature of 260 °C in split-less mode for 1 min. The fibre was then baked for 10 min at 270 °C in a second injector. The helium carrier gas flow rate was 3 mL/min. The initial GC oven temperature was 40 °C, which was held for 3 min before heating at 5 °C/min until 115 °C; increased at 3 °C/min until 166 °C; then increased at 10 °C/min until 210 °C was reached. The final temperature was held for 15 min, resulting in a total run time of 54.4 min. After a solvent delay of 3 min, the mass detector recorded a scan range between m/z 50 and 550 for untargeted volatile analysis. For targeted volatile analysis, single ion monitoring (SIM) groups were recorded. Between 3 min and 14 min m/z 58 and 100 were recoded for methy lisobutyl ketone (internal standard). M/z 57 and 72 were recorded for 3-octanone and m/z 55 and 70 for 1-octen-3-one between 14 min and 19.4 min. In another group, between 19.4 min and 23.5 min, m/z 45 and 55 were recorded for 2-octanol (internal standard) and m/z 57 and 72 for 1-octen-3-ol. A last group was recorded for the internal standard geosmin-*d3* (m/z 115 and 111), between 32.9 min and 38.6 min.

5.4.6 SPME-GC/MS data processing

For the untargeted volatile analysis the data (.CDF) was imported into MatLab (version R.2016a, The Mathworks Inc., MI, USA) using the iCDF program available at www.models.life.ku.dk/icdf. The sum of each mass ion intensity across the entire chromatogram was calculated and then normalised to the geometric mean of the internal standards (peak areas of m/z 58 for methyl isobutyl ketone and m/z 115 for geosmin-*d3*) for each sample replicate. M/z higher than 300 were excluded from analysis. Siloxane related m/z, including 75, 76, 110, 133, 147, 165, 177-180, 182, 189, 193-195, 197, 205, 207-214, 218-219, 223-231, 233-242, 245-255 and 257-260 were excluded from the analysis as they were due to SPME fibre breakdown products. The resulting matrix of m/z intensities was then pre-processed by applying a logarithm to the base 10, mean centring and variance scaling using the pareto standardisation. Orthogonal signal correction (OSC) to remove structured but uncorrelated information was applied prior to PLS-DA analysis (PLS_toolbox, v. 8.1.1, Eigenvector Research, Inc., WA, USA). Data was organised into the five classes representing the infection levels (0 = no visible signs of bunch rot, 1 = one or two berries in the bunch with bunch rots, 2 = one tenth to one quarter of the bunch with rot, 3 = one quarter to a half of the bunch with rot and a score of 4 = greater than half of the bunch affected with rot). To evaluate the efficacy of the models to predict fungal classes from the m/z data matrix cross validation using the leave on sample out approach was used. For each class in a given model m/z with the 20 highest selectivity ratios were selected for detailed inspection of associated VOCs.

A correlation matrix including all normalised m/z values was used to identify which of the 20 given m/z from the PLS-DA models correlated (m/z with highest R coefficients and lowest p values). Chromatograms were inspected for retention times at which at least two highly correlated m/z appeared. From the mass spectra of the so identified peaks the prevalent m/z was integrated.

For the targeted volatile analysis the quantification ions for internal standards and targeted compounds (see supplementary material Table S1) were integrated in Masshunter Qualitative Analysis (v. B.07.00, Agilent Technologies Inc., PA, USA). Peak areas of the targeted compounds were normalised to the internal standards and concentrations calculated based on the external 5-point linear calibrations ($R^2 = 0.999$).

For both targeted and un-targeted compounds, to identify the statistically significant differences between peak areas or concentrations, ANOVA and a post hoc test (Tukey) was conducted and the effect size was calculated (partial Eta-Squared) to determine the size of the significant differences (SPSS Statistics, v. 20, IBM, IL, USA).

Retention indices (RI) of the detected compounds were calculated based on an alkane series (C8-C40), measured using the GC/MS method described above, according to the equation of van den Dool and Kratz (Van den Dool and Kratz 1963). Compounds were identified at level 1, by comparing their RI and EI-MS spectra against authentic standards and the NIST2011 GC-MS metabolite (NIST, MD, USA) and the Massfinder4 Terpenoid (Dr. Hochmuth Scientific Consulting, Germany) database, or at level 2, by comparing their RI and EI-MS against the above databases and peer-reviewed scientific literature.

6. Results

The results relating to the ATR FTIR analysis of fungal and grape tissues, the GC/MS analysis of laboratory-inoculated grapes and the field-infected grape bunches are discussed separately in this section of the report.

6.1 ATR FTIR spectroscopy to discriminate fungal mycelium and grape berries inoculated with either *Aspergillus niger, A. carbonarius*, *Botrytis cinerea* or *Penicillium expansum.*

6.1.1 ATR FTIR of fungal mycelia

Exploratory data analysis of the 'fingerprint' region between 375 – 1850 cm^{-1} was conducted *via* a principal components analysis on the standard normal variates scaled and mean centred data. The first three principal components (PCs) capture 98.2% of data variance and demonstrate the ability to differentiate between fungal pathogen species employed in this study. This is best visualised when plotting PC2 against PC3 (Figure 5), in which clear groupings for each pathogen species are evident. An important observation is the ability to clearly differentiate between the two *Aspergillus* species. *Aspergillus spp.* are typically very similar to one another when inspected visually and will often require time-consuming and expensive molecular techniques for accurate identification. Inspection of the loadings associated with the PC2 and PC3 scores plot (Figure 6) show interesting portions of the IR spectra associated with the sample groupings. Loadings for PC2 have positive correlations at the wavenumbers 1740, 1205 and 950 cm^{-1} corresponding to lipids C=O stretching, amide III and polysaccharide stretching respectively (Salman, et al. 2012). A negative correlation at 1590 cm^{-1} associated with amide II N=H bending is also evident for the loading associated with PC2. Loadings associated with PC3 show positive correlations at 1650, 1000, 950 1150 1373 and 1310 corresponding to amide I C=O stretching, polysaccharide C-O stretching, C-N and amide III functional groups. A strongly negative correlation with amide II N-H bending is also evident in this loading. The ability to rapidly discriminant each fungal species using ATR FTIR signatures demonstrates the potential for combining IR with chemometric data analysis for pathogen identification.

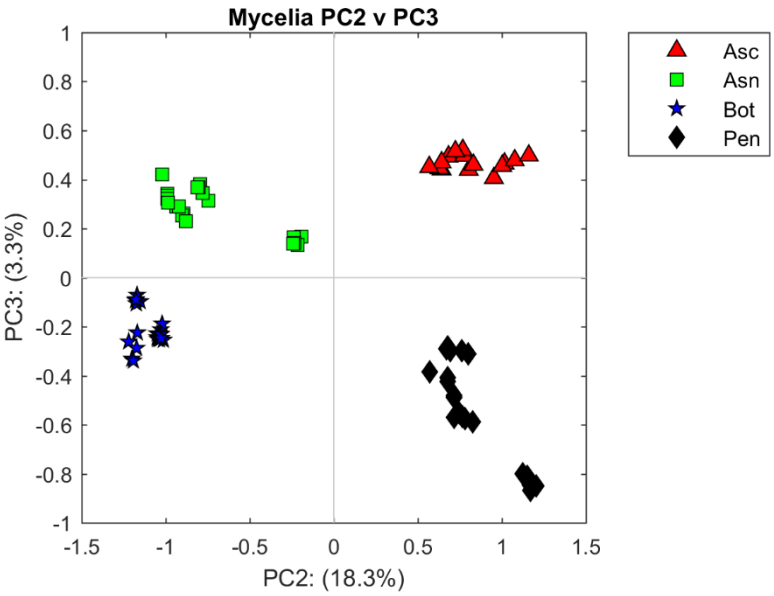
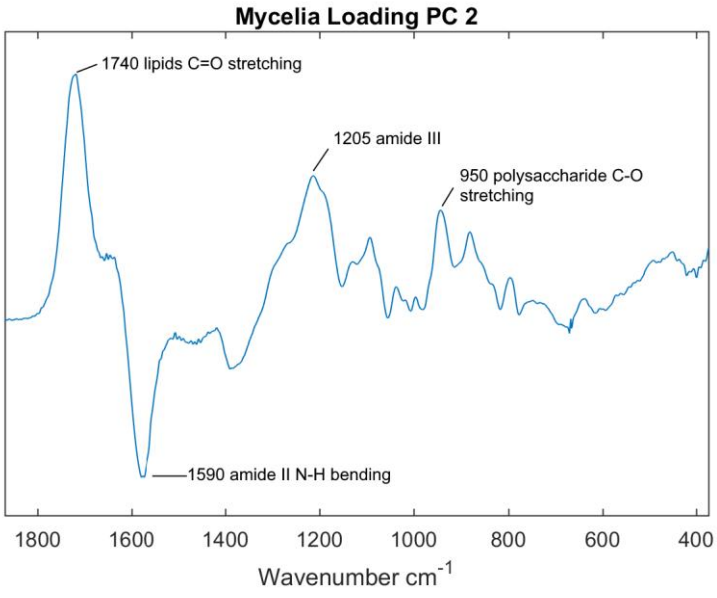
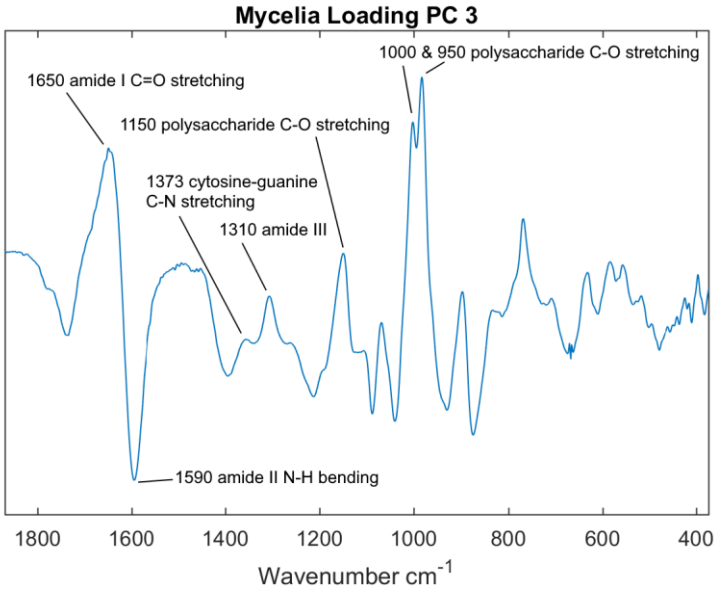


Figure 5: PCA scores plots of PC2 and PC3 from acquired FT-IR spectra of fungal mycelium homogenates cultured in synthetic grape juice medium with coding for fungal pathogen. *B. cinerea* (Bot); *A. carbonarius* (Asc); *A. niger (Asn);* and *P. expansum* (Pen).



(a)



(b)

Figure 6: PCA loadings plots of (a) PC2 and (b) PC3 from acquired FT-IR spectra of fungal mycelium homogenates cultured in synthetic grape juice medium.

6.1.2 Attenuated Total Reflectance Fourier Transform Infrared Spectroscopy (ATR FTIR) method development

A preliminary series of method development experiments enabled an increased level of sensitivity for the ATR FTIR using small quantities of grape berry extract concentrated *in-situ* on the ATR surface prior to spectral scanning (Appendix 5.2 - Supplementary Figure S1). A comparison of sample scans at room temperature (20 °C) and 60 °C revealed there was poor sensitivity for signal detection in the region from 375-2000 cm^{-1} at room temperature. This region of the spectra is important as C-C; C-O and C-N bond stretching, twisting and oscillation frequencies lead to important energy absorption patterns, which manifest in absorption spectra that correlate well with compositional data. A compromise between increasing analytical sensitivity and sample throughput was considered important. Hence, the final method incorporated a sample 'concentrating' time of 5 minutes at 60 °C on the ATR surface. Reproducibility of this method was determined using a single sample analysed 10 times with results considered appropriate for a pilot study (data not shown). Heated ATR-IR spectroscopy has been used for collection of wine spectra (Climaco-Pinto, et al. 2009) and the *in-situ* study of edible oil degradation (Pinto, et al. 2010), and is a simple and effective way to improve the sensitivity of the instrument. The mean IR spectra of samples from the berry infection trials (Figure 3) reveal a broad peak between 3000-3500 cm^{-1} which is consistent with O-H bond stretching typically related to moisture. The spectral region with the most interesting variation occurs between ~375 to 1850 cm^{-1} and this region was selected for data analysis.

6.1.3 Comparison of predictive model algorithms

Predictive models of berry pathogen using ATR FTIR spectra were developed using a range of approaches including latent variable methods; decision trees; aggregative nearest neighbour and support vector machines which collectively represent popular algorithms types for classification (Scott, et al. 2013). Receiver Operating Characteristic (ROC) curves, by definition, show true positive rate versus false positive rate (equivalently, sensitivity versus 1–specificity) for different thresholds of the various predictive models. When assessing various predictive models of class (berry pathogen) using independent test set data, i.e. samples that were not used to construct the predictive model but for which the class membership is known, overall model performance can be assessed and compared for the different classification approaches. The ROC curves (Figure 4) can also be used to find the threshold that maximizes the classification accuracy or to assess, in more broad terms, how the classifier performs in the regions of high sensitivity and high specificity. Confusion tables and confusion matrices for cross validation (CV) and the independent test sets (ITS) are presented in Appendix 5.1 -

Supplementary Table S1-S2 and Tables 3 and 4 respectively. Predictive model performance metrics including the proportion of true positive; false positive; false negative and true negative classification results, misclassification errors, precision, F1 value (an overall measure of model accuracy), and area under the ROC curve enable objective comparison of each model performance. A similar pattern of performance is evident for cross validation and test data sets for each predictive algorithm. Overall, best prediction for pathogen was achieved by the SVM models, followed by the random forest methods; with KNN and SIMCA models demonstrating overall lower performance for class prediction and higher misclassification errors.

Support vector models (SVM) demonstrated excellent class prediction for all pathogens and control samples. Therefore this approach should be explored further to determine the potential for use with large sample numbers and increased grape varieties. SVM are computationally intensive models but have outperformed other classification methods as evident by the lower misclassification errors (CV ~1%, ITS ~5%) and high area under curve (AUC) values from the ROC figures (CV: 0.98-1.00, ITS 0.83-1.00) and F1 values between 0.98-1.00. SVM methods are reported to provide excellent results for classification and prediction of chemical composition (Scott, et al. 2013,Wu, et al. 2008) in a wide range of applications. Interestingly SVM are well established methods in mathematics, image analysis and computing but are less popular in food chemistry (Brereton 2015). The ability for SVM to accommodate nonlinear data, which is frequently observed in biological systems, is a clear advantage for pattern recognition models. Such chemical data could be expected for primary microbial metabolites in infected grape berries in which transformation of substrate follows a logarithmic progression associated with population density.

Decision tree methods such as random forests models are promising methods with FT-IR spectra for prediction of pathogen class. In the present investigation bagged random forest models have performed with moderate levels of precision for classification of *Aspergillus carbonarius, A. niger* and control samples, with performance clearly diminishing for *B. cinerea* and *P. expansum* sample prediction. As ensemble random forest methods make use of a binary decision algorithm, additional information may be incorporated into models that include non-numerical data within the classifiers, for example, grape cultivar, growing region, and visual observations of vine and berry health. Such information could be used to improve predictive model performance, which may be particularly useful in detecting early stage infections. Fungal pathogens such as *Aspergillus* spp. and *P. expansum* are more likely to cause infections as secondary pathogens, or following berry damage and may be noticed in vineyards during bunch development, whereas *B. cinerea* is a necrotropic plant pathogen, frequently encountered within mature grape bunches and berry clusters where higher humidity levels promote more rapid growth (Steel, et al. 2013). Thus, incorporation of cultivar, maturity data, climatic

conditions and vineyard management approaches into the decision model would greatly assist the predictive model performance.

Table 3: Confusion table of class predictions for the independent test set samples. Sample abbreviations are as follows: *Aspergillus carbonarius* (Asc), *A. niger* (Asn), *Botrytis cinerea* (Bot), *Penicillium expansum* (Pen) and Control (Con). Predictive model abbreviations: Support Vector Model (SVM); Soft Independent Model of Class Analogy (SIMCA); K-Nearest Neighbour (KNN).

		Actual Class				
		Asc	Asn	Bot	Pen	Con
SVM	Predicted as Asc	6	0	0	0	0
	Predicted as Asn	2	7	0	0	0
	Predicted as Bot	0	0	8	2	0
	Predicted as Pen	0	0	0	5	0
	Predicted as Con	0	0	0	0	7
SIMCA	Predicted as Asc	6	3	0	0	0
	Predicted as Asn	2	7	4	1	1
	Predicted as Bot	0	0	8	2	4
	Predicted as Pen	0	0	6	6	0
	Predicted as Con	0	0	5	1	6
KNN	Predicted as Asc	5	0	0	0	0
	Predicted as Asn	2	7	1	0	0
	Predicted as Bot	1	0	5	4	2
	Predicted as Pen	0	0	0	2	1
	Predicted as Con	0	0	2	1	4
Random Forest	Predicted as Asc	5	0	0	0	0
	Predicted as Asn	3	7	0	0	0
	Predicted as Bot	1	0	8	3	5
	Predicted as Pen	0	0	0	4	0
	Predicted as Con	0	0	0	0	2

Table 4: Confusion matrix for prediction of the independent data set. Sample abbreviations are as follows: *Aspergillus carbonarius* (Asc), *A. niger* (Asn), *Botrytis cinerea* (Bot), *Penicillium expansum* (Pen) and Control (Con). Predictive model abbreviations: Support Vector Model (SVM); Soft Independent Model of Class Analogy (SIMCA); K-nearest Neighbour (KNN).

	Class	True Positive	False Positive	True Negative	False Negative	Misclassification error	Precision	Accuracy F1	Area Under Curve
SVM	Asc	0.75	0.00	1.00	0.25	0.05	1.00	0.86	0.970
	Asn	1.00	0.07	0.93	0.00	0.05	0.78	0.88	0.995
	Bot	1.00	0.07	0.93	0.00	0.05	0.80	0.89	0.996
	Pen	0.71	0.00	1.00	0.29	0.05	1.00	0.83	0.995
	Con	1.00	0.00	1.00	0.00	0.00	1.00	1.00	1.000
SIMCA	Asc	0.75	0.01	0.90	0.25	0.14	0.67	0.71	0.970
	Asn	1.00	0.27	0.73	0.00	0.22	0.47	0.64	0.962
	Bot	1.00	0.21	0.79	0.00	0.16	0.57	0.73	0.892
	Pen	0.86	0.20	0.80	0.14	0.19	0.50	0.63	0.957
	Con	0.86	0.20	0.80	0.14	0.19	0.50	0.63	0.933
KNN	Asc	0.63	0.00	1.00	0.38	0.08	1.00	0.77	0.875
	Asn	1.00	0.10	0.90	0.00	0.08	0.70	0.82	0.983
	Bot	0.63	0.24	0.76	0.38	0.27	0.42	0.50	0.808
	Pen	0.29	0.03	0.97	0.71	0.16	0.67	0.40	0.817
	Con	0.57	0.10	0.90	0.43	0.16	0.57	0.57	0.891
Random Forest	Asc	0.63	0.00	1.00	0.38	0.08	1.00	0.77	0.841
	Asn	1.00	0.10	0.90	0.00	0.08	0.70	0.82	0.986
	Bot	1.00	0.28	0.72	0.00	0.22	0.50	0.67	0.940
	Pen	0.57	0.00	1.00	0.43	0.08	1.00	0.73	0.995
	Con	0.29	0.00	1.00	0.71	0.14	1.00	0.44	0.931

6.1.4 Prediction of pathogen class

Random forest models performed well for classification of samples infected with *Aspergillus* to the species level, although imperfect prediction of class is noted. When predicted class was collapsed to the *Aspergillus* genus level, i.e. removal of species level information, the predictive model performance was improved with 100% true positive and true negative classification for random forest and SVM models (Table 4). The SIMCA approach also showed some improvement for genus level classification for *Aspergillus* but a decrease in predictive performance for true negative (false positive) prediction was evident. Overall SIMCA models have performed poorly for all pathogen classes.

Prediction of *Penicillium expansum* infected berries and discrimination from control samples was mixed. Overall model performance for prediction of *P. expansum* infected berries may have been impacted by the inclusion of the outlier samples previously identified by PCA of the FT-IR data, however, SVM and RF approaches were able to accommodate these and demonstrated the robustness of these approaches over the latent variable methods. The SIMCA and KNN models showed a decreased acuity for prediction of pathogen compared to the other models as indicated by higher misclassification errors, especially evident for prediction of *P. expansum.* Similar observations for class prediction were evident for *B. cinerea* infected berries for SIMCA and SVM models; with KNN models performing poorly.

Overall model prediction for pathogen class varied according to the model type. Generally, most models were capable of predicting pathogen class in the independent test samples with varying levels of misclassification error and accuracy. SVM models clearly outperformed other classification models followed by random forest methods and KNN; SIMCA models were the least reliable predictive models.

6.1.5 ATR FTIR of must homogenates containing up to 2 % infection

After the success observed with respect to the discrimination of fungal mycelia and infected berry homogenates, the ATR FTIR technique described above was applied to the analysis of must homogenates, acquired during the wine making process using bunches containing up to 2% by weight of infected bunches. Exploratory data analysis (Data not shown) of the 'fingerprint' region between 375 – 1850 cm^{-1} conducted *via* a principal components analysis was inconclusive and failed to demonstrate any clear discrimination between control and infected samples or between fungal species.

6.2 Volatile analysis of grape juices obtained from laboratory-inoculated berries and bunches

6.2.1 Validation of PLS-DA models of GC/MS data obtained from inoculated detached berry samples 2015 and inoculated bunch samples 2016 and 2017

PLS-DA models for each GC/MS data set were constructed with four latent variables (PC) which corresponded to eigenvalues greater than one for each PC. The explained variance for the calibration data was 74, 90 and 84%; the explained variance for pathogen class was 92, 75 and 86% for the detached berries 2015, the bunches 2016, and 2017 data sets, respectively (Appendix 5.1 - Supplementary Tables S3-5). Result of permutation testing for optimising orthogonal signal correction (OSC) for the 2016 bunch data set is presented in Appendix 5.1 - Supplementary Table S6. Model interpretation was not improved by using OSC and models for all data sets were subsequently developed without the use of signal correction. Validation of the PLS-DA models using permutation testing is presented in Appendix 5.2 - Supplementary Figures S6-8 for the detached berry, 2016 bunch and 2017 bunch trial respectively. AUROC and Q2 metrics for each sample class are presented for 1000 permutations of the data. Empirical P values derived from the permutation results and comparison with the true model outcomes for Q2 and AUROC support the assertion that all classes with the exception of *Aspergillus niger* in the 2016 bunch data set only, are reliably modelled. The GC/MS data for the individual experiments will be presented in the corresponding sections in the form of PLS-DA scores plots including 95 % confidence interval ellipses around the predicted classes (based on Hotelling T2 metrics). The scores plots from the PCAs of the individual experiments can be found in the supplementary data (Appendix 5.2 – Supplementary Figures S4 – S6). The comparison of results between the experiments will be addressed within the discussion section.

6.1.2 Inoculated detached Chardonnay berries

PLS-DA on the GC/MS grape juice data obtained from the inoculated detached berries is presented in Figure 7. The first two latent variables (PCs) explained 61 % of the variance. In this scores plot, sample classification according to pathogen was observed. *Botrytis cinerea* infected samples were separated from the other samples along PC1. *Aspergillus niger* and *A. carbonarius* infected samples were separated from the remaining samples along PC2. The control and *Penicillium expansum* infected samples could also be discriminated from the other samples along PC1 although the control samples appeared with the highest amount of variation within the class (see confidence interval ellipse). Along PC3 (8 %), *P. expansum* infected samples were discriminated from the remaining samples. The mass

ions (*m/z*) that provided the most discrimination for each class (85th percentile of selectivity ratios and VIPs >1) are tabulated in Appendix 5.1 – Supplementary Table S7 and the corresponding loadings plots are displayed in Appendix 5.2 – Supplementary Figures S7. Compounds attributed to these *m/z*, based on the identification procedure are tabulated in Table 5. *B. cinerea* infected samples were relatively highest in 1-octen-3-ol, and were the only fungal class in which 1,5-dimethylnaphthalene, 1,5-dimethyltetralin and 10 unknown sesquiterpenes were present, while *A. niger and A. carbonarius* were the only fungal classes where 2-(4-hexyl-2,5-dioxo-2,5dihydrofuran-3-yl)acetic acid was present. Control samples had significantly higher relative concentrations of three unknown compounds, as well as the aldehydes 3-hexenal, hexanal, (*E*)-2-hexenal, (*E,E*)-2,4-hexadienal, *p*-tolualdehyde and *β*-damascenone. The compounds separating *P. expansum* from the other samples along PC3 were *m*-cresol, 2-pentylfuran and *γ*-nonalactone. *A. niger* was discriminated from the remaining samples by relatively higher amounts of ethyl acetate and ethyl propionate.

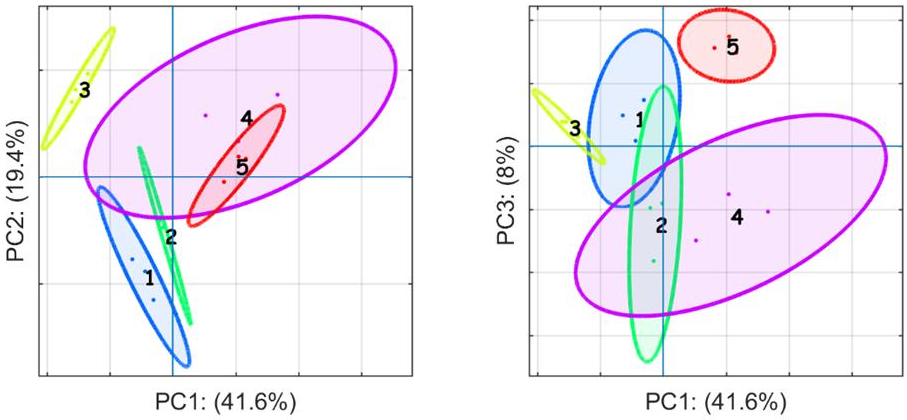


Figure 7: PLS-DA scores plots (PC1-3) of GC/MS grape juice data obtained from individual inoculated Chardonnay berries. Variance captured refers to the X-block of the data. Sample classes are denoted by 1: *A. carbonarius*, 2: *A. niger*, 3: *B. cinerea*, 4: Control, 5: *P. expansum*. Ellipses represent the 95 % confidence interval for each class, consisting of three replicates, based on Hotelling T^2 metrics.

Table 5: Compounds responsible for sample classification based on fungal pathogen for the grape juice samples obtained from individual inoculated Chardonnay berries, vintage 2015.

Compound	Level of ID[1]	RI cal[2]	RI lit[3]	Ref for RI lit[4]	Main m/z	Standardised peak areas[5]					Effect size (partial eta squared)
						Control	*B. cinerea*	*A. carbonarius*	*A. niger*	*P. expansum*	
Ethyl acetate	a	876	892	10	61	1^{a}	0^{a}	100^{a}	0^{a}	20^{a}	0.69
Ethyl propanoate	a	946	955	11	57	0^{a}	2^{a}	100^{b}	1^{a}	3^{a}	0.97
Unknown	b	1065	-	-	110	100^{c}	47^{a}	46^{a}	66^{ab}	71^{b}	0.99
Hexanal	a	1085	1089	2	56	100^{b}	0^{a}	0^{a}	6^{a}	3^{a}	0.98
Unknown	b	1114	-	-	109	100^{c}	50^{ab}	39^{a}	59^{b}	69^{b}	0.99
3-Hexenal	b	1151	1149	1	69	100^{c}	6^{ab}	1^{a}	15^{ab}	31^{b}	0.97
2-Pentyl furan	a	1245	1258	2	81	25^{a}	15^{a}	3^{a}	12^{a}	100^{b}	0.97
(*E*)-2-hexenal	a	1250	1248	3	55	100^{b}	2^{a}	0^{a}	14^{a}	5^{a}	0.99
(*E,E*)-2,4-Hexadienal	a	1432	1428	4	81	100^{b}	0^{a}	0^{a}	0^{a}	0^{a}	1.00
1-Octen-3-ol	a	1452	1466	6	57	3^{a}	100^{c}	18^{ab}	16^{ab}	33^{b}	0.99
Unknown sesquiterpene	b	1568	1455	7	145	0^{a}	100^{b}	0^{a}	0^{a}	0^{a}	0.95
p-Tolualdehyde	a	1667	1654	5	119	100^{a}	16^{a}	15^{a}	64^{a}	19^{a}	0.67
1,5-Dimethyl tetralin	a	1751	-	-	145	0^{a}	100^{b}	0^{a}	0^{a}	0^{a}	0.99
Unknown sesquiterpene	b	1763	-	-	119	0^{a}	100^{b}	0^{a}	0^{a}	0^{a}	0.96
ϐ-Damascenone	a	1831	1831	2	69	100^{b}	25^{a}	12^{a}	41^{a}	57^{ab}	0.93
Unknown	b	1837	-	-	115	100^{c}	45^{ab}	33^{a}	55^{b}	66^{b}	0.99
Phenylethyl alcohol	a	1915	1916	9	91	7^{a}	6^{a}	100^{b}	7^{a}	83^{b}	0.96

Unknown sesquiterpene	b	1928	-	-	143	0[a]	100[b]	0[a]	0[a]	0[a]	0.97
Unknown sesquiterpene	b	1933	-	-	202	0[a]	100[b]	0[a]	0[a]	0[a]	0.95
Unknown sesquiterpene	b	1970	-	-	200	0[a]	100[b]	0[a]	0[a]	0[a]	0.97
γ-Nonalactone	a	2046	2042	13	85	10[a]	9[a]	3[a]	3[a]	100[b]	0.97
Unknown sesquiterpene	b	2051	-	-	220	0[a]	100[b]	0[a]	0[a]	0[a]	0.98
1,5-Dimethyl naphthalene	a	2060	2048	8	156	0[a]	100[b]	0[a]	0[a]	0[a]	0.97
m-Cresol	a	2087	2088	12	108	4[a]	0[a]	0[a]	0[a]	100[b]	0.99
Unknown sesquiterpene	b	2100	-	-	118	0[a]	100[b]	0[a]	0[a]	0[a]	0.95
2-(4-hexyl-2,5-dioxo-2,5-dihydrofuran-3-yl)acetic acid	b	2119	-	-	126	0[a]	0[a]	28[ab]	100[b]	0[a]	0.77
Unknown sesquiterpene	b	2221	-	-	105	0[a]	100[b]	0[a]	0[a]	0[a]	0.97
Unknown sesquiterpene	b	2279	-	-	159	0[a]	100[b]	0[a]	0[a]	0[a]	0.97
Unknown sesquiterpene	b	2326	-	-	59	0[a]	100[b]	0[a]	0[a]	0[a]	0.97

[1] Level of identification: a) Metabolites were identified at level 1, by comparing their RI and EI-MS against authentic standards and the NIST2011 metabolite and Massfinder4 terpenoid database, b) Metabolites were identified at level 2, by comparing their RI and EI-MS against the above databases and peer-reviewed scientific literature.

[2] RI calculated based on alkane series (C8-C40), according to the equation of van den Dool and Kratz (section 2.3.1).

[3] RI reported in peer-reviewed scientific literature.

[4] Literature for RI: 1 (Serot, Prost, Visan, & Burcea, 2001), 2 (Welke, Manfroi, Zanus, Lazarotto, & Zini, 2012), 3 (Wang, Finn, & Qian, 2005), 4 (Wierda, Fletcher, Xu, & Dufour, 2006), 5 (Chung, Shing Yung, & Kim, 2001), 6 (Escudero, Cacho, & Ferreira, 2000), 7 (Tabanca, Demirci, Ozek, Kirimer, Baser, Bedir, et al., 2006), 8 (Chung, 1999), 9 (Ferreira, San Juan, Escudero, Culleré, Fernández-Zurbano, Saenz-Navajas, et al., 2009), 10 (Fan & Qian, 2006), 11 (Fang & Qian, 2005), 12 (López, Ferreira, Hernández, & Cacho, 1999), 13 (Miranda-Lopez, Libbey, Watson, & McDaniel, 1992). The bibliography can be found in the supplementary material (S.1.2 Reference list RI lit).

[5] MANOVA, Tukey HSD, and effect sizes were calculated based on the peak areas that were normalised to the internal standard peak areas. For visual ease in this table, these normalised peak areas have been further standardized to the maximum peak. The standardised areas of the compounds with the same superscript are not significantly different between samples, based on Tukey HSD.

6.2.3 Inoculated Chardonnay bunches from the 2016 vintage

PLS-DA of the GC/MS grape juice data obtained from the 10 % infected grape bunches in vintage 2016 resulted in scores plots depicted in Figure 8. The first two PCs explained 79.2 % of the variance. *Botrytis cinerea* infected and control samples are separated from the other samples and from each other along PC1 and PC2. Samples infected with *Penicillium expansum*, could be discriminated from *Aspergillus carbonarius* and *A. niger* samples along PC3 (5.4 %). The control samples were separated from the remaining along PC2. The *m/z* that provided the most discrimination for each class are tabulated in the supplementary data (Table S8) and the corresponding loadings plots are displayed in (Appendix 5.2 – Supplementary Figure S8. Compounds attributed to these *m/z* are tabulated in Table 6. *B. cinerea* infected samples were significantly higher in benzyl methyl ether, *γ*-eudesmol, benzaldehyde, 1,5-dimethylnaphthalene and several unknown sesquiterpenes), and were the only fungal class in which six sesquiterpenes were present. *A. niger* and *A. carbonarius* infected samples were highest in 2-(4-hexyl-2,5-dioxo-2,5dihydrofuran-3-yl)acetic acid, cadalene in addition to two unknown compounds (RI 1387 and 1545). Control samples were highest in methyl heptenone, 2-heptenal, (*E*)-2-hexenal, *o*-tolualdehyde and *p*-tolualdehyde. The compounds separating *P. expansum* infected samples from the other samples were 1-octen-3-ol, *m*-cresol, 2-pentylfuran and *γ*-nonalactone. Other compounds that were the highest in *P. expansum* infected samples were the ethyl esters ethyl decanoate, dodecanoate, hexadecanoate and linoleate and an unknown compound (RI 1501).

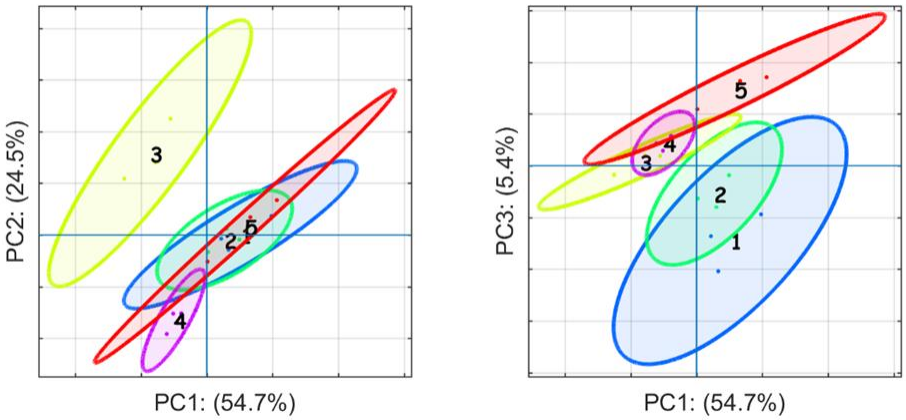


Figure 8: PLS-DA scores plots (PC1-3) of GC/MS grape juice data obtained from inoculated Chardonnay bunches, vintage 2016. Variance captured refers to the X-block of the data. Sample classes are denoted by 1: *A. carbonarius*, 2: *A. niger*, 3: *B. cinerea*, 4: Control, 5: *P. expansum*. Ellipses represent the 95 % confidence interval for each class, consisting of three replicates, based on Hotelling T^2 metrics.

Table 6: Compounds responsible for sample classification based on fungal pathogen for the grape juice samples obtained from inoculated Chardonnay bunches, vintage 2016.

Compound	Level of ID[1]	Accurate mass GC-Q-TOF	RI cal[2]	RI lit[3]	Ref for RI lit[4]	Main m/z	Standardised peak areas[5]					Effect size (partial eta squared)
							Control	*B. cinerea*	*A. carbonarius*	*A. niger*	*P. expansum*	
2-Pentyl furan	a	81.0339	1245	1258	13	81	25^{a}	37^{a}	34^{a}	20^{a}	100^{b}	0.98
(*E*)-2-Hexenal	a	55.0542	1250	1248	4	55	100^{c}	41^{a}	62^{ab}	68^{b}	58^{ab}	0.99
2-Heptenal	a	83.0489	1355	1342	3	83	100^{b}	50^{a}	44^{a}	36^{a}	28^{a}	0.94
6-Methyl-5-hepten-2-one	a	108.0932	1377	1367	2	108	100^{b}	77^{ab}	68^{a}	65^{a}	61^{a}	0.99
Unknown	b	137.0959	1387	-	-	137	72^{ab}	25^{a}	100^{b}	90^{ab}	66^{ab}	0.92
Benzyl methyl ether	a	91.0543	1419	1400	1	91	84^{a}	100^{b}	95^{ab}	97^{ab}	95^{ab}	1.00
1-Octen-3-ol	a	57.0338	1452	1466	7	57	20^{a}	51^{b}	27^{a}	25^{a}	100^{c}	1.00
Unknown	c	57.0336	1501	-	-	57	2^{a}	10^{a}	3^{a}	3^{a}	100^{b}	0.99
Unknown	b	192.1516	1545	-	-	192	57^{a}	75^{a}	100^{b}	76^{ab}	67^{a}	0.99
Benzaldehyde	a	106.0410	1549	1538	9	106	14^{a}	100^{b}	12^{a}	14^{a}	16^{a}	1.00
Unknown sesquiterpene	b	145.1017	1568	-	-	145	0^{a}	100^{b}	0^{a}	0^{a}	0^{a}	0.99
o-Tolualdehyde	a	120.0568	1638	1622	5	120	100^{b}	40^{a}	28^{a}	17^{a}	7^{a}	0.95
Ethyl decanoate	a	88.0519	1641	1635	10	88	8^{a}	7^{a}	63^{ab}	52^{ab}	100^{b}	0.82
p-Tolualdehyde	a	119.0497	1667	1654	6	119	100^{b}	40^{a}	29^{a}	20^{a}	8^{a}	0.95
Unknown sesquiterpene	b	185.1331	1733	-	-	185	12^{a}	100^{b}	0^{a}	0^{a}	0^{a}	0.99
Unknown sesquiterpene	b	119.0850	1763	-	-	119	0^{a}	100^{b}	0^{a}	0^{a}	0^{a}	0.96
Ethyl dodecanoate	a	88.0518	1845	1851	11	88	12^{a}	10^{a}	48^{ab}	33^{ab}	100^{b}	0.83
Unknown sesquiterpene	b	143.0855	1928	-	-	143	0^{a}	100^{b}	0^{a}	0^{a}	0^{a}	0.99
Unknown sesquiterpene	b	202.1715	1933	-	-	202	0^{a}	100^{b}	0^{a}	0^{a}	0^{a}	0.98

Unknown sesquiterpene	b	200.1557	1970	-	-	200	2[a]	100[b]	3[a]	4[a]	2[a]	1.00
γ-nonalactone	a	85.0286	2046	2042	14	85	4[a]	4[a]	6[a]	29[a]	100[b]	1.00
1,5-Dimethyl naphthalene	a	156.0941	2060	2048	8	156	2[a]	100[b]	2[a]	4[a]	2[a]	0.99
m-Cresol	a	108.0568	2087	2088	12	108	3[a]	2[a]	3[a]	3[a]	100[b]	0.99
2-(4-hexyl-2,5-dioxo-2,5-dihydrofuran-3-yl)acetic acid	b	126.0309	2119	-	-	126	1[a]	0[a]	100[c]	59[b]	1[a]	0.99
γ-Eudesmol	b	161.1201	2185	2195	16	161	21[a]	100[b]	22[a]	29[a]	31[a]	0.99
Unknown sesquiterpene	b	105.0697	2221	-	-	105	48[a]	100[b]	37[a]	50[a]	31[a]	0.99
Cadalene	b	183.1167	2252	2242	15	183	58[a]	47[a]	100[b]	73[ab]	64[a]	0.98
Ethyl hexadecanoate	a	88.0514	2254	2259	10	88	24[a]	39[a]	33[a]	21[a]	100[b]	0.93
Unknown sesquiterpene	b	159.1177	2279	-	-	159	17[a]	100[b]	17[a]	20[a]	13[a]	0.99
Unknown sesquiterpene	b	59.0485	2326	-	-	59	17[a]	100[b]	15[a]	20[a]	12[a]	0.98
Unknown	b	215.0885	>2500	-	-	215	0[a]	100[b]	0[a]	0[a]	0[a]	0.99
Ethyl linoleate	a	67.0530	>2500	2510	11	67	0[a]	10[a]	8[a]	3[a]	100[b]	0.80

[1] Level of identification: a) Metabolites were identified at level 1, by comparing their RI and EI-MS against authentic standards and the NIST2011 metabolite and Massfinder4 terpenoid database, b) Metabolites were identified at level 2, by comparing their RI and EI-MS against the above databases and peer-reviewed scientific literature.

[2] RI calculated based on alkane series (C8-C40), according to the equation of van den Dool and Kratz (section 2.3.1).

[3] RI reported in peer-reviewed scientific literature.

[4] Literature for RI: 1 (Whitfield, et al. 1981), 2 (Beauchêne, et al. 2000), 3 (Sérot, et al. 2002), 4 (Wang, et al. 2005), 5 (Steullet and Guerin 1994), 6 (Chung, et al. 2001), 7 (Escudero, et al. 2000), 8 (Chung 1999), 9 (Selli, et al. 2004), 10 (Selli, et al. 2006), 11 (Cantergiani, et al. 2001), 12 (López, et al. 1999), 13 (Welke,

et al. 2012), 14 (Miranda-Lopez, et al. 1992), 15 (Shiratsuchi, et al. 1994), 16 (Frizzo, et al. 2001). The bibliography can be found in the supplementary material (S.1.2 Reference list RI lit).

[5] MANOVA, Tukey HSD, and effect sizes were calculated based on the peak areas that were normalised to the internal standard peak areas. For visual ease in this table, these normalised peak areas have been further standardized to the maximum peak. The standardised areas of the compounds with the same superscript are not significantly different between samples, based on Tukey HSD.

6.2.4 Inoculated Chardonnay bunches from the 2017 vintage

PLS-DA of the GC/MS grape juice data obtained from the 10 % infected grape bunches in vintage 2017 resulted in scores plots depicted in Figure 9. The first two PCs explained 65.7 % of the variance. *Botrytis cinerea* infected samples were separated from the other samples along PC1. *Aspergillus carbonarius* infected samples were clearly separated from the other samples along PC2. Control samples, *A. niger* and *Penicillium expansum* infected samples clustered together along PC1 and PC2 and could barely be separated along PC3.The *m/z* that provided the most discrimination for each class are tabulated in the supplementary data (Appendix 5.1 – Supplementary Table S9) and the corresponding loadings plots are displayed in Appendix 5.2 – Supplementary Figures Figure S9. Compounds attributed to these *m/z* are tabulated in Appendix 5.1 – Supplementary Table S10. *B. cinerea* infected samples were highest in (*E*)-2-hexenal, *γ*-eudesmol, phenylethyl alcohol, benzaldehyde, ethyl hexadecanoate, 1,5-dimethyltetralin, 1,5-dimethylnaphthalene and some unknown sesquiterpenes and they were the only fungal class in which seven sesquiterpenes (RIs at 1763, 1928, 1933, 1970, 2221, 2326, >2500) were present (Appendix 5.1 – Supplementary Table S9). *A. carbonarius* and *A. niger* infected samples were highest in 2-(4-hexyl-2,5-dioxo-2,5dihydrofuran-3-yl)acetic acid, linalool oxide, benzyl alcohol and an unknown compound. *A. niger* infected samples were highest in 1-octen-3-ol and 2-nonen-1-ol while *A. carbonarius* infected samples were highest in phenylethyl acetate and styrene. Control samples were highest in 1-dodecanol and pentanoic acid, 2,2,4-trimethyl-3-carboxyisopropyl, isobutyl ester. The compounds separating *P. expansum* infected samples from the other samples were *m*-cresol, 2-pentylfuran, *γ*-nonalactone and ethyl linoleate.

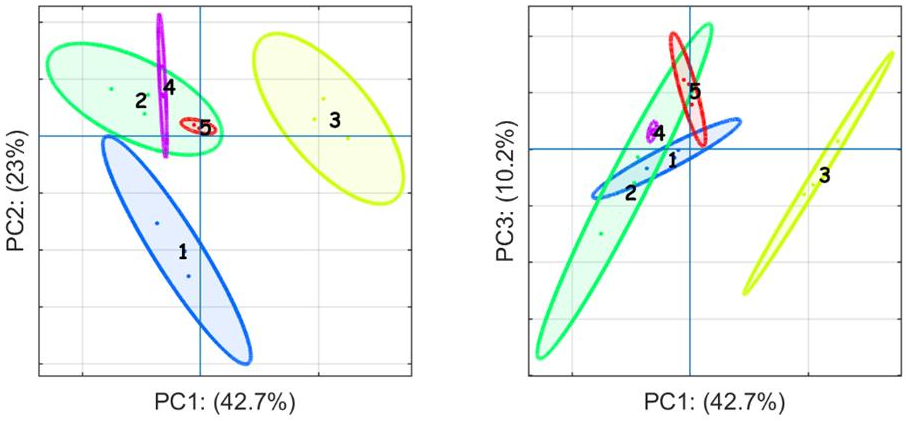


Figure 9: PLS-DA scores plots (PC1-3) of GC/MS grape juice data obtained from inoculated Chardonnay bunches, vintage 2017. Variance captured refers to the X-block of the data. Sample classes are denoted by 1: A. carbonarius, 2: A. niger, 3: B. cinerea, 4: Control, 5: P. expansum. Ellipses represent the 95 % confidence interval for each class, consisting of three replicates, based on Hotelling T^2 metrics.

6.2.5 Conclusions from volatile analysis of laboratory-inoculated bunches

In this study the impact of four grapevine fungal pathogens on the chemical composition of grape juices obtained from fully inoculated *V. vinifera* (cv Chardonnay) detached berries (vintage 2015) and obtained from 10 % inoculated bunches (vintage 2016 and 2017) were investigated. The cultivar Chardonnay was selected as it is the predominant white grape variety grown in Australia (Statistsics 2015) and is widely grown in many other countries (Harding and Robinson 2015).

An untargeted metabolomics approach for identification of volatile profiles from SPME-GC/MS data was undertaken in which the summed mass ion ratio (*m/z*) data matrices across the entire chromatograms were used for discriminant analysis. Such an approach has been reported before (Berna, et al. 2009) and is advantageous as the resulting data matrices are time independent and re-alignment of peaks, which is computationally intensive and requires close inspection of the data sets for selection of appropriate elution time windows, is not required (Schmidtke, et al. 2013). Furthermore, it allowed for rapid removal of *m/z* that were SPME fibre-related, thereby simplifying the downstream process of putative peak identification. Validated model performance for class discrimination was excellent for all data and class sets with the exception the *Aspergillus niger* class for the 2016 infected bunch data. Inspection of the PCs 1-3 for this model shows *A. niger* and *A. carbonarious* classes are largely superimposed (Figure 8), whereas these are more separate in the other models (Figures 7 and 9), and supports the observations that *A. niger* samples are easily misclassified as *A. carbonarious* within this data. Such misclassifications do not invalidate the overall results for the identification of compounds as potential biomarkers as data from the detached berries and the 2017 bunch data sets are reliably modelled. The poor performance of the 2016 bunch data set to accurately discriminate *A. niger* from *A. carbonarious* should also be viewed with consideration to the closer phylogenetic relationship of these two *Aspergillus* species compared to the *Botrytis* and *Penicillium* strains used in the investigation, and to the ability to differentiate from the un-inoculated control samples. Ion chromatograms were extracted from the correlated *m/z* triplets that were identified using the SR and VIP information from the validated PLS-DA models. The so identified peaks with potential discriminatory value were integrated and the resulting compounds and peak areas were further interrogated for information that enabled identification of sample class. The additional GCqToF measurements assisted in the identification of these compounds.

The analysis of grape juice samples revealed that a number of compounds were unique, or present at significantly different concentrations for each of the fungal pathogens investigated in all three data sets. This suggested that at levels of 10 % infection changes in chemical profiles of juices are detectable and might also be detectable by olfaction (not tested in the current study). Some differences between

vintages were apparent. For example, (*E*)-2-hexenal and *p*-tolualdehyde were detected in samples of the detached berry juices in vintage 2015 and the grape bunch juices in 2016. In contrast, (*E*)-2-hexenal and *p*-tolualdehyde levels were lower or not found at all in juice from grape bunches in 2017. Benzaldehyde and two unknown compounds (RI 1733 and >2500) were identified as possible indicator compounds for *B. cinerea* infected samples in both years of grape bunch inoculation (2016 and 2017), but levels did not discriminate *B. cinerea* infected samples from other infected samples in the detached berry juice samples. The concentration of benzaldehyde in grape juice and wine has been reported to be dependent on the variety, and in Chardonnay grapes it has been described as a characteristic volatile compound (González-Barreiro, et al. 2015). Benzaldehyde has further been reported as a metabolite produced by *B. cinerea* (Bailly, et al. 2006) and is known to be formed from benzyl alcohol (Delfini, et al. 1991). In the current study, benzaldehyde was detected in relatively low concentrations in grape juices of bunches infected with either *P. expansum*, *A. niger* or *A. carbonarius* when compared with the significantly higher concentrations in *B. cinerea* infected bunch samples. This suggested that benzaldehyde had potential as a marker metabolite for *B. cinerea* infected grape bunches across both vintages. However, as no significant differences were observed in the benzaldehyde content for the different fungal infections in the detached berry experiment, it was not considered a marker compound for this work.

P. expansum infected samples produced more 2-pentylfuran than samples infected with the other three pathogens investigated. A number of *Penicillium* species other than *P. expansum* have been reported to produce 2-pentylfuran (Jeleń and Wasowicz 1998). However, other fungi such as *Fusarium coeruleum* and *Phytophthora infestans* have also been reported to be 'disease specific producers' of 2-pentylfuran (Vikram, et al. 2004). As 2-pentylfuran was still detected in significant amounts in samples infected with pathogens other than *P. expansum* in the current study, it cannot be considered as a unique marker compound for *P. expansum* infected samples.

Only compounds that contributed to sample discrimination based on a specific infection fungus in all three experiments, and that were significantly different from the remaining sample classes will be considered as possible marker compounds and will be further discussed. The criteria for significant difference was an effect size of greater than 0.75, indicating a measure of strength of significance based on Eta-squared (where 0=low and 1=high). Possible marker compounds for *B. cinerea* infected samples included several sesquiterpenes (RI 1568, 1763, 1928, 1933, 1970, 2221, 2279, 2326) and 1,5-dimethylnaphthalene. Samples infected with *A. niger*, and in particular *A. carbonarius* consistently had higher amounts of 2-(4-hexyl-2,5-dioxo-2,5dihydrofuran-3-yl)acetic acid while for *P. expansum* infected samples the potential marker compounds were *m*-cresol and *γ*-nonalactone (Table 5 and 6, Figure 11).

The volatile *m*-cresol, found as marker compound for *P. expansum* inoculated samples in our investigations has previously been reported as an intermediate metabolite in the production of patulin. Patulin is a toxin produced by 13 *Penicillium* species including *P. expansum* and a limited number of *Aspergillus* species, namely *A. clavatus*, *A. giganteus and A. longivesica* (Puel, et al. 2010). Previously reported in wine, *m*-cresol is typically an indicator of oak contact, extracted from thermo-degraded lignin and microbial activity (Cerdán, et al. 2002,Loscos, et al. 2007). High levels of cresols in grapes have also been related to smoke pollution (Hayasaka, et al. 2010). *m*-Cresol in grapes has also been reported during berry raisining (Noguerol-Pato, et al. 2013). From our work it is clear that *P. expansum* infected samples had higher levels of *m*-cresol with a negligible amount being produced in the samples infected with the other fungi.

γ-Nonalactone has previously been reported as an active aroma compound in young wines, and as a contributor to prune aroma in aged wines, with concentrations dependent on grape variety, yeast strain and vintage (Ferreira, et al. 2000,Hernández-Orte, et al. 2008,Pons, et al. 2008). *γ*-Nonalactone is not commonly reported in grapes or grape must but rather after fermentation where it is produced by the yeast (Loscos, et al. 2007). In the current study, *γ*-nonalactone was detected in grape juices infected with different fungal pathogens, with its concentration being significantly higher in *P. expansum* inoculated samples compared to all other treatments. This result suggests that *γ*-nonalactone might be produced through fungal metabolic action in the grapes, and that it might be an indicator for fungal bunch rot infection, in particular *P. expansum* infections.

2-(4-Hexyl-2,5-dioxo-2,5dihydrofuran-3-yl)acetic acid (or 2-carboxymethyl-3-hexylmaleic acid anhydride) has been isolated from *A. niger* strain cultures a number of times (Almassi, et al. 1994,Weidenmüller, et al. 1972). It has been reported as a metabolite in the biotransformation of *β*-ionone, an intermediate in the degradation of carotenoids (Larroche, et al. 1995). Although 2-(4-hexyl-2,5-dioxo-2,5dihydrofuran-3-yl)acetic acid has been previously reported in wine, its identity has not been validated and the nature of its origin has not been discussed (García-Carpintero, et al. 2011). In the current study 2-(4-hexyl-2,5-dioxo-2,5dihydrofuran-3-yl)acetic acid was detected in samples infected with *A. ni*ger and *A. carbonarius* and its identification was based at level 2 (see Table 5). As this compound was not available commercially and the synthesis was not straight forward, further experiments are required in order to confirm its identity. 2-(4-hexyl-2,5-dioxo-2,5dihydrofuran-3-yl)acetic acid was barely detectable in the control and other inoculated samples and so appears to have a promising potential as marker compound for *A. ni*ger and *A. carbonarius* inoculated samples.

Dimethylnaphthalene compounds have been described in the scientific literature as possessing petroleum-like aroma, and they are generally derived from beta-carotene break down products

(Baldock and Hayasaka 2004,LaRoe and Shipley 1970). In the current study, 1,5-dimethylnaphthalene was almost exclusively found in samples inoculated with *B. cinerea*. The hydrocarbon structure of 1,5-dimethylnaphthalene suggests that this compound may have been produced by the breakdown of grape carotenoids, due to the enzymatic effects of *B. cinerea* infection.

Sesquiterpenes (C_{15}) can be found in grapes themselves (predominantly in the epicuticular wax layer of the skin) and are believed to contribute to plant defence or resistance mechanisms against pathogens such as fungi (Schwab and Wüst 2015). Comparison of the sesquiterpenes that were possible marker compounds for *B. cinerea* to available RI and mass spectral data of grape-derived sesquiterpenes (Petronilho, et al. 2014) was performed. However, no identification of the specific sesquiterpene structure could be made, which may indicate that *B. cinerea* might induce production of sesquiterpene by grapes as a specific defence against infection. It is also possible that the fungus may produce these sesquiterpenes de novo, potentially to contribute to increased virulence and toxicity (Fehlhaber, et al. 1974). One group of sesquiterpenes, namely (+)-4-epieremophil-9-en-11-ols, was recently isolated from *B. cinerea* strains and found to be involved in the conidiation process (Pinedo, et al. 2016). The sesquiterpenes found in the current study with *m/z* 145, 143, 200 and 159 (RI 1568, 1928, 1970 and 2279) appear to have eremophilane scaffolds of the molecular formulas $C_{15}H_{22}$, $C_{15}H_{20}$ or $C_{15}H_{22}O$. These structures also show similarities with *β*-vatirenene and amorpha-2,4,7(11)-triene when comparing the mass spectra with the NIST and Massfinder spectral databases. Three (+)-4-epieremophil-9-en-11-ols, namely (+)-4-epieremophil-9-en-2α,11-diol, (+)-4-epieremophil-9-ene-1α,2α,11-triol, (+)-4-epieremophil-9-en-2α,8β,11-triol, were isolated and purified by the University of Cádiz, Spain and kindly provided to our group. The compounds were analysed using a cool liquid-injection GC/MS method but were not consistent (identical *m/z* and RI) with the marker compounds from the *B. cinerea* infected samples, detected using the current SPME-GC/MS method. However, when a hot injection GC/MS method (as used in the current study) was used, the isolated sesquiterpene compounds generated several breakdown products that were in agreement with the marker compounds in this study (RI 1568, 1928, 1970, 2279, Appendix 5.3 - Supplementary Figures S10, S11, S12 and S13, respectively). This suggests that the four *B. cinerea* marker compounds may be breakdown products, as induced by hot injection GC analysis, of (+)-4-epieremophil-9-en-11-ol type compounds. However, further work is required to confirm their identity, possibly including different extraction methodologies and analysis techniques, which was beyond the scope of the current study. Further collaboration with the research group of the University of Cádiz is intended.

One limitation of this study is that it is common that different types of bunch rots appear simultaneously in the vineyard. The impact of significant amounts of multiple infections on the

proposed marker compounds is the logical next phase of fungal chemical marker investigations. This is important as some compounds, such as *γ*-nonalactone or 2-pentylfuran have been reported to be produced by different yeast or fungal organisms (Jeleń and Wasowicz 1998,Loscos, et al. 2007), and may even be present in healthy fruit in significant amounts, as shown in the current study. Therefore, the use of such compounds as markers requires further investigation. The applicability of these identified marker compounds for field infected grape samples and grapes from different regions, as well as varieties also requires further validation.

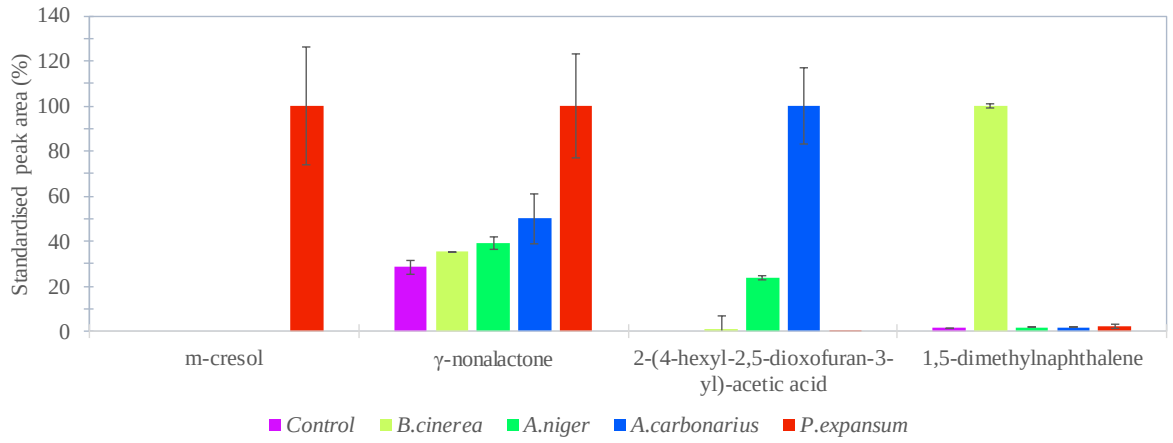


Figure 11: Bar plot of marker compounds of the whole bunch juices from inoculated bunches 2017. Peak areas were normalised to the highest peak area of a compound across all. Error bars represent the standard deviations between triplicate samples.

6.2.6 Sensory difference testing

To determine the effect of the fungal inoculations on the juice, difference testing was performed to compare the inoculated samples against the control using triangle tests. Participants were able to perceive the difference between the control and all 4 inoculation treatments with a high degree of certainty ($P<0.01$ - $P<0.001$). Panellists noted that earthy, mouldy and musty characters were common descriptors used to describe the infected juice samples. All juice treatments also had diminished fruit characters, irrespective of the bunch rot type. However there were some differences noted, with Botrytis samples appearing to have the most obvious earthy character while juice from grapes affected with *Penicillium* had noticeable herbal vegetal, tomato-leaf characters.

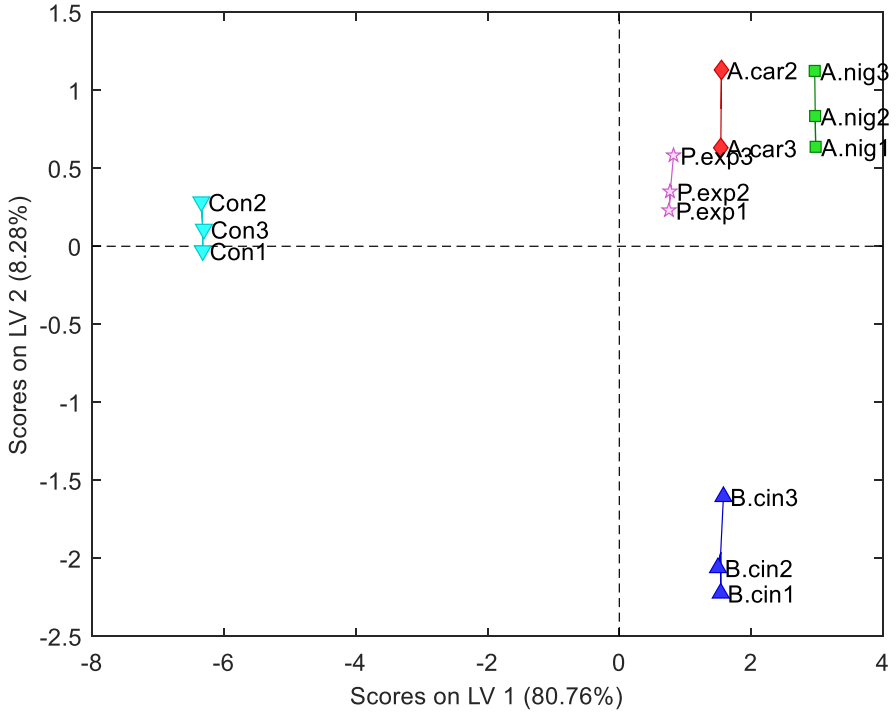
6.3 Volatile analysis of wines made from laboratory-inoculated grapes

6.3.1 Wines from inoculated bunches 2016 and 2017

The laboratory inoculated grape bunches infected with the four fungal pathogens investigated were vinified and the wine analysed by GC/MS using the same methodology as that described above for the analysis of the unfermented grape juices. PLS-DA scores and loadings plots for the data for the 2016 and 2017 trials are presented in Figures 12 and 13 and the corresponding compounds responsible for classification based on pathogen are listed in Tables 8 and 9 respectively.

For the 2016 vintage samples, LV1 captured 80.76% of variance and an immediate loss of variance is captured from LV2 onwards (only 8.28% and less) (Figure 12a). The most discriminated sample in this PLS-DA model was the control, which was shifted to the negative side of LV1. *B. cinerea* samples appeared separate from the remaining samples along LV2 (Figure 12b). Only a small number of compounds were found to discriminate pathogen classes, however, they were mostly not significant (see Table 8). The only significant discriminating compounds were an unknown which was relatively higher in *B. cinerea* samples (RI1330), 2-(4-hexyl-2,5-dioxo-2,5-dihydrofuran-3-yl)acetic acid, which was significantly highest in *A. carbonarius* samples and the two compounds ethyl cinnamate and an unknown (RI 1286) highest in *P. expansum* infected samples. The discriminating compounds that were found in the unfermented grape juices may have been lost during the winemaking process.

Figure 12a: PLS-DA scores and loadings plots of GC/MS wine data obtained from inoculated Chardonnay bunches, vintage 2016. Sample classes are denoted by diamonds*: A. carbonarius*, squares: *A. niger*, triangles: *B. cinerea*, upside down triangles: Control, stars: *P. expansum*.



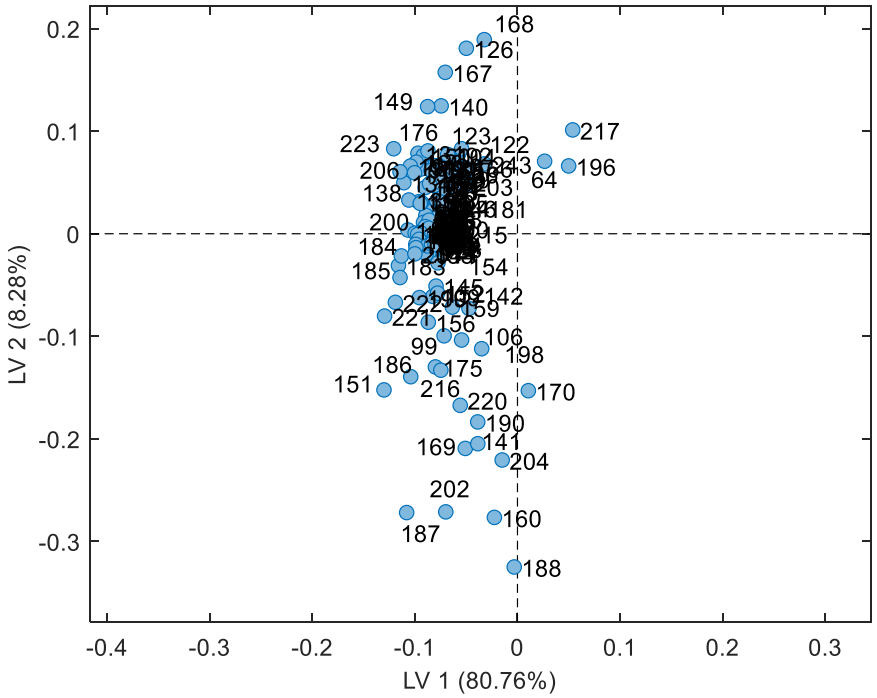


Figure 12b

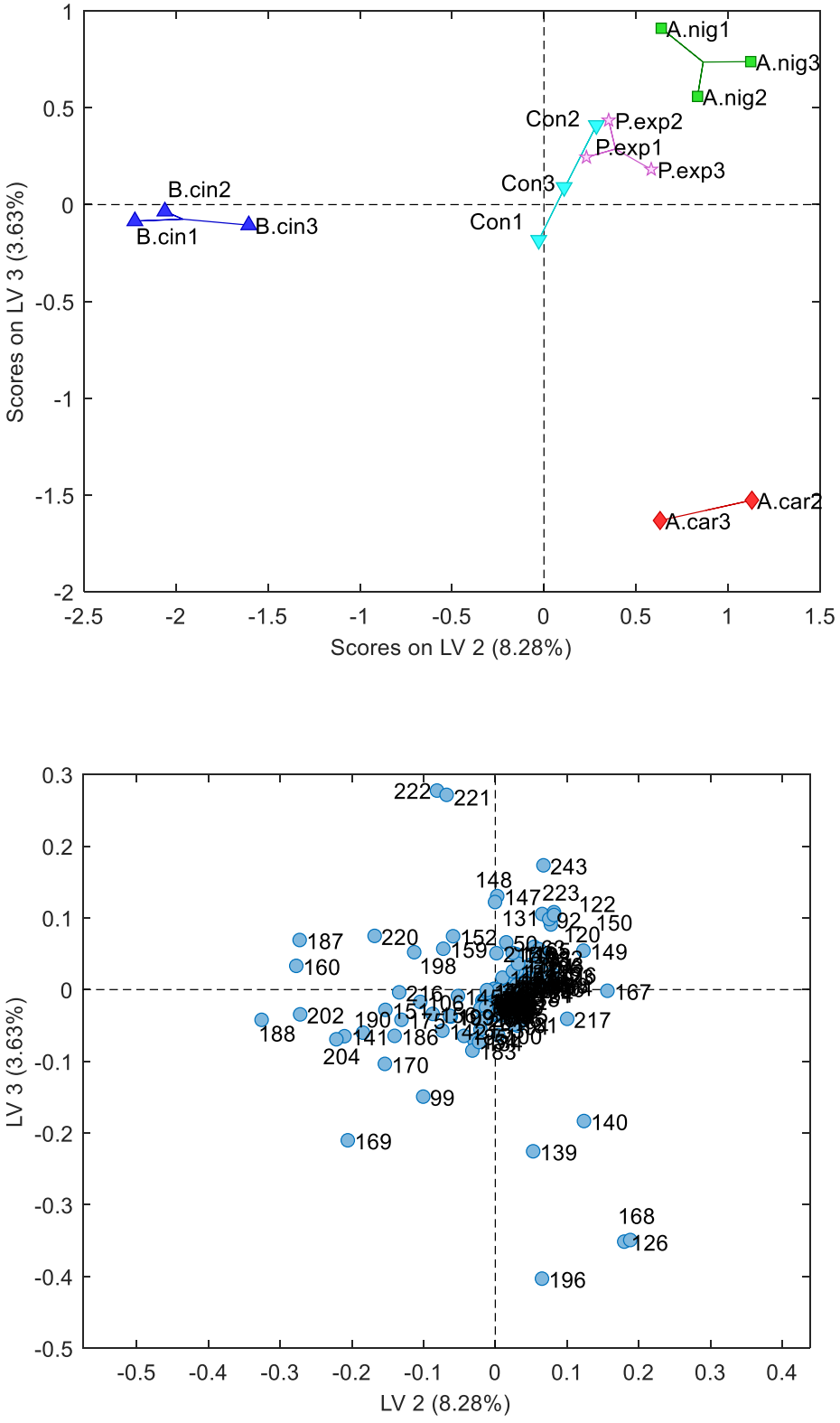
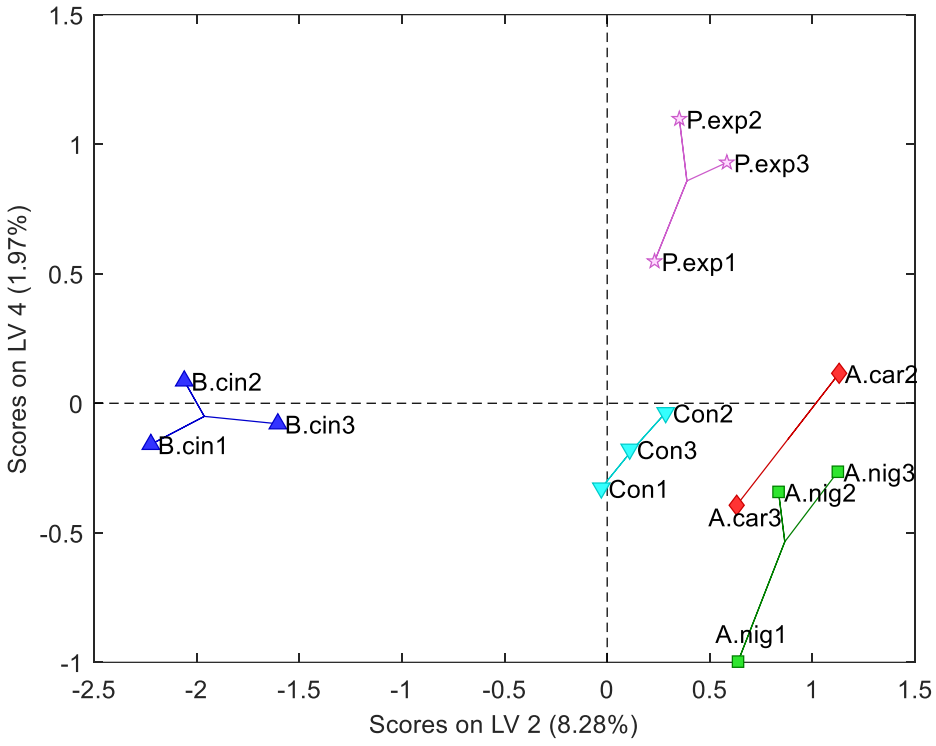

A.nig1
A.nig3
A.nig2
Con2
P.exp2
P.exp1
P.exp3
Con3
Con1
B.cin2
B.cin3
B.cin1
A.car2
A.car3
Scores on LV 3 (3.63%)
Scores on LV 2 (8.28%)
LV 3 (3.63%)
LV 2 (8.28%)

Figure 12b continued



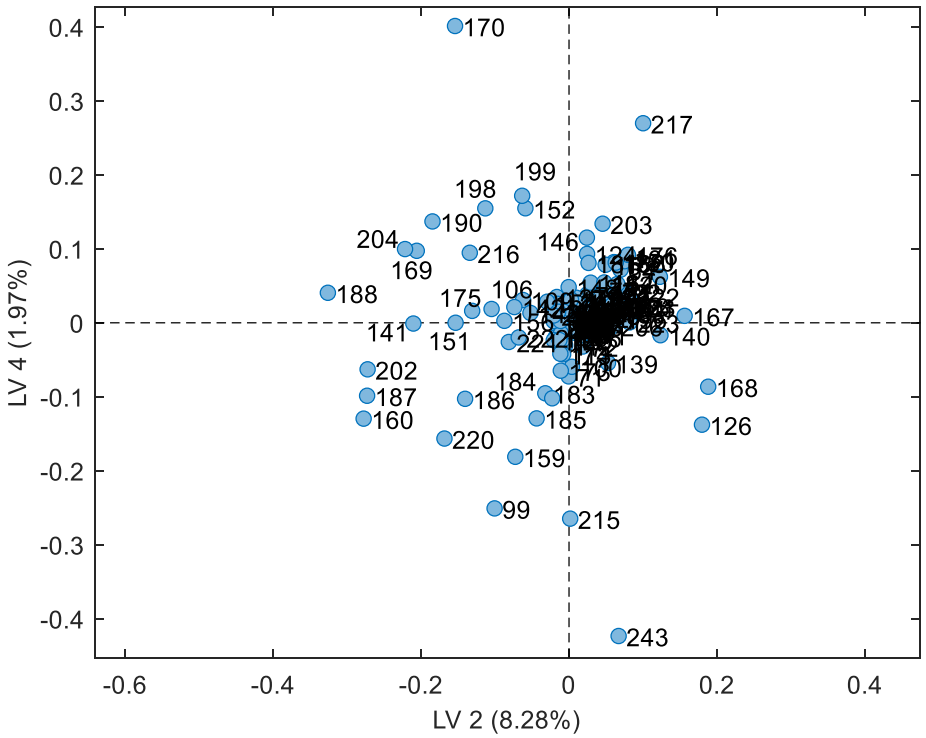


Table 8: Compounds responsible for sample classification based on fungal pathogen for the wine samples obtained from inoculated Chardonnay bunches, vintage 2016 (10% INFECTION). Data handling and processing was carried out as described previously for grape juice analysis.

Compound	Level of ID[1]	RI cal[2]	RI lit[3]	Ref for RI Lit[4]	Main m/z	Standardised peak areas[5]				
						Control	*B. cinerea*	*A. carbonarius*	*A. niger*	*P. expansum*
Unknown	-	1286	-	-	104	28^{a}	28^{a}	33^{a}	36^{a}	$\mathbf{92^{b}}$
Unknown	-	1305	-	-	119	0^{a}	57^{a}	0^{a}	0^{a}	0^{a}
Unknown	-	1330	-	-	119	0^{a}	$\mathbf{63^{b}}$	0^{a}	0^{a}	0^{a}
Unknown	-	1742	-	-	151	3^{a}	54^{a}	4^{a}	4^{a}	4^{a}
Unknown	-	1756	-	-	157	54^{a}	76^{b}	96^{c}	$84^{b,c}$	78^{b}
Unknown	-	2091	-	-	151, 109	2^{a}	56^{a}	12^{a}	1^{a}	5^{a}
Unknown	-	2097	-	-	151, 109	2^{a}	56^{a}	11^{a}	1^{a}	5^{a}
2-(4-hexyl-2,5-dioxo-2,5-dihydrofuran-3-yl)acetic acid	b	2119	-	-	126	0^{a}	0^{a}	$\mathbf{94^{c}}$	15^{b}	0^{a}
Ethyl cinnamate	a	2150	1	2112	131	6^{a}	14^{a}	48^{b}	41^{b}	$\mathbf{87^{c}}$

[1] Level of identification: a) Metabolites were identified at level 1, by comparing their RI and EI-MS against authentic standards and the NIST2011 metabolite and Massfinder4 terpenoid database, b) Metabolites were identified at level 2, by comparing their RI and EI-MS against the above databases and peer-reviewed scientific literature.

[2] RI calculated based on alkane series (C8-C40), according to the equation of van den Dool and Kratz (section 2.3.1 in main manuscript).

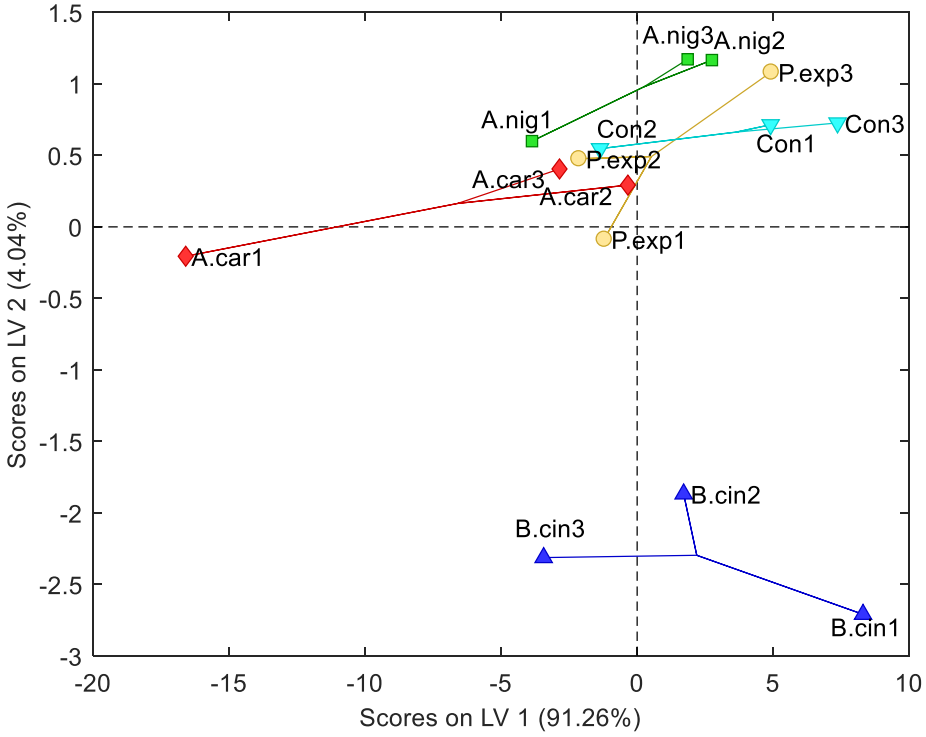
[3] RI reported in peer-reviewed scientific literature.

[4] Literature for RI: 1 (Pino, J.A.; Marbot, R., Volatile flavour constituents of acerola (Malpighia emarginata DC.) fruit, J. Agric. Food Chem., 2001, 49, 12, 5880-5882).

[5] MANOVA and Tukey HSD was calculated based on the peak areas that were normalised to the internal standard peak areas. For visual ease in this table, these normalised peak areas have been further standardized to the maximum peak. The standardised areas of the compounds with the same superscript are not significantly different between samples, based on Tukey HSD.

Figure 13a illustrates that LV1 captured 91.26% of variance and an immediate loss of variance is captured from LV2 onwards (only 4.04% and less) (Figure 13b) for the 2017 vintage samples. The most discriminated sample in this PLS-DA model is the *B. cinerea*, which is shifted to the negative side of LV2. Only a small number of compounds were found to discriminate *B. cinerea* from the remaining samples (see Table 9). The only significantly discriminating compounds were three unknowns which was relatively higher in *B. cinerea* samples (RI 1764, 1930 and 1935) and again, in agreement to the previous vintage, 2-(4-hexyl-2,5-dioxo-2,5-dihydrofuran-3-yl)acetic acid, which was significantly highest in *A. carbonarius* samples. The majority of the discriminating compounds that were found in the unfermented grape juices may have been lost during the fermentation and winemaking process.

Figure 13a: PLS-DA scores and loadings plots of GC/MS wine data obtained from inoculated Chardonnay bunches, vintage 2017. Variance captured refers to the X-block of the data. Sample classes are denoted by diamonds: *A. carbonarius*, squares: *A. niger*, triangles: *B. cinerea*, upside down triangles: Control, stars: *P. expansum*.



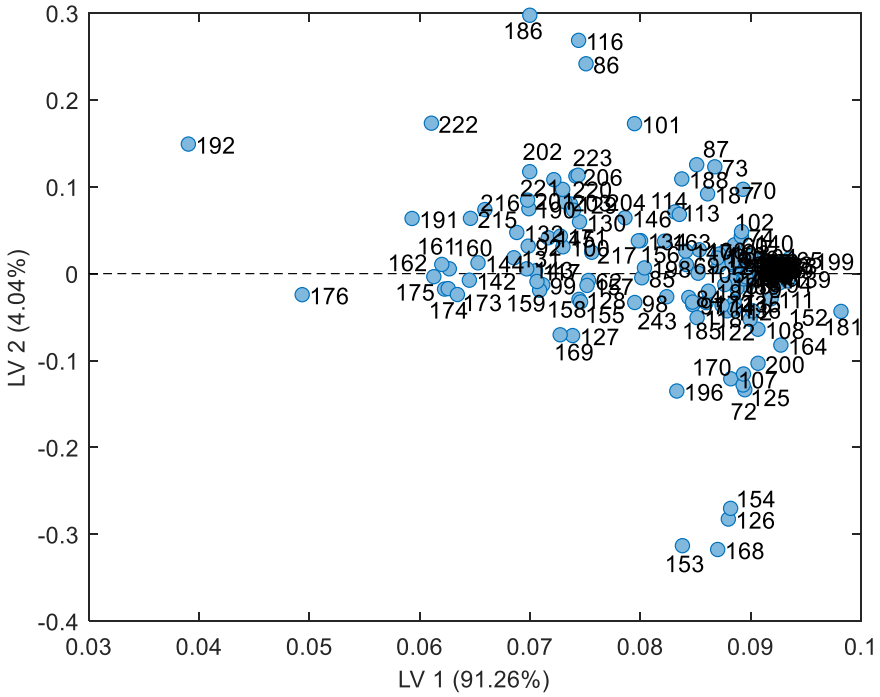
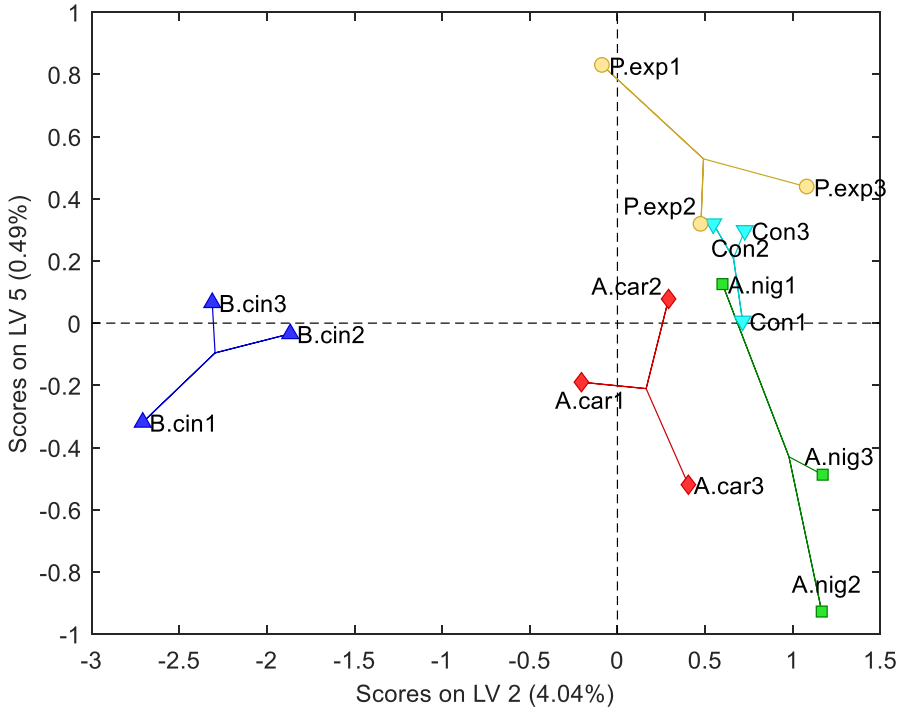

LV 2 (4.04%)
LV 1 (91.26%)
0.3
0.2
0.1
0
-0.1
-0.2
-0.3
-0.4
0.03
0.04
0.05
0.06
0.07
0.08
0.09
0.1
186
116
86
222
101
192
202
223
87
73
206
188
187
70
221
220
216
215
191
130
146
113
102
161
160
162
217
176
175
142
174
173
159
158
155
243
185
122
108
164
127
169
170
200
107
196
125
72
154
126
153
168

Figure 13b


Scores on LV 5 (0.49%)
Scores on LV 2 (4.04%)
1
0.8
0.6
0.4
0.2
0
-0.2
-0.4
-0.6
-0.8
-1
-3
-2.5
-2
-1.5
-1
-0.5
0
0.5
1
1.5
P.exp1
P.exp3
P.exp2
Con3
Con2
A.car2
A.nig1
Con1
B.cin3
B.cin2
B.cin1
A.car1
A.nig3
A.car3
A.nig2

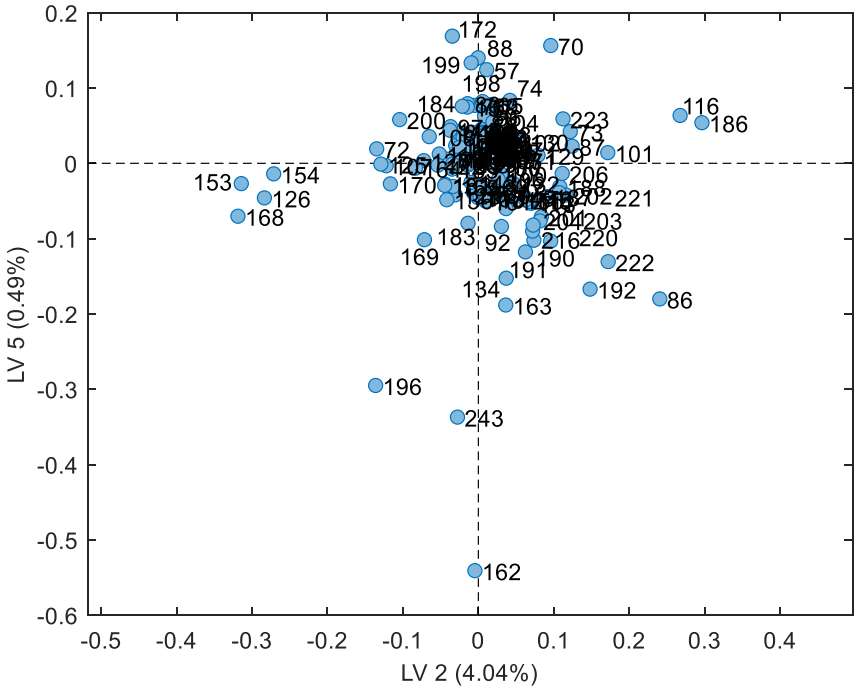

LV 5 (0.49%)
LV 2 (4.04%)
0.2
0.1
0
-0.1
-0.2
-0.3
-0.4
-0.5
-0.6
-0.5
-0.4
-0.3
-0.2
-0.1
0
0.1
0.2
0.3
0.4
172
88
70
199
57
198
74
184
116
186
200
223
73
72
101
153
154
126
168
206
221
170
203
183
92
216
220
169
190
222
191
134
192
86
163
196
243
162

Table 9: Compounds responsible for sample classification based on fungal pathogen for the wine samples obtained from inoculated Chardonnay bunches, vintage 2017 (10% INFECTION). Data handling and processing was carried out as described previously for grape juice analysis.

Compound	Level of ID[1]	RI cal[2]	RI lit[3]	Ref for RI Lit[4]	Main m/z	Standardised peak areas[5]				
						Control	*B. cinerea*	*A. carbonarius*	*A. niger*	*P. expansum*
Isoamyl acetate	b	1128	1131	1	70	100^{b}	49^{a}	$62^{a,b}$	57^{a}	$70^{a,b}$
Ethyl hexanoate	b	1269	1270	2	88	100^{b}	$81^{a,b}$	$73^{a,b}$	62^{a}	$90^{a,b}$
Unknown	-	1764	-	-	119	0^{a}	**100^{b}**	0^{a}	0^{a}	0^{a}
Unknown	-	1930	-	-	143	0^{a}	**100^{a}**	0^{a}	0^{a}	0^{a}
Unknown	-	1935	-	-	202	0^{a}	**100^{b}**	0^{a}	0^{a}	0^{a}
2-(4-hexyl-2,5-dioxo-2,5-dihydrofuran-3-yl)acetic acid	b	2119	-	-	126	0^{a}	0^{a}	**100^{b}**	7^{a}	0^{a}

[1] Level of identification: a) Metabolites were identified at level 1, by comparing their RI and EI-MS against authentic standards and the NIST2011 metabolite and Massfinder4 terpenoid database, b) Metabolites were identified at level 2, by comparing their RI and EI-MS against the above databases and peer-reviewed scientific literature.

[2] RI calculated based on alkane series (C8-C40), according to the equation of van den Dool and Kratz (section 2.3.1 in main manuscript).

[3] RI reported in peer-reviewed scientific literature.

[4] Literature for RI: 1 (Castello, G.; Vezzani, S.; Gerbino, T., Gas chromatographic separation and automatic identification of complex mixtures of organic solvents in indrustrial wates, J. Chromatogr., 1991, 585, 2, 273-280); 2 (Culleré, L.; Escudero, A.; Cacho, J.; Ferreira, V., Gas chromatography-olfactometry and chemical quantitative study of the aroma of six premium auality Spanish aged red wines, J. Agric. Food Chem., 2004, 52, 6, 1653-1660).

[5] MANOVA and Tukey HSD were calculated based on the peak areas that were normalised to the internal standard peak areas. For visual ease in this table, these normalised peak areas have been further standardized to the maximum peak. The standardised areas of the compounds with the same superscript are not significantly different between samples, based on Tukey HSD.

For both years (2016 and 2017) of the trial the classification of wine samples based on pathogen was not as obvious as for the grape juice data prior to fermentation. Based on the GC/MS volatile profiles it was not straight forward to discriminate the wines, less compounds significantly differed between treatments (see Table 8 and 9), suggesting that some of the compounds identified in the grapes had not survived the fermentation process.

Wine made from grapes inoculated with *B. cinerea* were most easily discriminated based on a few unknown compounds while wine made from *A. carbonarius* inoculated grapes was discriminated based on 2-(4-hexyl-2,5-dioxo-2,5-dihydrofuran-3-yl)acetic acid. It seems that these compounds survive the winemaking process. Further investigation is required to determine the chemical identities of the above compounds and their sensory properties and importance to grape and wine flavour and quality from bunch rot affected fruit.

6.3.2 Use of fining agents to ameliorate wine faults

The wines made from the laboratory inoculated grapes in 2016 and 2017 were treated with fining agents to assess their ability to remove the fungal-induced sensory impacts on the wines. For wine made with grapes infected with any of the fungal pathogens investigated in this project, the additions of carbon (300 and 500 ppm) caused the treatments to be perceived (aroma) as significantly different to the un-fined wine ($p < 0.05$). PVPP (dosed at 1000 ppm & 500 ppm) only had an effect at the higher dosage rate. The exception was those wines made from grapes affected with *A. niger*, wherein no effect was perceived. Isinglass (dosed at 50 and 20 ppm) had no perceived effect.

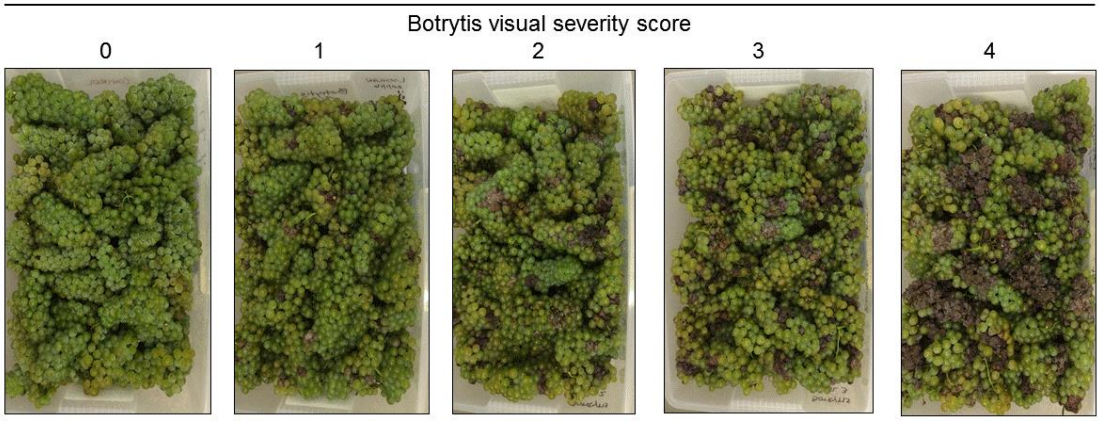
6.4 Thresholds for Botrytis grey mould contamination of wine grapes

6.4.1 Ergosterol as an estimate of fungal biomass

Ergosterol, a sterol present in fungal membranes (Mercer 1984) was used as an indicator of fungal biomass in bunch rot affected grapes. To establish this assay, the ergosterol content of fungal mycelium was determined in the absence of host plant material. Three isolates of *B. cinerea* were grown in culture and the mycelium freeze-dried. The average ergosterol content was 3.6mg per g dry weight of fungus. From this data a biomass conversion factor (BCF) of 0.3 was calculated. This allowed the dry weight of fungal mycelium present in a batch of grapes to be calculated. The ergosterol content of the two Aspergillus and one Penicillium isolate examined ranged from 2.92 to 7.75 mg of ergosterol per g dry weight of fungus. The ergosterol content of the fungal isolates examined in this study was similar to that reported by other authors, (Porep, et al. 2014).

6.4.2 Botrytis-affected grapes harvested in 2016 from the Hunter Valley

The ergosterol concentration in the homogenised must samples from Hunter Valley grape samples collected in 2016 with the five severities of grey mould infection was quantified by HPLC. In the visually uninfected fruit, (i.e. severity level score 0), a concentration of 0.17 mg/kg ergosterol was detected. As to be expected, the concentration of ergosterol increased with increasing visual severity levels of infection from 0.83, 2.57, 4.44 and 12.62 mg/kg for severity levels 1, 2, 3 and 4 respectively. This equated to fungal biomass values of 0.07, 0.34, 1.05, 1.82 and 5.16 g dry weight of fungus per kg wet weight of grapes for each of the five severity levels from 0 to 5 respectively. The ergosterol content of the musts and fungal biomass of each of the five batches of grapes with different levels of Botrytis severity are depicted in figure 14.



Ergosterol (mg) / kg wet wt. grapes				
0.17	0.83	2.57	4.44	12.62
Fungal biomass in g dry wt. / kg wet wt. grapes				
0.07	0.34	1.05	1.82	5.16

Figure 14: Ergosterol concentration and fungal biomass in the five batches with different severities of Botrytis infection based on a visual assessment.

6.4.3 Musts, juices and wines: glycerol, gluconic acid and acetic acid contents

Konelab analysis of musts, juices and wines showed increasing concentrations of a number of compounds with increasing levels of infection (Table 10). Glycerol and gluconic acid increased with increased levels of infection in all three sample matrices. Acetic acid was only detectable in wines, and it also increased with increasing levels of infection. Gluconic acid concentration, in both must and juice samples, increased significantly (based on ANOVA followed by Tukey HSD test) only in the fruit with a severity score of 2, i.e. an ergosterol content of 2.57 mg/kg. In wines gluconic acid only significantly increased at severity level 3, i.e. an ergosterol content of 4.44 mg/kg. Glycerol appeared slightly variable in musts only increasing slightly at levels at the highest level of infection, i.e. at ergosterol levels of 12.62 mg/kg. Acetic acid concentrations showed a significant increase in wines from severity level 2. In agreement with the ergosterol content of musts, being significantly increased at level 2, 3, and 4, gluconic acid concentrations in must or juice, glycerol concentrations in juice and acetic concentrations in wines might be used as an estimate for spoilage.

Table 10: Concentration of glycerol, gluconic acid and acetic acid in must, juice and wine obtained from Konelab analysis. Concentrations of compounds are contrasted to the ergosterol concentration of the samples original must. Samples with different letters are significantly different ($p < 0.05$) using MANOVA followed by a Tukey HSD test.

	Compound	Concentration (standard deviation)				
		E0.17[1]	**E0.83**	**E2.57**	**E4.44**	**E12.62**
Must	**Glycerol [g/L]**	2.5 (±3.9)^{ab}	0.3 (±0.1)^{a}	0.8 (±0.0)^{ab}	1.7 (±0.1)^{ab}	5.1 (±0.2)^{b}
	Gluconic acid [mg/L]	6.0 (±0.0)^{a}	7.7 (±0.6)^{a}	11.0 (±1.0)^{b}	15.0 (±1.7)^{c}	29.0 (±1.7)^{d}
	Acetic acid [g/L]	n.d.	n.d.	n.d.	n.d.	n.d.
Juice	**Glycerol [g/L]**	n.d.^{a}	0.1 (±0.0)^{a}	0.8 (±0.0)^{b}	1.5 (±0.1)^{c}	4.8 (±0.1)^{d}
	Gluconic acid [mg/L]	4.7 (±0.6)^{a}	5.0 (±0.0)^{a}	8.3 (±0.6)^{b}	12.3 (±0.6)^{c}	26.7 (±0.6)^{d}
	Acetic acid [g/L]	n.d.	n.d.	n.d.	n.d.	n.d.
Wine	**Glycerol [g/L]**	5.6 (±0.2)^{a}	6.4 (±0.2)^{b}	7.4 (±0.3)^{c}	8.1 (±0.2)^{d}	11.6 (±0.2)^{e}
	Gluconic acid [mg/L]	3.0 (±0.0)^{a}	4.0 (±0.0)^{a}	6.0 (±0.0)^{a}	10.3 (±0.6)^{b}	23.3 (±3.2)^{c}
	Acetic acid [g/L]	0.2 (±0.0)^{a}	0.2 (±0.0)^{a}	0.9 (±0.2)^{b}	0.8 (±0.1)^{b}	0.8 (±0.1)^{b}

[1] E: Ergosterol content of must samples [mg/kg].

6.4.4 Juice and wines: volatile compounds

The GC/MS data for the untargeted volatile analysis of juices and wine samples using PLS-DA is displayed in form of PLS-DA scores and loadings plots in Figure 15.

In both data sets, the grape juice samples and wine samples, were organised into the five classes (levels of infection) each for PLS-DA.

The first two latent variables (LVs) of the PLS-DA model for the grape juices explained 80.71 % of the variation and samples were well discriminated according to their level of infection, i.e. the uninfected (0) and low infected samples, (severity level 1) were separated from the higher infected samples along LV1 (Figure 14). The 20 mass ions (m/z) that provided the most discrimination between class one and five were selected based on the highest selectivity ratios and are tabulated in the supplementary material (**Table S2**). Compounds responsible for these m/z are tabulated in Table 11. Compounds that decreased with increasing level of infection were (*E*)- and (*Z*)-2-hexenal and hexanal. Compounds that increased with increasing levels of infection were 3-octanone, 1-octen-3-one, (*E*)-3-hexenol, 3-octanol, 1-octen-3-ol, 2-pentyl furan and benzaldehyde. A number of compounds only evolved at infection level of severity levels 1 and 2 and above, namely 1,5-dimethyltetralin, 1,5-dimethylnaphthalene, ethyl linoleate a number of unknowns (RI: 1560, 1610) and a number of unknown sesquiterpenes (RI: 1717, 1764, 1930, 1935, 1971, 2053, 2220, 2228, 2302, 2320).

The targeted compounds 3-octanone, 3-octanone and 1-octen-3-ol were detected in significantly increasing concentrations with increased levels of infection (Table 11).

The first two latent variables (LVs) of the PLS-DA model for the wine samples explained 75.53 % of the variation and samples were again discriminated according to their level of infection, i.e. the low infected samples, i.e. severity levels 1, were separated from the higher infected samples along LV1 (Figure 14). The 20 mass ions (m/z) that provided the most discrimination between class one and five were selected based on the highest selectivity ratios and are tabulated in the supplementary material (**Table S3**). Compounds responsible for these m/z are tabulated in Table 12.

The only compound that significantly decreased with increased levels of infection was vinyl guaiacol, it decreased significantly with increasing severity of Botrytis. Compounds that increased with increasing levels of infections were benzaldehyde, the sesquiterpenes at RI 2000, 2089, 2119 and ethyl-3-hydroxydodecanoate. Compounds that were not detected in visually healthy fruit (visual score 0) but were detected in at infection levels from 1 or 2 onwards were the unknowns at RI 1554, 1973, 2090 and 2351 and some unknown sesquiterpenes at RI 1667, 1695, 1739, 1743, 1842, 1918, 1958, 1961, 2098, 2119, 2271 and 2282.

The targeted compounds 3-octanone and 1-octen-3-ol were detected in increasing concentrations as seen in the grape juices, at comparatively lower concentrations, while 3-octanone was not detected (Table 12).

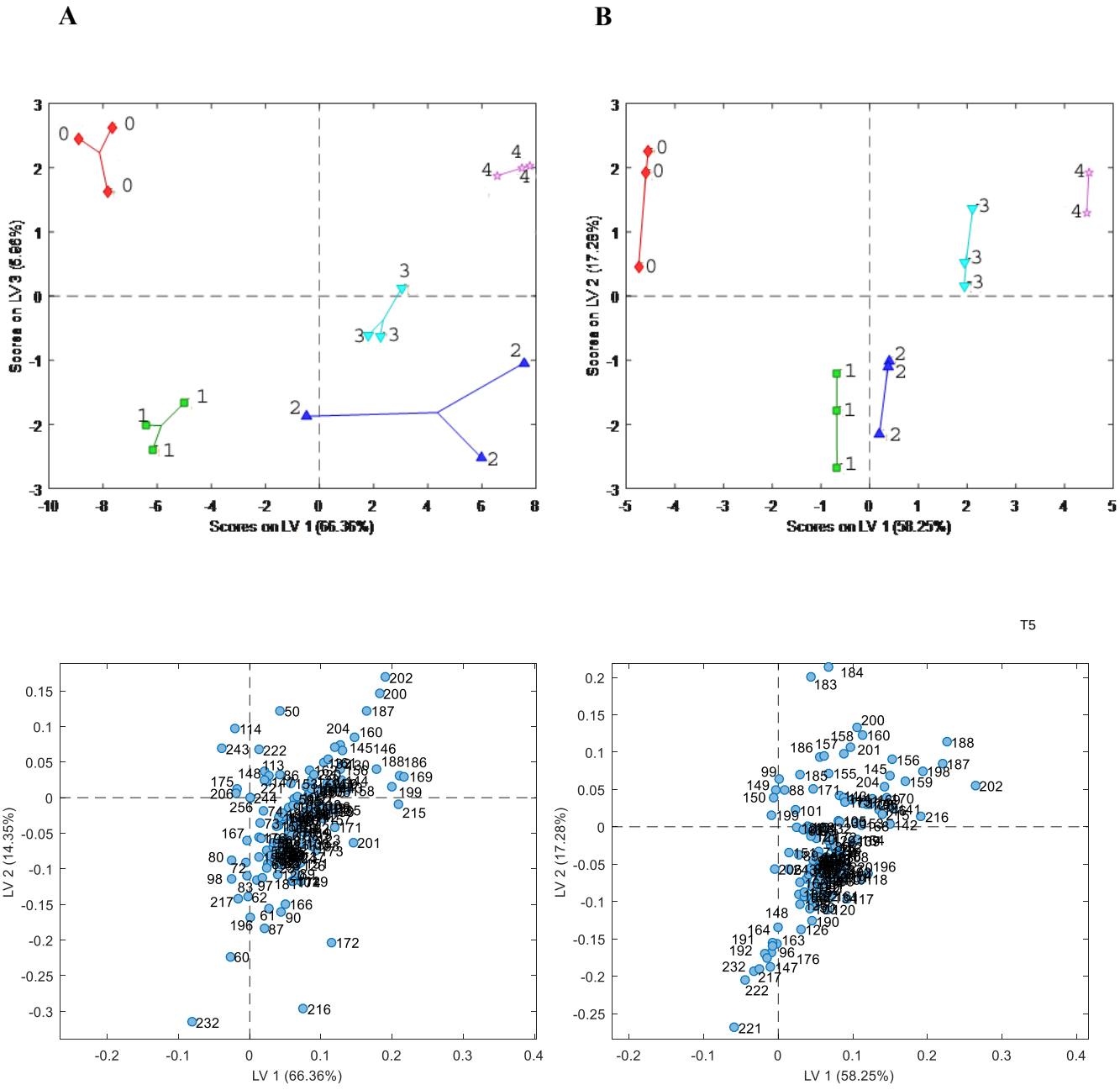


Figure 15: PLS-DA scores (top) and leadings (bottom) plot of GC/MS grape juice (A) and wine (B) data obtained from field infected Chardonnay bunches with increasing severity levels of infection starting from 0 (diamonds); 1 (squares); 2 (triangles); 3 (upside down triangles) and 4 (stars).

Table 11: Compounds responsible for sample classification based on the level of infection for **the grape juice samples** obtained from field infected Chardonnay berries, identified using untargeted and targeted volatile analysis.

Untargeted compound	Level of ID[1]	RT	RI cal[2]	RI lit[3]	Ref for RI lit	Main m/z	Standardised peak areas[4] for different levels of Botrytis severity[5]				
							0	1	2	3	4
Hexanal	a	10.9	1085	1089	Welke et al. 2012	**56**	**100^{b}**	21^{a}	6^{a}	5^{a}	10^{a}
(Z)-2-Hexenal	b	14.46	1230	1236	Lopéz-Tamames et al. 1997	**83**	**100^{b}**	37^{a}	16^{a}	12^{a}	8^{a}
2-Pentyl furan	a	14.7	1245	1258	Welke et al. 2012	**81**	4^{a}	15^{ab}	42^{bc}	54^{c}	**100^{d}**
(*E*)-2-Hexenal	a	15.01	1250	1248	Wang et al. 2005	**55**	**100^{b}**	38^{a}	17^{a}	13^{a}	10^{a}
3-Octanone	a	15.77	1273	1263	Mo et al. 2009	**57**	17^{a}	17^{a}	32^{a}	54^{a}	**100^{b}**
1-Octen-3-one	a	17.24	1321	1317	Cho et al. 2007	**70**	8^{a}	20^{ab}	41^{bc}	53^{c}	**100^{d}**
(*E*)-3-Hexenol	a	19.694	1396	1391	Baser et al. 2004	**67**	19^{a}	40^{ab}	57^{bc}	72^{c}	**100^{d}**
3-Octanol	a	19.78	1401	1400	Cho et al. 2006	**59**	5^{a}	9^{a}	6^{a}	14^{a}	**100^{b}**
1-Octen-3-ol	a	21.47	1452	1466	Escudero et al. 2000	**57**	6^{a}	13^{a}	28^{ab}	47^{b}	**100^{c}**
Benzaldehyde	a	24.51	1549	1536	Selli et al.2004	**106**	14^{a}	26^{ab}	70^{bc}	80^{c}	**100^{c}**
Unknown	b	24.99	1560	-	-	**145**	0^{a}	3^{a}	30^{a}	36^{ab}	**100^{b}**
Unknown	b	26.67	1610			**105**	0^{a}	0^{a}	7^{a}	18^{a}	**100^{b}**
Unknown sesquiterpene	b	30.45	1717	-	-	**105**	0^{a}	0^{a}	16^{a}	25^{a}	**100^{b}**
1,5-Dimethyltetralin	a	31.59	1751	-	-	**145**	0^{a}	1^{a}	7^{a}	19^{a}	**100^{b}**
Unknown sesquiterpene	b	32.01	1764	-	-	**119**	0^{a}	9^{a}	42^{b}	41^{b}	**100^{c}**
Unknown sesquiterpene	b	37.06	1930	-	-	**143**	0^{a}	5^{a}	31^{b}	41^{b}	**100^{c}**
Unknown sesquiterpene	b	37.18	1935	-	-	**202**	0^{a}	3^{a}	18^{ab}	34^{b}	**100^{c}**
Unknown sesquiterpene	b	37.99	1971	-	-	**200**	0^{a}	3^{a}	29^{b}	40^{b}	**100^{c}**
Unknown sesquiterpene	b	39.62	2053	-	-	**220**	0^{a}	0^{a}	9^{a}	27^{a}	**100^{b}**
1,5-Dimethylnaphthalene	a	39.76	2060	-	-	**156**	0^{a}	3^{a}	24^{b}	36^{b}	**100^{c}**

Unknown sesquiterpene	b	42.8	2220	-	-	**161**	0[a]	0[a]	9a	21[a]	**100[b]**
Unknown sesquiterpene	b	42.88	2228	-	-	**105**	0[a]	2[ab]	10[ab]	24[b]	**100[c]**
Unknown sesquiterpene	b	44.10	2302	-	-	**159**	0[a]	4[a]	26[b]	41[b]	**100[c]**
Unknown sesquiterpene	b	45.24	2320	-	-	**59**	0[a]	4[ab]	14[b]	29[c]	**100[d]**
Ethyl linoleate	a	52.23	>2500	2510	Cantergiani et al. 2001	**67**	0[a]	0[a]	4[a]	27[a]	**100[b]**

Targeted compound							**Concentration [ng/L] (standard error)**				
3-Octanone	a	15.77	1273	1263	Mo et al. 2009	**57**	116 (±201)[a]	779 (±402)[ab]	1568 (±962)[ab]	2541 (±261)[b]	4908 (±1327)[c]
1-Octen-3-one	a	17.24	1321	1317	Cho et al. 2007	**55**	365 (±201)[a]	815 (±202)[ab]	1591 (±386)[ab]	2383 (±403)[b]	4328 (±1155)[c]
1-Octen-3-ol	a	21.47	1452	1466	Escudero et al. 2000	**57**	945 (±462)[a]	2436 (±444)[ab]	13037 (±1686)[bc]	17292 (±4372)[cd]	28215 (±8641)[d]

[1] Level of identification: a) Metabolites were identified at level 1, by comparing their RI and EI-MS against authentic standards and the NIST2011 metabolite and Massfinder4 terpenoid database, b) Metabolites were identified at level 2, by comparing their RI and EI-MS against the above databases and peer-reviewed scientific literature.

[2] RI calculated based on alkane series (C8-C40), according to the equation of van den Dool and Kratz.

[3] RI reported in peer-reviewed scientific literature.

[4] MANOVA and Tukey HSD were calculated based on the peak areas that were normalised to the internal standard peak areas. For visual ease in this table, these normalised peak areas have been further standardized to the maximum peak. The standardised areas of the compounds with the same superscript are not significantly different between samples, based on Tukey HSD.

[5]Levels of Botrytis severity are depicted in figure 2

Note, RI for the compounds in grape juices vary slightly from RI in wine samples due to sample matrix effects.

Table 12: Compounds responsible for sample classification based on the level of infection for the **wine samples** obtained from field infected Chardonnay berries, identified using untargeted and targeted volatile analysis.

Untargeted compound	Level of ID[1]	RT	RI cal[2]	RI lit[3]	Ref for RI lit	Main m/z	Standardised peak areas[4] for different levels of Botrytis severity[5]				
							0	1	2	3	4
Isoamyl acetate	a	11.9	1128	1126	Gurbutz et al 2006	**70**	70^{ab}	72^{ab}	49^{a}	61^{ab}	$\mathbf{100^{b}}$
Benzaldehyde	a	24.27	1536	1536	Selli et al.2004	**106**	18^{a}	28^{a}	37^{ab}	53^{b}	$\mathbf{100^{c}}$
Unknown	b	24.8	1554	-	-	**145**	0^{a}	4^{a}	17^{b}	38^{c}	$\mathbf{100^{d}}$
Unknown sesquiterpene	b	28.7	1667	-	-	**189**	0^{a}	2^{ab}	14^{bc}	27^{c}	$\mathbf{100^{d}}$
Unknown sesquiterpene	b	29.7	1695	-	-	**108**	0^{a}	3^{ab}	17^{bc}	29^{c}	$\mathbf{100^{d}}$
Unknown sesquiterpene	b	31.2	1739	-	-	**119**	0^{a}	0^{a}	17^{ab}	29^{b}	$\mathbf{100^{c}}$
Unknown sesquiterpene	b	31.32	1743	-	-	**159**	0^{a}	0^{a}	10^{ab}	30^{b}	$\mathbf{100^{c}}$
Phenylethyl acetate	a	33.65	1829	1825	Tatsuka et al 1990	**104**	61^{a}	79^{ab}	55^{a}	71^{a}	$\mathbf{100^{b}}$
Unknown sesquiterpene	b	34.54	1842	-	-	**202**	0^{a}	0^{a}	1^{ab}	31^{b}	$\mathbf{100^{c}}$
Isoamyl acetamide	b	34.9	1853	1866	Kim et al. 2004	**73**	0^{a}	2^{ab}	14^{bc}	25^{c}	$\mathbf{100^{d}}$
Unknown sesquiterpene	b	36.78	1918	-	-	**143**	0^{a}	0^{a}	2^{a}	32^{b}	$\mathbf{100^{c}}$
Unknown sesquiterpene	b	37.58	1958	-	-	**143**	0^{a}	0^{a}	10^{b}	21^{c}	$\mathbf{100^{d}}$
Unknown sesquiterpene	b	37.7	1961	-	-	**200**	0^{a}	0^{a}	5^{a}	33^{b}	$\mathbf{100^{c}}$
Unknown	b	38.05	1973	-	-	**183**	0^{a}	1^{a}	9^{a}	30^{b}	$\mathbf{100^{c}}$
Unknown sesquiterpene	b	38.65	2000	-	-	**143**	2^{a}	4^{a}	12^{a}	66^{b}	$\mathbf{100^{c}}$
Unknown sesquiterpene	b	40.30	2089	-	-	**198**	1^{a}	5^{ab}	14^{b}	32^{c}	$\mathbf{100^{d}}$
Unknown	b	40.32	2090	-	-	**118**	0^{a}	1^{a}	8^{a}	24^{b}	$\mathbf{100^{c}}$
Unknown sesquiterpene	b	40.46	2098	-	-	**157**	0^{a}	2^{a}	8^{a}	22^{a}	$\mathbf{100^{b}}$
Unknown sesquiterpene	b	40.86	2119	-	-	**185**	8^{a}	14^{a}	27^{b}	38^{c}	$\mathbf{100^{d}}$
Vinyl guaiacol	a	42.33	2195	2194	Choi et al 2002	**150**	36^{ab}	$\mathbf{100^{c}}$	74^{bc}	8^{a}	3^{a}
Unknown sesquiterpene	b	43.98	2271	-	-	**159**	0^{a}	6^{a}	20^{ab}	57^{b}	$\mathbf{100^{c}}$
Unknown sesquiterpene	b	44.22	2282	-	-	**198**	0^{a}	3^{a}	11^{a}	30^{b}	$\mathbf{100^{c}}$

Ethyl-3-hydroxydodecanoate	b	44.75	2306	-	-	**117**	36[a]	76[b]	80[b]	85[b]	**100[b]**
9-Decenoic acid	b	45.23	2324	2335	Xu et al. 2007	**55**	50[a]	**100[b]**	85[ab]	84[ab]	85[ab]
Unknown	b	45.95	2351	-	-	**196**	0[a]	3[ab]	12[b]	31[c]	**100[d]**
Dihydrobenzofuran	b	46.98	2390	-	-	**120**	24[a]	80[bc]	**100[c]**	47[a]	52[ab]

Targeted compound							**Concentration [ng/L] (standard error)**				
3-Octanone	a	15.89	1277	1263	Mo et al. 2009	**57**	0 (±0)[a]	0 (±0)[a]	0 (±0)[a]	1099 (±102)[b]	2753 (±302)[c]
1-Octen-3-one	a	17.26	1322	1317	Cho et al. 2007	**55**	n.d	n.d	n.d	n.d	n.d
1-Octen-3-ol	a	21.49	1454	1466	Escudero et al. 2000	**57**	0 (±0)[a]	2562 (±320)[ab]	5496 (±1960)[bc]	8449 (±1636)[c]	14395 (±14)[d]

[1] Level of identification: a) Metabolites were identified at level 1, by comparing their RI and EI-MS against authentic standards and the NIST2011 metabolite and Massfinder4 terpenoid database, b) Metabolites were identified at level 2, by comparing their RI and EI-MS against the above databases and peer-reviewed scientific literature.

[2] RI calculated based on alkane series (C8-C40), according to the equation of van den Dool and Kratz.

[3] RI reported in peer-reviewed scientific literature.

[4] MANOVA and Tukey HSD were calculated based on the peak areas that were normalised to the internal standard peak areas. For visual ease in this table, these normalised peak areas have been further standardized to the maximum peak. The standardised areas of the compounds with the same superscript are not significantly different between samples, based on Tukey HSD.

[5]Levels of Botrytis severity are depicted in figure 2

6.4.5 Sensory analysis of wines made from field-infected grapes

Wine made from grape bunches with different severity levels of Botrytis grey mould, harvested from the Hunter valley trial in 2016 were analysed by a sensory panel. A triangle test was conducted where participants were asked to identify a wine that was different from two other identical ones. Wine made from grapes a Botrytis severity level of 2 (i.e. ≥ 1.05 g of dry weight of fungus / kg wet weight of grapes or ≥ 2.57 mg/kg ergosterol) were perceived as different from wine made with uninfected grapes. Wine made with grapes with the lowest level of grey mould (i.e. severity level of 1, or 0.34 g of dry weight of fungus / kg wet weight of grapes or ≥ 0.83 mg ergosterol / kg wet weight of grapes) could not be differentiate by the panel (table 13). This suggest that the threshold for Botrytis contamination of chardonnay grapes destined for wine, is between 0.34 to 1.05 g dry weight of fungus / kg fresh weight of grapes range. Volatile compounds as well as ergosterol, gluconic acid, glycerol and acetic acid concentrations in must, juice or wine are in agreement with the sensory thresholds, which indicate a level of infection above 0.34 g/kg of dry weight of fungus (or 0.83 mg/kg ergosterol) in grapes might lead to negative quality impacts on the resulting wines.

Table 13: Sensory analysis of chardonnay wines made with different severity levels of Botrytis grey mould. A triangle test was conducted where participants were asked to identify a wine that was different from two other identical ones.

Comparison of wines made from grapes with different severity levels* of Botrytis grey mould	Number of correct responses
0 vs. 1	8/15 (NSD)
0 vs. 2	13/15 (SD p<0.01)
0 vs. 3	12/15 (SD p<0.01)
0 vs. 4	15/15 (SD p<0.01)

* Botrytis severity levels are depicted in figure 2. NSD = Not significantly different, SD = significantly different.

In further work, three fining agents, bentonite (300 ppm or 500 ppm), potassium caseinate (150 ppm or 300ppm) and Phila exel, a yeast protein polysaccharide extract (200 ppm or 400 ppm) were trailed to ameliorate wine faults due to Botrytis. Of these only bentonite at 500 ppm significantly altered the aroma characters of the wine.

7. Outcome/Conclusion:

Achieving the objectives set out in the original application were hampered by the seasonal variability in the incidence of bunch rots in the field. In particular the climatic conditions in the Eastern states of Australia in the final years of the project (2017 and 2018) were not conducive to grey mould or other bunch riot diseases. Low to insignificant severities of Botrytis grey mould were recorded in the vineyards used for this work. To overcome these limitations, bunches were inoculated in the laboratory. Project conclusions are discussed below.

7.1 Potential use of ATR FTIR for bunch rot discrimination

ATR FTIR was able to distinguish mycelium of the four fungal species investigated and demonstrated promising results with respect to the ability to distinguish between the visually similar *Aspergillus spp.*. *Vitis vinifera* berries infected with pure cultures of these grapevine pathogens could also be differentiated with varying levels of precision and classification depending on the algorithm used for model development. These findings illustrate the potential of ATR FTIR coupled with chemometrics to develop predictive models of fungal bunch rot occurrence on wine grapes. While the technique will also have to be evaluated using field examples of naturally occurring bunch rots using a larger sample set, the findings illustrate the potential of ATR FTIR to provide a rapid indication of grape contamination prior to wine making. The choice of predictive model is an important consideration to the development of a successful rapid method for discrimination of these fungal pathogens in grape berry homogenates. Non-linear methods such as bagged random forests or transformation of data from non-linear to a linear hyperplane such as occurs with SVM, prove to be the most promising approach for predictive modelling. The fungal organisms investigated in this study also cause losses of yield and quality in other fruit crops, thus the technique may also have applicability in other food production processes.

7.2 Marker compounds for bunch rot discrimination

Potential volatile fungal marker compounds were identified in the juices from Chardonnay grapes infected with different fungi. *B. cinerea* had higher concentrations of 1,5-dimethylnaphthalene and a number of unknown sesquiterpenes/sesquiterpene fragments (some possibly due to (+)-4-epieremophil-9-en-11-ol isomers or break down products) while *P. expansum* infected samples were consistently highest in *m*-cresol and *γ*-nonalactone. *A. niger* and *A. carbonarius* infected samples

produced the tentatively identified 2-(4-hexyl-2,5-dioxo-2,5dihydrofuran-3-yl)acetic acid. These marker compounds form a good basis on which to establish the identity of the major infecting grapes.

In all grape juices, from individually infected berries and infected whole bunches collected in two growing seasons, *B. cinerea* infected samples could be readily discriminated from the other fungal species investigated. This could be achieved due to the higher abundancies of 1,5-dimethylnaphthalene, benzaldehyde and several unidentified sesquiterpenes or fragments thereof. Samples infected with *A. niger* and *A. carbonarius* had relatively higher levels of 2-(4-hexyl-2,5-dioxo-2,5dihydrofuran-3-yl)acetic acid while *P. expansum* infected samples were relatively higher in *γ*-nonalactone, 2-pentylfuran and *m*-cresol. The majority of marker compounds did not seem to be stable during the winemaking process and were not responsible for discrimination of samples based on pathogen present on the grapes used to make the corresponding wines. However, compounds that appeared to discriminated wines based on pathogens were some sesquiterpenes and/or their breakdown products in the case of *B. cinerea* and 2-(4-hexyl-2,5-dioxo-2,5dihydrofuran-3-yl)acetic in the case of *A. carbonarius*. Hence, it is suggested to confirm the chemical identity of those compounds and to investigate their sensory perception importance in wine. It is hitherto unclear if these compounds may contribute to the perceived differences in the bunch rot affected wines.

7.3 Thresholds for grey mould contamination of Chardonnay grapes.

Various techniques have been proposed to measure Botrytis contamination of grapes. These techniques include spectral imaging, such as NIR and immuno-detection to measure Botrytis antigens. Immuno-diagnostic kits are simple to use but require calibration. Furthermore such technology may have greater applicability in the analysis of finished wines rather than with grape samples (Dewey, et al. 2013). Methods involving measures of the fungal sterol ergosterol to determine fungal biomass present in plant tissues (Porep, et al. 2014) hold some promise for more accurate measures of Botrytis contamination of grapes and have been trialled online in a commercial setting (Porep, et al. 2015). For this reason measurements of fungal ergosterol were used in the current study to more accurately quantify the amount of fungal biomass and hence Botrytis bunch rot in field infected grape samples. Infected bunches were sorted into one of five levels of severity infection and based on the measurements of ergosterol it was determined that the infection scores of 0, 1, 2, 3, and 4 (figure 2) corresponded to 0.07, 0.34, 1.05, 1.82 and 5.16 g dry weight of fungus per kg fresh weigh of grapes respectively. The ergosterol recorded in the apparently disease free grapes (0) was not necessarily due to *B. cinerea*, but rather represents the background yeast and fungal population naturally residing

on the berry surface. These fungal organisms are saprophytes and are generally found on the surfaces of all fruit tissues including grape berries (Barata, et al. 2011).

Grape bunches infected with grey mould accumulated multiple compounds, including 3-octanone, 1-octen-3-one and 1-octen-3-ol that were detected in grape juice samples at concentrations exceeding olfactory detection thresholds (ranges 0.12 - 4.91 µg/L, 0.37 - 4.33 µg/L and 0.95 - 28.22 µg/L, respectively). These observations correlated well with the degree of grey mould infection present on the grapes. Low levels of these compounds (0.12 µg/L, 0.37 µg/L and 0.95 µg/L, respectively) were also present in juice from apparently disease-free grapes, highlighting the difficulty of obtaining complete disease free fruit from vineyards in growing seasons when there is a high incidence of Botrytis. Wine made from grape bunches infected with grey mould accumulated 1-octen-3-ol and 1-octen-3-one as previously reported (La Guerche, et al. 2006). Concentrations of these compounds reduced after fermentation, with the most severely tainted wine samples having 2.75 µg/L and 14.40 µg/L of 3-octanone and 1-octen-3-ol, respectively while 1-octen-3-one was not detected in the final wine.

From a sensory point of view wines made from grapes where one or two berries in the bunch were affected with botrytis were not significantly different from wine made with disease-free bunches. Wine made with grapes that had >/= 10% of the bunch infected with Botrytis could be discriminated from wine made from the disease-free bunches, suggesting that the sensory threshold for wine is between 0.35 and 1.00 g dry weight of fungus per kg wet weight of grapes. Furthermore, in juice samples, glycerol was an indicator of fungal infection and increased significantly between severity levels 1 and 2. Volatile compounds that behaved in a similar manner in juice samples included 1,5-dimethylnaphthalene and a variety of unknown sesquiterpenes (RI: 1764, 1930, 1971 and 2302). In wine this pattern of severity levels, 0 and 1 being significantly lower in concentration of volatile compounds, was observed for an unknown at RI 1554 and two sesquiterpenes (RI 1958 and 2119). Acetic acid concentration also significantly increased from infection level 1 to 2.

A significant sensory difference was not observed between wines from apparently healthy fruit and level 1. Nevertheless compounds that significantly decreased in grape juices from apparently healthy fruit to the infection level 1 were (*E*)- and (*Z*)-2-hexenal and hexanal, indicating that low levels of infection can already lead to loss of varietal aroma compounds. Recent work has shown the ability of hexenal to react with glutathione in juice (Clark and Deed 2018), and such a mechanism may be relevant to the decrease in (E)- and (Z)-2-hexenal as a consequence of grape fungal infection inducing elevated concentrations of glutathione in the grape. The product from hexenal reaction with glutathione was a precursor to 3-mercapto-1-hexanol, a compound responsible for passionfruit

flavour in wine. In wine samples, significant increases of glycerol and ethyl-3-hydroxydodecanoate were observed (from 0 to 1), indicating that these compounds may be useful for the detection of spoilage that is expressed in wine made from slightly infected fruit.

It is well known that grapes infected with *B. cinerea* have increased levels of glycerol, gluconic acid and acetic acid due to the metabolism of *B. cinerea* or due to infections with other microbes that occur as a result of the *B. cinerea* infection (Barbe, et al. 2002,Šehović, et al. 2004,Zoecklein 2012). From these compounds, gluconic acid and glycerol have been used as indicators for the levels of infections in grapes. In the current study we relate the concentrations of these compounds to the level of infection expressed in the ergosterol content. Volatile compounds such as 1,5-dimethylnaphthalene and some sesquiterpenes may also be used as potential marker compounds for *B. cinerea* bunch rot. Furthermore, it may be worth to quantify the hexanal and 2-hexenal concentrations in grape juices in order to then validate the threshold at which the concentration is so low in the juices that one can assume a *B. cinerea* infection. However, validation is required also investigating other fungal bunch rots in order to ensure that the decrease only appears when grapes are infected with *B. cinerea* but not with other fungal rots.

In conclusion, findings from the project have opened up new opportunities to quantify bunch rot contamination of wine grapes. Further validation of the work is required, and the work needs to be extended to include wine grape varieties other than chardonnay.

8. Recommendations:

The following recommendations are made as a result of the research conducted in this project.

Recommendation 1

ATR FTIR analysis was able to discriminate detached chardonnay grape berries inoculated with either *Botrytis cinerea, Aspergillus niger, Aspergillus carbonarius* or *Penicillium expansum*. The technique was simple to use, but more limited results were obtained with whole bunches infected with one of these fungal pathogens. It is recommended that ATR FTIR be explored further as a tool to differentiate machine harvested grapes arriving at the winery.

Recommendation 2

A number of marker compounds were identified in grape juices from grapes infected with either *Botrytis cinerea, Aspergillus niger, Aspergillus carbonarius* or *Penicillium expansum*. The potential to use these compounds as indicators of bunch rot spoilage warrants further investigation. Identification of these compounds as markers for bunch rot type requires confirmation and validation using field infected samples. This area of work could also be extended to include other fungal pathogens associated with bunch rot diseases of grapes, and in particular bitter rot (*Greeneria uvicola*) and ripe rot (*Colletotrichum* spp.). Some desirable compounds such as *β*-damascenone were depleted in bunch rot affected grapes. Aside from the identified compounds, grapes infected with any one of the bunch rot pathogens examined, accumulated a number of unknown compounds that are yet to be identified. The role (if any) these unidentified compounds potentially have on grape and wine quality should be investigated.

Recommendation 3

Outcomes from this research indicate that the likely threshold for bunch rot contamination of wine grapes is in the region of 0.34 to 1.05 g dry weight of fungal biomass per kg wet weight of grapes. These two levels of severity are equivalent with one or two berries in a bunch and up to 10% of a bunch infected with grey mould. Based on the data gathered, making wine with low levels of Botrytis, (i.e. < 2 berries per bunch infected) is likely to have minimal impact on wine quality. This of course will depend on the number of berries in a bunch and other factors. This estimate is based on the ergosterol content of just three *Botrytis cinerea* isolates grown on laboratory media. A vineyard affected with grey mould contains potentially hundreds of different *B. cinerea* isolates, which may differ in their ergosterol content based on their genotype. Furthermore the ergosterol content of fungal mycelium may vary depending upon the growing conditions and will also vary between different fungal species.

This natural variability in the ergosterol content of fungal tissues needs to be examined further in order to more accurately calculate the biomass of fungal tissues in infected grapes.

The thresholds for bunch rot contamination of wine grapes calculated in this project was based on only one grape variety and one growing season. Further validation and fine tuning of the actual threshold is required, possibly by examining wine grape varieties other than chardonnay. Different thresholds are also likely to exist for the non-Botrytis bunch rots.

It is recommended that the applicability of ergosterol as a measure of fungal biomass be further investigated using a greater range of fungal isolates and fungal species grown under different environmental conditions and that bunch rot thresholds should be examined in additional wine grape cultivars.

Appendix 1: Communication

Communication of outcomes during the project

Steel, C. C., Schwarz, L. J., Schmidtke, L. M., Clark, A. C. and Blackman, J. W. (2016). Analysis of mushroom-like aromas found in wine prepared from *Botrytis cinerea* diseased Chardonnay grapes. Proceedings of the 16th Australian Wine Industry Technical Conference, Poster 186. Adelaide 24th – 28th July 2016.

Steel, C. C., Schwarz, L. J., Schmidtke, L. M., Blackman, J. W., Clark, A. C. and Schueuermann, C. (2016). ATR FTIR and GC-MS techniques for *Botrytis cinerea* detection and evaluation of grape and wine quality. Key Note Presentation 2.2. XVII International Botrytis Symposium, Santa Cruz, Chile, 23rd to 28th October 2016.

Steel, C. C. (2017). Determining the impacts of Bunch rots on wine quality - thresholds for contamination. Chardonnay workshop, NSW DPI, Orange, NSW. 31st May 2017.

Schueuermann, C., Schmidtke, L. M., Schwarz, L. J. Steel, C. C., Blackman, J. W. and Clark, A. C. (2017). A GC-MS and PTR-MS Untargeted Metabolomics Approach for the Identification of Fungal Marker Compounds in Grape Juice and Wine. 10th In Vino Analytica Scientia, Salamanca, Spain. 17th to 20th July 2017.

Schueuermann, C., Steel, C. C., Schmidtke, L. M., Blackman, J. W. Schwarz, L. J. and Clark, A. C. (2017). Determining the impact of Botrytis bunch rot on grape quality to inform disease management decisions. Poster 335, Science Protecting Plant Health Conference, Brisbane, 26 – 28th September 2017.

Steel, C. C. (2018). Grape bunch rots and thresholds for wine contamination. AWRI webinar, 19th January 2018. https://www.youtube.com/watch?v=5B-qp4umOBo&feature=youtu.be

Christopher C Steel, Lachlan J Schwarz, John W Blackman, Andrew C Clark and Leigh M Schmidtke (2018) Determining bunch rot impact on wine quality - thresholds for contamination, In NSW DPI 2018/19 Grapevine Management Guide. Publisher NSW DPI, Orange, NSW. pp 21 – 23. (In Press, publication date August 2018).

Journal articles

Schueuermann, C, Steel, C C, Blackman, J, Clark, A C, Schwarz, L J, Moraga, J, Collado I G and Schmidtke, L M (2018) A GC-MS Untargeted Metabolomics Approach for the Identification of Fungal Marker Compounds in Grape Juice. Food Chemistry **270,** 375-384. https://doi.org/10.1016/j.foodchem.2018.07.057

Schmidtke, L.M. Schwarz, L.J. Schueuermann C. and Steel C.C. (201?). Discrimination of *Aspergillus* spp., *Botrytis cinerea* and *Penicillium expansum* in grape berries by ATR FTIR spectroscopy. American Journal of Enology and Viticulture – *Accepted June 2018 - subject to minor revisions.*

Appendix 2: Intellectual Property

No intellectual property arose from the work.

Appendix 3: References

Almassi, F., E.L. Ghisalberti, and C.Y. Rowland (1994) Alkylcitrate-derived metabolites from *Aspergillus niger*. Journal of Natural Products 57, 833-836.

Australian Bureau of Statistsics, 2015, "Key wine variety figures", (Australian Bureau of Statistsics, 2015), http://www.abs.gov.au/ausstats/abs@.nsf/mf/1329.0.55.002.

Bailly, S., V. Jerkovic, J. Marchand-Brynaert, and S. Collin (2006) Aroma Extraction Dilution Analysis of Sauternes Wines. Key Role of Polyfunctional Thiols. Journal of Agricultural and Food Chemistry 54, 7227-7234. doi: 10.1021/jf060814k.

Baldock, G.A. and Y. Hayasaka (2004) Screening method for petroleum-derived aromatic hydrocarbons in wine. Australian Journal of Grape and Wine Research 10, 17-25.

Barata, A., E. Campo, M. Malfeito-Ferreira, V. Loureiro, J. Cacho, and V. Ferreira (2011) Analytical and sensorial characterization of the aroma of wines produced with sour rotten grapes using GC-O and GC-MS: Identification of key aroma compounds. Journal of Agricultural and Food Chemistry 59, 2543-2553.

Barbe, J.-C., G. de Revel, and A. Bertrand (2002) Gluconic acid, its lactones, and SO2 binding phenomena in musts from botrytized grapes. Journal of Agricultural and Food Chemistry 50, 6408-6412.

Beauchêne, D., J. Grua-Priol, T. Lamer, M. Demaimay, and F. Quémeneur (2000) Concentration by pervaporation of aroma compounds from *Fucus serratus*. Journal of Chemical Technology and Biotechnology 75, 451-458.

Behr, M., E. Cocco, A. Lenouvel, C. Guignard, and D. Evers (2013) Earthy and Fresh Mushroom Off-Flavors in Wine: Optimized Remedial Treatments. Americal Journal of Enology and Viticulture 64, 545 - 549.

Belli, N., S. Marin, V. Sanchis, and A.J. Ramos (2004) Influence of water activity and temperature on growth of isolates of *Aspergillus* section *Nigri* obtained from grapes. International Journal of Food Microbiology 96, 19-27. doi: 10.1016/j.ijfoodmicro.2004.03.004.

Berna, A.Z., S. Trowell, D. Clifford, W. Cynkar, and D. Cozzolino (2009) Geographical origin of Sauvignon Blanc wines predicted by mass spectrometry and metal oxide based electronic nose. Analytica Chimica Acta 648, 146-152. doi: https://doi.org/10.1016/j.aca.2009.06.056.

Bianchi, F., M. Careri, A. Mangia, and M. Musci (2007) Retention indices in the analysis of food aroma volatile compounds in temperature-programmed gas chromatography: Database creation and evaluation of precision and robustness. Journal of Separation Science 30, 563-572.

Brereton, R.G. (2015) Pattern recognition in chemometrics. Chemometrics and Intelligent Laboratory Systems 149, 90-96. doi: https://doi.org/10.1016/j.chemolab.2015.06.012.

Cantergiani, E., H. Brevard, Y. Krebs, A. Feria-Morales, R. Amado, and C. Yeretzian (2001) Characterisation of the aroma of green Mexican coffee and identification of mouldy/earthy defect. European Food Research and Technology 212, 648-657.

Cerdán, T.G., S.R. Mozaz, and C.A. Azpilicueta (2002) Volatile composition of aged wine in used barrels of French oak and of American oak. Food Research International 35, 603-610.

Chung, H.Y. (1999) Volatile components in crabmeats of Charybdis feriatus. Journal of Agricultural and Food Chemistry 47, 2280-2287.

Chung, H.Y., I.K. Shing Yung, and J.-S. Kim (2001) Comparison of volatile components in dried scallops (*Chlamys farreri* and *Patinopecten yessoensis*) prepared by boiling and steaming methods. Journal of Agricultural and Food Chemistry 49, 192-202.

Clark, A.C. and R.C. Deed (2018) The Chemical Reaction of Glutathione and trans-2-Hexenal in Grape Juice Media To Form Wine Aroma Precursors: The Impact of pH, Temperature, and Sulfur Dioxide. Journal of Agricultural and Food Chemistry 66, 1214-1221.

Climaco-Pinto, R., A.S. Barros, N. Locquet, L. Schmidtke, and D.N. Rutledge (2009) Improving the detection of significant factors using ANOVA-PCA by selective reduction of residual variability. Analytica Chimica Acta 653, 131-142.

Delfini, C., P. Gaia, L. Bardi, G. Mariscalco, M. Contiero, and A. Pagliara (1991) Production of benzaldehyde, benzyl alcohol and benzoic acid by yeasts and *Botrytis cinerea* isolated from grape musts and wines. Vitis - Journal of Grapevine Research 30, 253-263.

Dewey, F.M. and U. Meyer (2004) Rapid, quantitative Tube immunoassays for on-site detection of Botrytis, Aspergillus and Penicillium antigens in grape juice. Analytica Chimica Acta 513, 11-19. doi: 10.1016/j.aca.2003.11.088.

Dewey, F.M., C.C. Steel, and S.J. Gurr (2013) Lateral Flow Devices to rapidly determine levels of stable Botrytis antigens in table and dessert wines American Journal of Enology and Viticulture 64, 291-295.

Diguta, C.F., A.M. Tanase, F. Matei, and C.P. Cornea (2016) Rapid detection of *Aspergillus carbonarius* in Romanian vineyards. Romanian Biotechnological Letters 21, 11875-11880.

Elad, Y., B. Williamson, P. Tudzynski, and N. Delen (2004) Botrytis: Biology, Pathology and Control. (Springer.

Escudero, A., J. Cacho, and V. Ferreira (2000) Isolation and identification of odorants generated in wine during its oxidation: a gas chromatography-olfactometric study. European Food Research and Technology 211, 105-110.

Farrés, M., S. Platikanov, S. Tsakovski, and R. Tauler (2015) Comparison of the variable importance in projection (VIP) and of the selectivity ratio (SR) methods for variable selection and interpretation. Journal of Chemometrics 29, 528-536. doi: 10.1002/cem.2736.

Fehlhaber, H.W., R. Geipel, H.J. Mercker, R. Tschesche, K. Welmar, and F. Schönbeck (1974) Botrydial, ein Sesquiterpen-Antibiotikum aus der Nährlösung des Pilzes Botrytis cinerea. European Journal of Inorganic Chemistry 107, 1720-1730.

Ferreira, V., R. López, and J.F. Cacho (2000) Quantitative determination of the odorants of young red wines from different grape varieties. Journal of the Science of Food and Agriculture 80, 1659-1667. doi: 10.1002/1097-0010(20000901)80:11<1659::AID-JSFA693>3.0.CO;2-6.

Frizzo, C., L. Serafini, E. Dellacassa, D. Lorenzo, and P. Moyna (2001) Essential oil of *Baccharis uncinella* DC. from Southern Brazil. Flavour and Fragrance Journal 16, 286-288.

García-Carpintero, E.G., E. Sánchez-Palomo, and M. González-Viñas (2011) Aroma characterization of red wines from cv. Bobal grape variety grown in La Mancha region. Food Research International 44, 61-70.

González-Barreiro, C., R. Rial-Otero, B. Cancho-Grande, and J. Simal-Gándara (2015) Wine Aroma Compounds in Grapes: A Critical Review. Critical Reviews in Food Science and Nutrition 55, 202-218. doi: 10.1080/10408398.2011.650336.

Grassin, C. and D. Dobourdieu (1989) Quantitative determination of Botrytis laccase in musts and wines by the syringaldazine test. Journal of Science Food Agriculture 48, 369 - 376.

Gürbüz, O., J.M. Rouseff, and R.L. Rouseff (2006) Comparison of aroma volatiles in commercial Merlot and Cabernet Sauvignon wines using gas chromatography-olfactometry and gas chromatography-mass spectrometry. Journal of Agricultural and Food Chemistry 54, 3990-3996.

Harding, J. and J. Robinson (2015) The Oxford companion to wine. (Oxford University Press: New York, USA).

Hayasaka, Y., G.A. Baldock, M. Parker, K.H. Pardon, C.A. Black, M.J. Herderich, and D.W. Jeffery (2010) Glycosylation of Smoke-Derived Volatile Phenols in Grapes as a Consequence of Grapevine Exposure to Bushfire Smoke. Journal of Agricultural and Food Chemistry 58, 10989-10998. doi: 10.1021/jf103045t.

Hernández-Orte, P., M. Cersosimo, N. Loscos, J. Cacho, E. Garcia-Moruno, and V. Ferreira (2008) The development of varietal aroma from non-floral grapes by yeasts of different genera. Food Chemistry 107, 1064-1077. doi: https://doi.org/10.1016/j.foodchem.2007.09.032.

Hill, G.N., K.J. Evans, R.M. Beresford, and R.G. Dambergs (2014) Comparison of methods for the quantification of botrytis bunch rot in white wine grapes. Australian Journal of Grape and Wine Research 20, 432-441.

Jeleń, H. and E. Wasowicz (1998) Volatile fungal metabolites and their relation to the spoilage of agricultural commodities. Food Reviews International 14, 391-426. doi: 10.1080/87559129809541170.

Kim, T.H., J.H. Shin, H.H. Baek, and H.J. Lee (2001) Volatile flavour compounds in suspension culture of Agastache rugosa Kuntze (Korean mint). Journal of the Science of Food and Agriculture 81, 569-575.

Krakowska, B., D. Custers, E. Deconinck, and M. Daszykowski (2016) The Monte Carlo validation framework for the discriminant partial least squares model extended with variable selection methods applied to authenticity studies of Viagra® based on chromatographic impurity profiles. Analyst 141, 1060-1070.

Ky, I., B. Lorrain, M. Jourdes, G. Pasquier, M. Fermaud, L. Geny, P. Rey, B. Doneche, and P.L. Teissedre (2012) Assessment of grey mould (*Botrytis cinerea*) impact on phenolic and sensory quality of Bordeaux grapes, musts and wines for two consecutive vintages. Australian Journal of Grape and Wine Research 18, 215-226.

Lakens, D. (2013) Calculating and reporting effect sizes to facilitate cumulative science: a practical primer for t-tests and ANOVAs. Frontiers in Psychology 4. doi: 10.3389/fpsyg.2013.00863.

LaRoe, E.G. and P.A. Shipley (1970) Whiskey composition: formation of alpha-and beta-ionone by the thermal decomposition of beta-carotene. Journal of Agricultural and Food Chemistry 18, 174-175. doi: 10.1021/jf60167a012.

Larroche, C., F. Grivel, C. Creuly, and J. Gros (1995) Fed batch biotransformation of β-ionone by Aspergillus niger immobilized in Ca-alginate beads. In: Bioflavour 95, Eds. P. Étiévant and P. Schreier (Inra Editions: Paris) pp. 309-314.

López, R., V. Ferreira, P. Hernández, and J.F. Cacho (1999) Identification of impact odorants of young red wines made with Merlot, Cabernet Sauvignon and Grenache grape varieties: a comparative study. Journal of the Science of Food and Agriculture 79, 1461-1467. doi: 10.1002/(SICI)1097-0010(199908)79:11<1461::AID-JSFA388>3.0.CO;2-K.

Loscos, N., P. Hernandez-Orte, J. Cacho, and V. Ferreira (2007) Release and Formation of Varietal Aroma Compounds during Alcoholic Fermentation from Nonfloral Grape Odorless Flavor Precursors Fractions. Journal of Agricultural and Food Chemistry 55, 6674-6684. doi: 10.1021/jf0702343.

Mercer, E.I. (1984) The biosynthesis of ergosterol. Pesticide Science 15, 133-155.

Meunier, M. and C.C. Steel (2009) Effect of *Colletotrichum acutatum* ripe rot on the composition and sensory attributes of Cabernet Sauvignon grapes and wine. Australian Journal of Grape and Wine Research 15, 223-227.

Miranda-Lopez, R., L.M. Libbey, B.T. Watson, and M. McDaniel (1992) Odor analysis of Pinot Noir wines from grapes of different maturities by a gas chromatography-olfactometry technique (Osme). Journal of Food Science 57, 985-993.

Noguerol-Pato, R., M. González-Álvarez, C. González-Barreiro, B. Cancho-Grande, and J. Simal-Gándara (2013) Evolution of the aromatic profile in Garnacha Tintorera grapes during raisining and comparison with that of the naturally sweet wine obtained. Food Chemistry 139, 1052-1061. doi: https://doi.org/10.1016/j.foodchem.2012.12.048.

Petronilho, S., M.A. Coimbra, and S.M. Rocha (2014) A critical review on extraction techniques and gas chromatography based determination of grapevine derived sesquiterpenes. Analytica Chimica Acta 846, 8-35.

Pinar, A.L., D. Rauhut, E. Ruehl, and A. Buettner (2017) Effects of Bunch Rot (*Botrytis cinerea*) and Powdery Mildew (*Erysiphe necator*) Fungal Diseases on Wine Aroma. Frontiers in Chemistry 5, 20-20.

Pinedo, C., J. Moraga, J. Barua, V.E. González-Rodríguez, J. Aleu, R. Durán-Patrón, A.J. Macías-Sánchez, J.R. Hanson, M. Viaud, R. Hernández-Galán, C. Garrido, and I.G. Collado (2016) Chemically Induced Cryptic Sesquiterpenoids and Expression of Sesquiterpene Cyclases in Botrytis cinerea Revealed New Sporogenic (+)-4-Epieremophil-9-en-11-ols. ACS Chemical Biology 11, 1391-1400. doi: 10.1021/acschembio.5b00931.

Pinto, R.C., N. Locquet, L. Eveleigh, and D.N. Rutledge (2010) Preliminary studies on the mid-infrared analysis of edible oils by direct heating on an ATR diamond crystal. Food Chemistry 120, 1170-1177.

Pons, A., V. Lavigne, F. Eric, P. Darriet, and D. Dubourdieu (2008) Identification of Volatile Compounds Responsible for Prune Aroma in Prematurely Aged Red Wines. Journal of Agricultural and Food Chemistry 56, 5285-5290. doi: 10.1021/jf073513z.

Porep, J.U., S. Mrugala, M.S.P. Nikfardjam, and R. Carle (2015) Online Determination of Ergosterol in Naturally Contaminated Grape Mashes Under Industrial Conditions at Wineries. Food and Bioprocess Technology 8, 1455-1464.

Porep, J.U., R. Walter, A. Kortekamp, and R. Carle (2014) Ergosterol as an objective indicator for grape rot and fungal biomass in grapes. Food Control 37, 77-84. doi: http://dx.doi.org/10.1016/j.foodcont.2013.09.012.

Puel, O., P. Galtier, and I.P. Oswald (2010) Biosynthesis and toxicological effects of patulin. Toxins 2, 613-631.

Quijada-Morin, N., F. Garcia, K. Lambert, A.-S. Walker, L. Tiers, M. Viaud, F.-X. Sauvage, C. Hirtz, and C. Saucier (2018) Strain effect on extracellular laccase activities from *Botrytis cinerea*. Australian Journal of Grape and Wine Research 24, 241-251.

Rebière, L., A.C. Clark, L.M. Schmidtke, P.D. Prenzler, and G.R. Scollary (2010) A robust method for quantification of volatile compounds within and between vintages using headspace-solid-phase micro-extraction coupled with GC-MS - Application on Semillon wines. Analytica Chimica Acta 660, 149-157.

Roessler, E.B., R.M. Pangborn, J.L. Sidel, and H. Stone (1978) Expanded statistical tables for estimating significance in paired preference, paired difference, duo-trio and triangle tests. Journal of Food Science 34, 940 - 941.

Rousseaux, S., C.F. Diguta, F. Radoï-Matei, H. Alexandre, and M. Guilloux-Bénatier (2014) Non-Botrytis grape-rotting fungi responsible for earthy and moldy off-flavors and mycotoxins. Food Microbiology 38, 104-121. doi: http://dx.doi.org/10.1016/j.fm.2013.08.013.

Saito, S., K.J. Dunne, K.J. Evans, K. Barry, L. Cadle-Davidson, and W.F. Wilcox (2013) Optimisation of techniques for quantification of Botrytis cinerea in grape berries and receptacles by quantitative polymerase chain reaction. Australian Journal of Grape and Wine Research 19, 68-73.

Salman, A., A. Pomerantz, L. Tsror, I. Lapidot, R. Moreh, S. Mordechai, and M. Huleihel (2012) Utilizing FTIR-ATR spectroscopy for classification and relative spectral similarity evaluation of different *Colletotrichum coccodes* isolates. Analyst 137, 3558-3564.

Samuelian, S.K., L.A. Greer, S. Savocchia, and C.C. Steel (2011) Detection and monitoring of *Greeneria uvicola* and *Colletotrichum acutatum* development on grapevines by real-time PCR. Plant Disease 95, 298-303. doi: 10.1094/pdis-07-10-0537.

Schmidtke, L.M., J.W. Blackman, A.C. Clark, and P. Grant-Preece (2013) Wine Metabolomics: Objective Measures of Sensory Properties of Semillon from GC-MS Profiles. Journal of Agricultural and Food Chemistry 61, 11957-11967. doi: 10.1021/jf403504p.

Schmidtke, L.M., J.P. Smith, M.C. Muller, and B.P. Holzapfel (2012) Rapid monitoring of grapevine reserves using ATR-FT-IR and chemometrics. Analytica Chimica Acta 732, 16-25.

Schwab, W. and M. Wüst (2015) Understanding the Constitutive and Induced Biosynthesis of Mono- and Sesquiterpenes in Grapes (*Vitis vinifera*): A Key to Unlocking the Biochemical Secrets of Unique Grape Aroma Profiles. Journal of Agricultural and Food Chemistry 63, 10591-10603. doi: 10.1021/acs.jafc.5b04398.

Scott, E.S., "Objective measures for powdery mildew - Wine Australia Report UA 12 - 02", (University of Adelaide, Adelaide SA, Australia, 2012), pp. 100.

Scott, I.M., W. Lin, M. Liakata, J.E. Wood, C.P. Vermeer, D. Allaway, J.L. Ward, J. Draper, M.H. Beale, D.I. Corol, J.M. Baker, and R.D. King (2013) Merits of random forests emerge in evaluation of chemometric classifiers by external validation. Analytica Chimica Acta 801, 22-33.

Šehović, Đ., V. Petravić, and V. Marić (2004) Glycerol and wine industry glycerol determination in grape must and wine. Kemija u industriji: časopis kemičara i tehnologa Hrvatske 53, 505-516.

Selli, S., T. Cabaroglu, A. Canbas, H. Erten, C. Nurgel, J. Lepoutre, and Z. Gunata (2004) Volatile composition of red wine from cv. Kalecik Karası grown in central Anatolia. Food Chemistry 85, 207-213.

Selli, S., A. Canbas, T. Cabaroglu, H. Erten, and Z. Günata (2006) Aroma components of cv. Muscat of Bornova wines and influence of skin contact treatment. Food Chemistry 94, 319-326.

Sérot, T., C. Regost, and J. Arzel (2002) Identification of odour-active compounds in muscle of brown trout (*Salmo trutta*) as affected by dietary lipid sources. Journal of the Science of Food and Agriculture 82, 636-643.

Shiratsuchi, H., M. Shimoda, K. Imayoshi, K. Noda, and Y. Osajima (1994) Volatile flavor compounds in spray-dried skim milk powder. Journal of Agricultural and Food Chemistry 42, 984-988.

Steel, C.C., "Assessment of fungal rots of grapes and their impacts on wine quality - Wine Australia Report NWG 12-01", (National Wine and Grape Industry Centre, Charles Sturt University, Wagga Wagga, NSW, Australia, 2014), pp. 48.

Steel, C.C., J.W. Blackman, and L.M. Schmidtke (2013) Grapevine Bunch Rots: Impacts on Wine Composition, Quality, and Potential Procedures for the Removal of Wine Faults. Journal of Agricultural and Food Chemistry 61, 5189-5206. doi: 10.1021/jf400641r.

Steel, C.C., L.A. Greer, and S. Savocchia (2007) Studies on *Colletotrichum acutatum* and *Greeneria uvicola*: Two fungi associated with bunch rot of grapes in sub-tropical Australia. Australian Journal of Grape and Wine Research 13, 23-29. doi: doi:10.1111/j.1755-0238.2007.tb00068.x.

Steel, C.C., L.A. Greer, S. Savocchia, and S.K. Samuelian (2011) Effect of temperature on *Botrytis cinerea*, *Colletotrichum acutatum* and *Greeneria uvicola* mixed fungal infection of *Vitis vinifera* grape berries. Vitis 50, 69-71.

Steullet, P. and P.M. Guerin (1994) Identification of vertebrate volatiles stimulating olfactory receptors on tarsus I of the tick *Amblyomma variegatum Fabricius* (Ixodidae). Journal of Comparative Physiology A: Neuroethology, Sensory, Neural, and Behavioral Physiology 174, 27-38.

Szymańska, E., E. Saccenti, A. Smilde, and J. Westerhuis (2012) Double-check: validation of diagnostic statistics for PLS-DA models in metabolomics studies. Metabolomics 8, 3-16. doi: 10.1007/s11306-011-0330-3.

Tabanca, N., B. Demirci, T. Ozek, N. Kirimer, K.H.C. Baser, E. Bedir, I.A. Khan, and D.E. Wedge (2006) Gas chromatographic-mass spectrometric analysis of essential oils from *Pimpinella* species gathered from Central and Northern Turkey. Journal of Chromatography A 1117, 194-205.

Tatsuka, K., S. Suekane, Y. Sakai, and H. Sumitani (1990) Volatile constituents of kiwi fruit flowers: simultaneous distillation and extraction versus headspace sampling. Journal of Agricultural and Food Chemistry 38, 2176-2180.

Van den Dool, H. and P.D. Kratz (1963) A generalization of the retention index system including linear temperature programmed gas—liquid partition chromatography. Journal of Chromatography A 11, 463-471.

Van den Dool, H. and P.D. Kratz (1963) A generalization of the retention index system including linear temperature programmed gas - liquid partition chromatography. Journal of Chromatography A 11, 463-471.

Vikram, A., B. Prithiviraj, and A. Kushalappa (2004) Use of volatile metabolite profiles to discriminate fungal diseases of Cortland and empire apples. Journal of Plant Pathology, 215-225.

Wang, Y., C. Finn, and M.C. Qian (2005) Impact of growing environment on chickasaw blackberry (Rubus L.) aroma evaluated by gas chromatography olfactometry dilution analysis. Journal of Agricultural and Food Chemistry 53, 3563-3571.

Weidenmüller, H.L., F. Cavagna, H.W. Fehlhaber, and P. Präve (1972) 2-Carboxymethyl-3-n-hexyl-maleic acid anhydride, a novel metabolite from an aspergillus. Tetrahedron Letters 13, 3519-3522. doi: http://dx.doi.org/10.1016/S0040-4039(01)94088-2.

Welke, J.E., V. Manfroi, M. Zanus, M. Lazarotto, and C.A. Zini (2012) Characterization of the volatile profile of Brazilian Merlot wines through comprehensive two dimensional gas chromatography time-of-flight mass spectrometric detection. Journal of Chromatography A 1226, 124-139.

Westerhuis, J.A., H.C.J. Hoefsloot, S. Smit, D.J. Vis, A.K. Smilde, E.J.J. van Velzen, J.P.M. van Duijnhoven, and F.A. van Dorsten (2008) Assessment of PLSDA cross validation. Metabolomics 4, 81-89. doi: 10.1007/s11306-007-0099-6.

Whitfield, F., S. Shea, K. Gillen, and K. Shaw (1981) Volatile components from the roots of *Acacia pulchella* R. Br. and their effect on *Phytophthora cinnamomi* Rands. Australian Journal of Botany 29, 195-208.

Wu, S., H. Zorn, U. Krings, and R.G. Berger (2005) Characteristic volatiles from young and aged fruiting bodies of wild *Polyporus sulfureus* (Bull.: Fr.) Fr. Journal of Agricultural and Food Chemistry 53, 4524-4528.

Wu, X., V. Kumar, J. Ross Quinlan, J. Ghosh, Q. Yang, H. Motoda, G.J. McLachlan, A. Ng, B. Liu, P.S. Yu, Z.-H. Zhou, M. Steinbach, D.J. Hand, and D. Steinberg (2008) Top 10 algorithms in data mining. Knowledge and Information Systems 14, 1-37. doi: 10.1007/s10115-007-0114-2.

Zoecklein, B. (2012) Enology Notes# 161. Virginia Tech 2012.

Appendix 4:

Staff

Christopher C Steel	NWGIC, Charles Sturt University (Project leader)
John W Blackman	NWGIC, Charles Sturt University
Andrew C Clark	NWGIC, Charles Sturt University
Campbell Meeks	NWGIC, Charles Sturt University (Experimental winemaker)
Leigh M Schmidtke	NWGIC, Charles Sturt University
Claudia Schueuermann	NWGIC, Charles Sturt University (WA Post-doctoral scientist)
Lachlan J Schwarz	NWGIC, Charles Sturt University (WA Post-doctoral scientist)

Collaborators

Isidro G Collado	Universidad de Cádiz, Spain
Javier Moraga	Universidad de Cádiz, Spain

Appendix 5: Supplementary information, figures and tables

Appendix 5.1 - Supplementary Tables

Table S1: Confusion table of class predictions from cross validation of predictive models using k=10 fold data splits. Samples abbreviations are as follows: *Aspergillus carbonarius* (Asc), *Aspergillus niger* (Asn), *Botrytis cinerea* (Bot), *Penicillium expansum* (Pen) and Control (Con). Predictive model abbreviations: Support Vector Model (SVM); Soft Independent Model of Class Analogy (SIMCA); K-nearest Neighbour (KNN).

		Actual Class				
		Asc	Asn	Bot	Pen	Con
SVM	Predicted as Asc	22	0	0	0	0
	Predicted as Asn	0	22	0	0	0
	Predicted as Bot	0	0	0	0	22
	Predicted as Pen	0	0	0	23	0
	Predicted as Con	0	1	23	0	0
SIMCA	Predicted as Asc	22	3	0	0	0
	Predicted as Asn	0	23	11	1	14
	Predicted as Bot	0	0	22	3	10
	Predicted as Pen	0	2	12	23	9
	Predicted as Con	0	1	12	1	23
KNN	Predicted as Asc	20	2	0	0	0
	Predicted as Asn	2	15	1	2	2
	Predicted as Bot	0	5	14	3	8
	Predicted as Pen	0	1	2	14	2
	Predicted as Con	0	0	5	4	11
Random Forest	Predicted as Asc	21	0	0	0	0
	Predicted as Asn	1	21	0	1	0
	Predicted as Bot	0	1	15	2	6
	Predicted as Pen	0	0	0	19	0
	Predicted as Con	0	1	7	1	17

Table S2: Confusion matrix for prediction from cross validation. Samples abbreviations are as follows: *Aspergillus carbonarius* (Asc), *Aspergillus niger* (Asn), *Botrytis cinerea* (Bot), *Penicillium expansum* (Pen) and Control (Con). Predictive model abbreviations: Support Vector Model (SVM); Soft Independent Model of Class Analogy (SIMCA); K-nearest Neighbour (KNN).

	Class	True Positive	False Positive	True Negative	False Negative	Misclassification error	Precision	Accuracy F1
SVM	Asc	1.00	0.00	1.00	0.00	0.00	1.00	1.00
	Asn	0.96	0.00	1.00	0.04	0.01	1.00	0.98
	Bot	1.00	0.00	1.00	0.00	0.00	1.00	1.00
	Pen	1.00	0.01	0.99	0.00	0.01	0.96	0.98
	Con	1.00	0.00	1.00	0.00	0.00	1.00	1.00
SIMCA	Asc	1.00	0.03	0.97	0.00	0.03	0.88	0.94
	Asn	1.00	0.29	0.71	0.00	0.23	0.47	0.64
	Bot	1.00	0.14	0.86	0.00	0.12	0.63	0.77
	Pen	1.00	0.16	0.84	0.00	0.12	0.62	0.77
	Con	1.00	0.26	0.74	0.00	0.20	0.50	0.67
KNN	Asc	0.91	0.02	0.98	0.09	0.04	0.91	0.91
	Asn	0.65	0.08	0.92	0.35	0.13	0.68	0.67
	Bot	0.64	0.18	0.82	0.36	0.21	0.47	0.54
	Pen	0.48	0.10	0.90	0.52	0.19	0.55	0.51
	Con	0.61	0.06	0.94	0.39	0.12	0.74	0.67
Random Forest	Asc	0.95	0.00	1.00	0.05	0.01	1.00	0.98
	Asn	0.91	0.02	0.98	0.09	0.04	0.91	0.91
	Bot	0.68	0.10	0.90	0.32	0.14	0.63	0.65
	Pen	0.74	0.10	0.90	0.26	0.13	0.65	0.69
	Con	0.83	0.00	1.00	0.17	0.04	1.00	0.90

Table S3: PLSDA Model characteristics of the GC/MS grape juice data obtained from the inoculated detached berries 2015.

PC	Eigenvalue	Variance X block	Cumulative X Variance	Variance Y Block	Cumulative Y Variance
1	26.4	41.6	41.6	23.6	23.6
2	12.3	19.4	61.1	23.8	47.4
3	5.1	8.0	69.0	23.5	70.9
4	3.4	5.3	74.4	21.1	92.1

Table S4: PLSDA Model characteristics of the GC/MS grape juice data obtained from the inoculated bunches 2016.

PC	Eigenvalue	Variance X block	Cumulative X Variance	Variance Y Block	Cumulative Y Variance
1	11.3	54.7	54.7	19.8	19.8
2	5.0	24.5	79.3	22.3	42.2
3	1.1	5.4	84.6	53.1	65.2
4	1.0	5.0	89.6	9.3	74.6

Table S5: PLSDA Model characteristics of the GC/MS grape juice data obtained from the inoculated bunches 2017.

PC	Eigenvalue	Variance X block	Cumulative X Variance	Variance Y Block	Cumulative Y Variance
1	9.0	42.7	42.7	43.3	24.3
2	4.8	23.0	65.8	23.6	47.9
3	2.2	10.2	76.0	19.6	67.5
4	1.6	7.6	83.6	18.2	85.7

Table S6: P-values from permutation testing for determining the appropriate number of orthogonal components for the 2016 inoculated bunches data set. Empirical P values determined from R^2Y values derived from 1000 permutations of data.

	Number of orthogonal components			
	0	1	2	3
Class 1 (A. carbonarius)	0.006	0.005	0.007	0.007
Class 2 (A. niger)	0.007	0.105	0.088	0.102
Class 3 (B. cinerea)	0.001	0.001	0.001	0.001
Class 4 (Control)	0.003	0.002	0.003	0.007
Class 5 (P. expansum)	0.002	0.004	0.002	0.003

Table S7: Mass ions (m/z) among 85th percentile of the selectivity ratios for a given class from PLS-DA of the GC/MS grape juice data obtained from the individual inoculated berries. M/z with VIP scores higher than 1 are indicated bold.

A. carbonarius	*A. niger*	*Control*	*P. expansum*	*B. cinerea*
54	60	51	**90**	**128**
56	78	52	**107**	**130**
57	85	**53**	**108**	**131**
61	99	55	119	**141**
67	**107**	**62**	134	**143**
72	125	63	139	**144**
82	**126**	65	153	**145**
88	129	**66**	161	**146**
89	**140**	**68**	167	**155**
92	151	**69**	**168**	**156**
102	154	70	**169**	**159**
104	166	79	176	**160**
114	167	**80**	183	**185**
122	**168**	81	192	186
135	**181**	**83**	198	**187**
136	186	84	**199**	**200**
137	**196**	**97**	**201**	**204**
163	217	**98**	**202**	**220**

Table S8: Mass ions (m/z) among 85th percentile of the selectivity ratios for a given class from PLS-DA of the GC/MS grape juice data obtained from the inoculated bunches 2016. M/z with VIP scores higher than 1 are indicated bold.

A. carbonarius	*A. niger*	*Control*	*P. expansum*	*B. cinerea*
92	56	77	**50**	57
94	**72**	78	**72**	66
101	94	105	79	67
113	121	117	81	72
123	124	**120**	**96**	80
124	**126**	**128**	**103**	82
126	**134**	**131**	104	**100**
127	137	132	**107**	**106**
136	**139**	**141**	**108**	**145**
137	**166**	**142**	114	**156**
139	**168**	154	**149**	**160**
140	**175**	**155**	**162**	**185**
144	**181**	**159**	**163**	**186**
168	**185**	**160**	**176**	**187**
169	190	**170**	190	**198**
174	**196**	174	**192**	**202**
196	**217**	**188**	243	**204**
256	**232**	**199**	244	**215**

Table S9: Mass ions (m/z) among 85th percentile of the selectivity ratios for a given class from PLS-DA of the GC/MS grape juice data obtained from the inoculated bunches 2017. M/z with VIP scores higher than 1 are indicated bold.

A. carbonarius	***A. niger***	***Control***	***P. expansum***	***B. cinerea***
65	55	77	**79**	**106**
66	60	78	82	116
91	68	**89**	88	**131**
92	69	**96**	89	**141**
94	70	103	**90**	**144**
100	71	118	93	**145**
104	83	**119**	101	**146**
112	84	125	**107**	**155**
122	85	**134**	**108**	**156**
125	93	**135**	**109**	**158**
126	**109**	161	**114**	**159**
127	111	162	**124**	**160**
139	**114**	**163**	**136**	**187**
140	**124**	**164**	137	**188**
150	137	166	**138**	**198**
153	**138**	181	168	**200**
168	152	**196**	199	**201**
169	173	203	**215**	**202**
196	174	**244**	**256**	**220**

Table S10: Compounds responsible for sample classification based on fungal pathogen for the grape juice samples obtained from inoculated Chardonnay bunches, vintage 2017.

Compound	Level of ID[1]	Accurate mass GC-Q-TOF	RIc[2]	RI lit[3]	Lit for RI Lit[4]	Main m/z	Standardised peak areas[5]					Effect size (partial eta squared)
							Control	*B. cinerea*	*A. carbonarius*	*A. niger*	*P. expansum*	
2-Pentyl furan	a	81.0339	1245	1258	15	81	42^{ab}	65^{bc}	43^{ab}	17^{a}	100^{c}	0.95
(*E*)-2-Hexenal	a	55.0542	1250	1248	4	55	33^{a}	100^{b}	26^{a}	17^{a}	19^{a}	0.99
Styrene	a	104.0539	1292	1264	3	104	9^{a}	8^{a}	100^{b}	8^{a}	11^{a}	0.98
1-Octen-3-ol	a	57.0338	1452	1466	6	57	6^{a}	16^{a}	56^{b}	100^{c}	13^{a}	0.99
***trans*-Linalool oxide**	a	59.0444	1463	1463	5	59	60^{a}	58^{a}	100^{c}	95^{bc}	72^{ab}	0.99
Unknown	b	192.1516	1545	-	-	192	53^{a}	68^{a}	100^{b}	87^{b}	61^{a}	1.00
Benzaldehyde	a	106.0410	1549	1538	12	106	20^{a}	100^{c}	22^{a}	17^{a}	35^{b}	1.00
Unknown sesquiterpene	b	145.1017	1568	1455	7	145	2^{a}	100^{b}	3^{a}	3^{a}	4^{a}	1.00
***trans*-2-Nonen-1-ol**	a	57.0292	1717	1713	8	57	87^{b}	42^{a}	42^{a}	100^{b}	39^{a}	0.99
Unknown sesquiterpene	b	185.1331	1733	-	-	185	58^{b}	100^{c}	0^{a}	6^{a}	0^{a}	0.97
1,5-Dimethyl tetralin	a	145.0903	1751	-	-	145	0^{a}	100^{b}	0^{a}	0^{a}	1^{a}	0.99
Unknown sesquiterpene	b	119.0850	1763	-	-	119	0^{a}	100^{b}	0^{a}	0^{a}	0^{a}	0.96
Phenylethyl acetate	a	104.0540	1829	1825	9	104	0^{a}	0^{a}	100^{b}	0^{a}	0^{a}	0.95
Pentanoic acid, 2,2,4-trimethyl-3-carboxyisopropyl, isobutyl ester	b	71.0438	1884	1866	2	71	100^{b}	65^{a}	69^{ab}	53^{a}	62^{a}	0.99
Benzylalcohol	a	108.0478	1889	1886	9	108	91^{b}	49^{a}	100^{b}	97^{b}	87^{b}	0.99
Phenylethyl alcohol	a	91.0470	1926	1922	9	91	8^{a}	100^{b}	7^{a}	7^{a}	22^{a}	0.99
Unknown sesquiterpene	b	143.0855	1928	-	-	143	0^{a}	100^{b}	0^{a}	0^{a}	0^{a}	1.00

Unknown sesquiterpene	b	202.1715	1933	-	-	202	0[a]	100[b]	0[a]	0[a]	0[a]	1.00
Unknown sesquiterpene	b	200.1557	1970	-	-	200	0[a]	100[b]	0[a]	0[a]	0[a]	0.99
1-Dodecanol	a	55.0503	1975	1981	1	55	100[b]	66[a]	77[a]	66[a]	75[a]	1.00
γ-Nonalactone	a	85.0286	2046	2042	16	85	29[a]	35[a]	50[a]	39[a]	100[b]	0.95
1,5-Dimethyl naphthalene	a	156.0941	2060	2048	10	156	1[a]	100[b]	2[a]	2[a]	2[a]	1.00
***m*-Cresol**	a	108.0568	2087	2088	14	108	0[a]	0[a]	0[a]	0[a]	100[b]	0.92
2-(4-hexyl-2,5-dioxo-2,5-dihydrofuran-3-yl)acetic acid	b	126.0309	2119	-	-	126	0[a]	1[ab]	100[c]	24[b]	0[a]	0.98
γ-Eudesmol	b	161.1200	2185	2195	11	161	65[a]	100[b]	63[a]	51[a]	46[a]	0.99
Unknown sesquiterpene	b	105.0697	2221	-	-	105	0[a]	100[b]	0[a]	0[a]	0[a]	0.95
Ethyl hexadecanoate	a	88.0514	2254	2259	13	88	21[a]	100[b]	28[ab]	47[ab]	76[ab]	0.87
Unknown sesquiterpene	b	159.1177	2279	-	-	159	1[a]	100[b]	1[a]	1[a]	2[a]	1.00
Unknown sesquiterpene	b	59.0485	2326	-	-	59	0[a]	100[b]	0[a]	0[a]	0[a]	0.98
Unknown sesquiterpene	b	215.0885	>2500	-	-	215	0[a]	100[b]	0[a]	0[a]	0[a]	0.97
Ethyl linoleate	a	67.0530	>2500	2510	5	67	10[a]	97[b]	37[ab]	47[ab]	100[b]	0.89

[1] Level of identification: a) Metabolites were identified at level 1, by comparing their RI and EI-MS against authentic standards and the NIST2011 metabolite and Massfinder4 terpenoid database, b) Metabolites were identified at level 2, by comparing their RI and EI-MS against the above databases and peer-reviewed scientific literature.

[2] RI calculated based on alkane series (C8-C40), according to the equation of van den Dool and Kratz (section 2.3.1 in main manuscript).

[3] RI reported in peer-reviewed scientific literature.

[4] Literature for RI: 1 (Gürbüz, et al. 2006), 2 (Wu, et al. 2005), 3 (Bianchi, et al. 2007), 4 (Wang, et al. 2005), 5 (Cantergiani, et al. 2001), 6 (Escudero, et al. 2000), 7 (Tabanca, et al. 2006), 8 (Kim, et al. 2001), 9 (Tatsuka, et al. 1990), 10 (Chung 1999), 11 (Frizzo, et al. 2001), 12 (Selli, et al. 2004), 13 (Selli, et al. 2006), 14 (López, et al. 1999) , 15 (Welke, et al. 2012), 16 (Miranda-Lopez, et al. 1992).

[5] MANOVA, Tukey HSD, and effect sizes were calculated based on the peak areas that were normalised to the internal standard peak areas. For visual ease in this table, these normalised peak areas have been further standardised to the maximum peak. The standardised areas of the compounds with the same superscript are not significantly different between samples, based on Tukey HSD.

Appendix 5.2 - Supplementary Figures

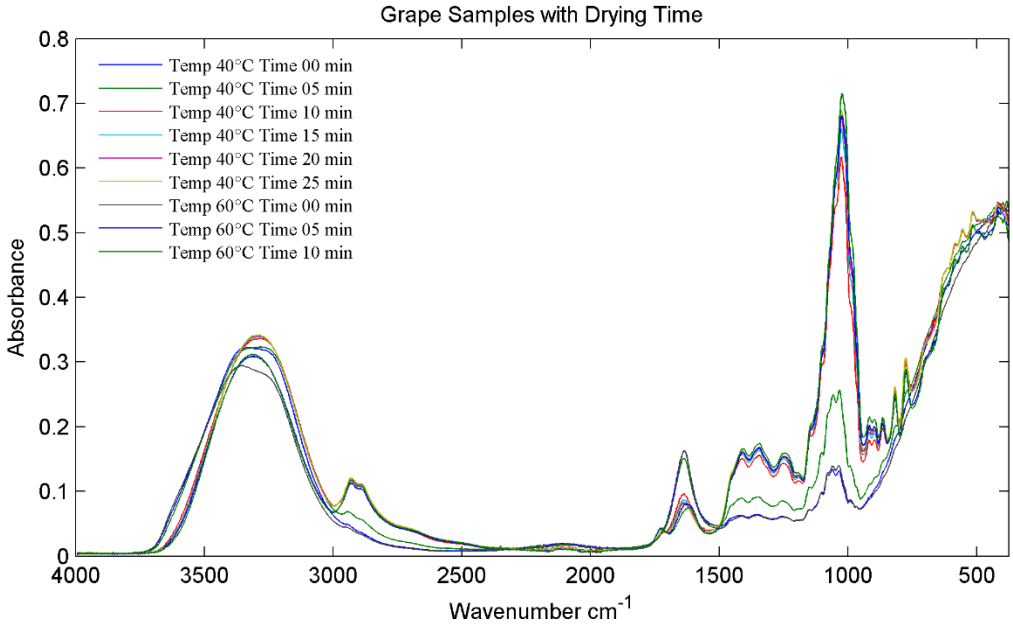


Figure S1: ATR-FTIR scans of berry extract samples at varying time and temperature combinations.

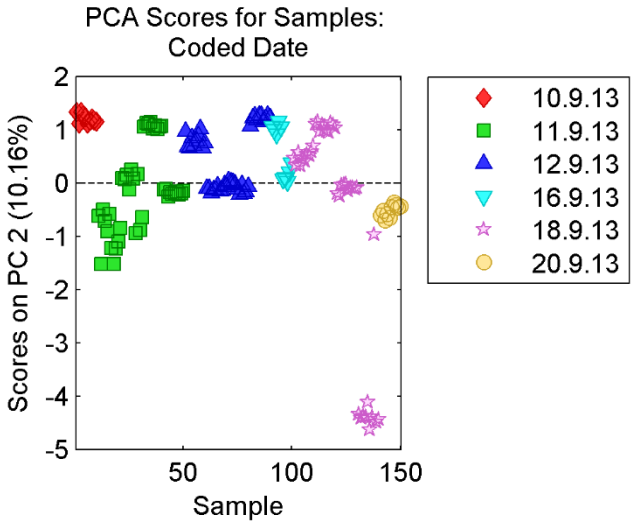


Figure S2: Principal component analysis of berry homogenate samples with coding for date of analysis illustrating separation of a subset of samples due to poor baseline correction.

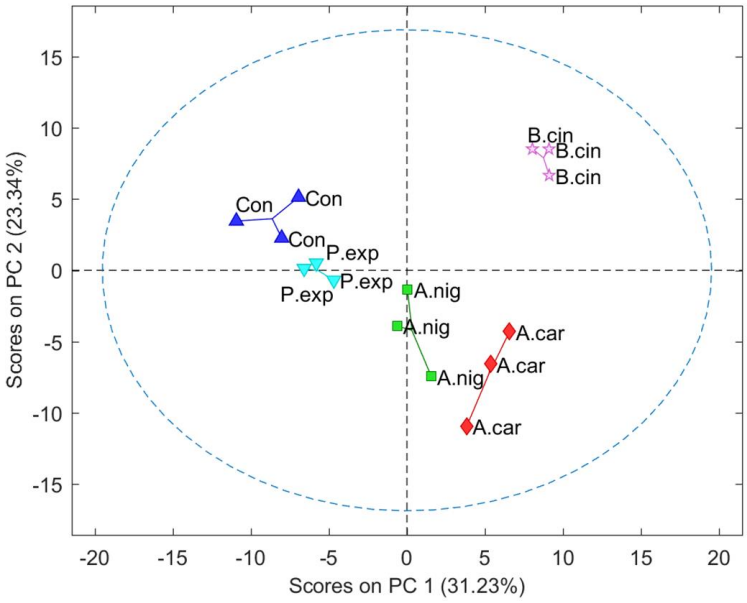


Figure S3: Scores plots of GC/MS grape juice data obtained from individual inoculated Chardonnay berries, showing PC1 versus PC2. Control, triangles: infected with *P. expansum*, upside down triangles; *A. niger*, squares; *A. carbonarius*, diamonds; *B. cinerea*, stars.

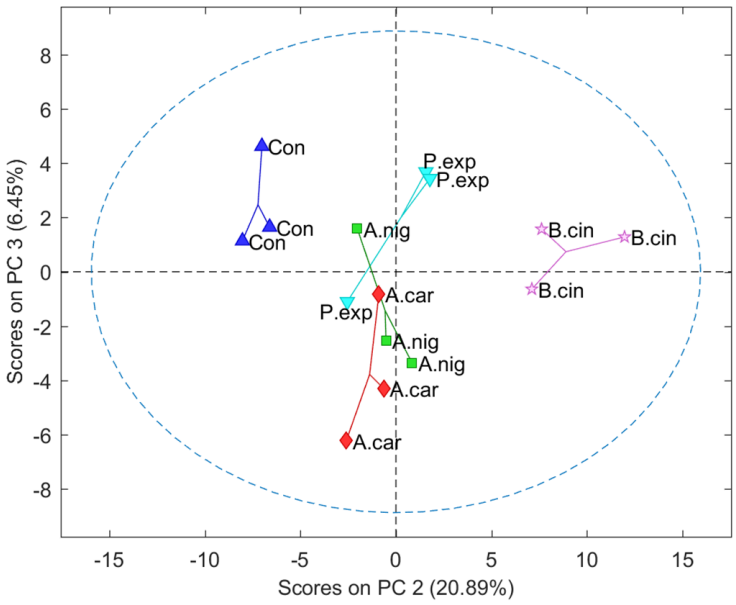


Figure S4: PCA scores plots of GC/MS grape juice data obtained from inoculated Chardonnay bunches, vintage 2016, showing PC2 versus PC3. Control, triangles: infected with *P. expansum*, upside down triangles; *A. niger*, squares; *A. carbonarius*, diamonds; *B. cinerea*, stars.

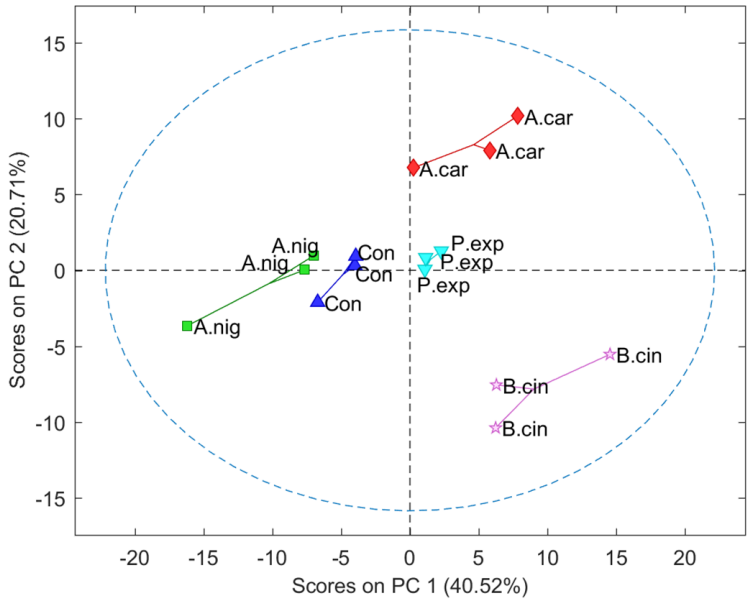


Figure S5: PCA scores plots of GC/MS grape juice data obtained from inoculated Chardonnay bunches, vintage 2017, showing PC1 versus PC2. Control, triangles: infected with *P. expansum*, upside down triangles; *A. niger*, squares*; A. carbonarius*, diamonds; *B. cinerea*, stars.

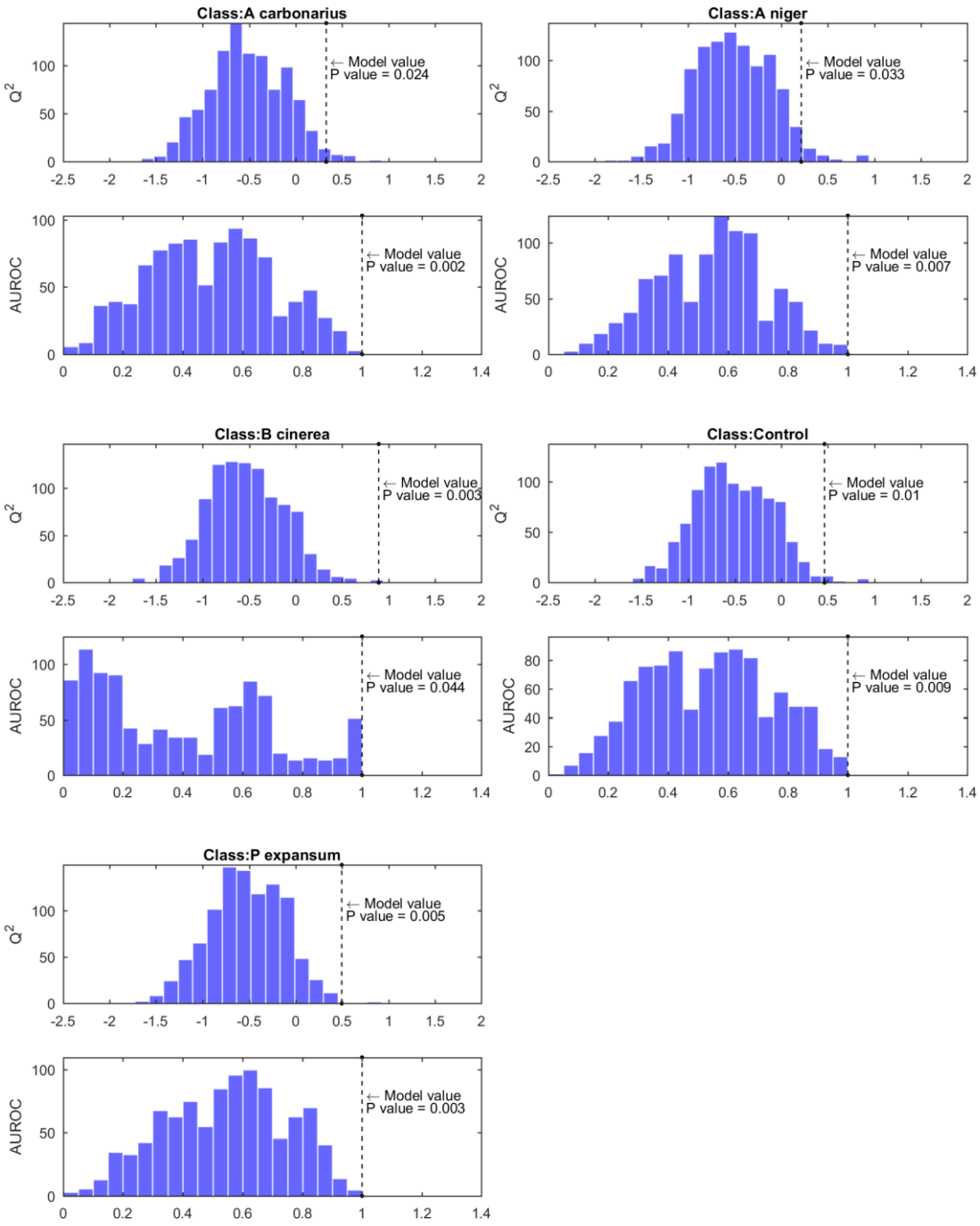


Figure S6: Validation of PLSDA models for class assignment of the GC/MS data obtained from inoculated detached berries 2015. Results based on cross model validation predictions (vertical dashed line) compared to permuted data using Q^2 and area under the ROC (AUROC) curve. Empirical P values determined from 1000 permutations of data.

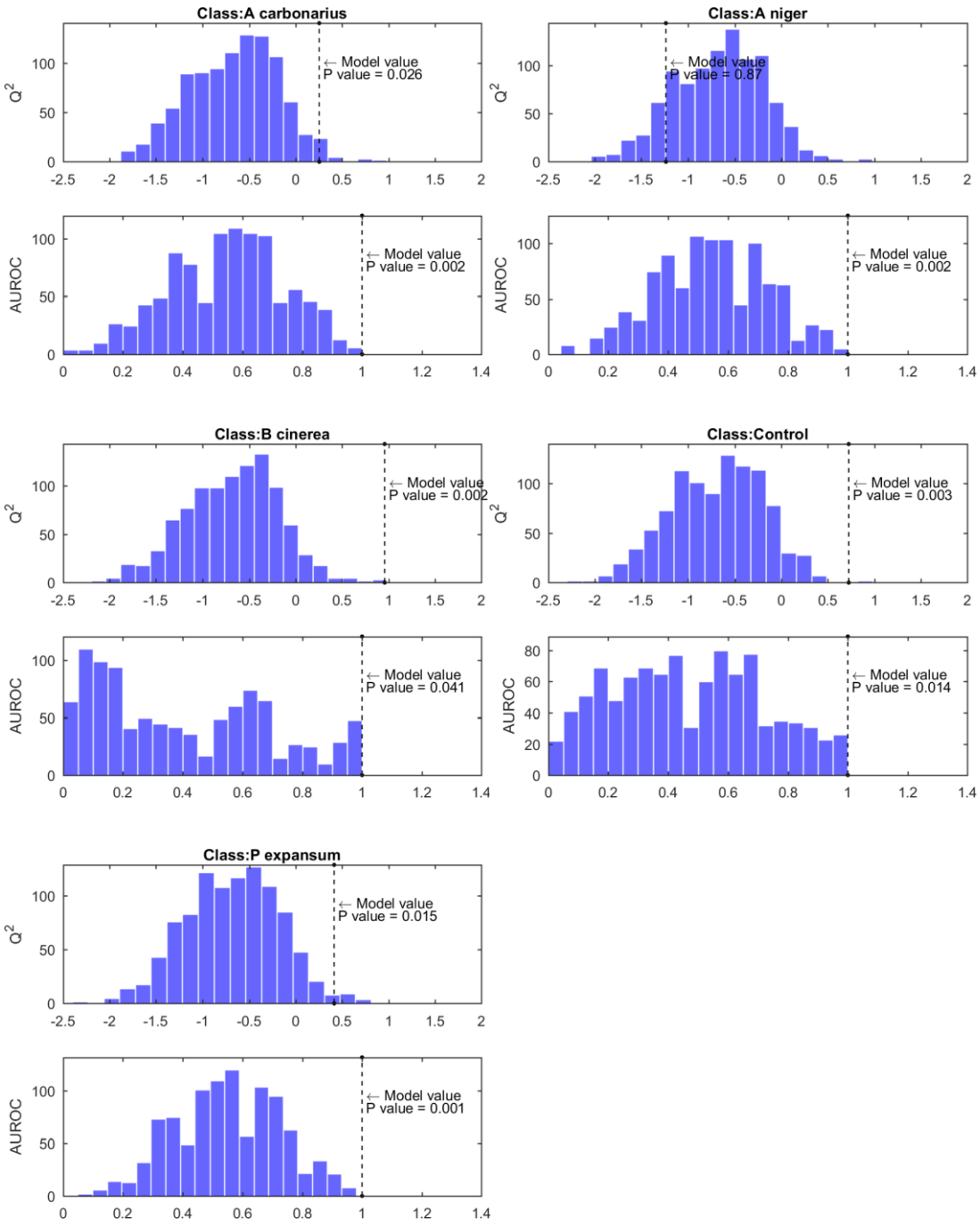


Figure S7: Validation of PLSDA models for class assignment of the GC/MS data obtained from inoculated bunches 2016. Results based on cross model validation predictions (vertical dashed line) compared to permuted data using Q^2 and area under the ROC (AUROC) curve. Empirical P values determined from 1000 permutations of data.

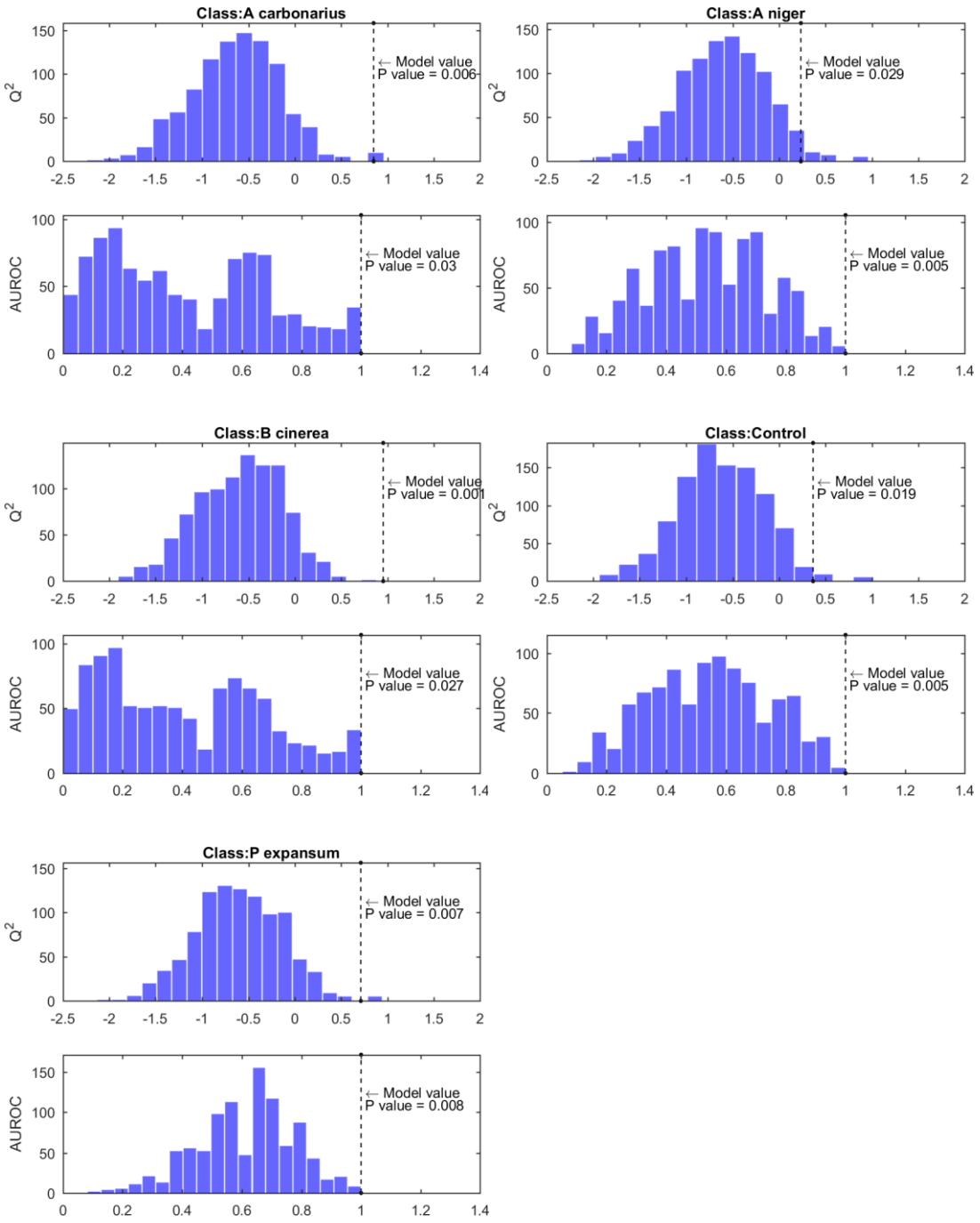


Figure S8: Validation of PLSDA models for class assignment of the GC/MS data obtained from inoculated bunches 2017. Results based on cross model validation predictions (vertical dashed line) compared to permuted data using Q^2 and area under the ROC (AUROC) curve. Empirical P values determined from 1000 permutations of data.

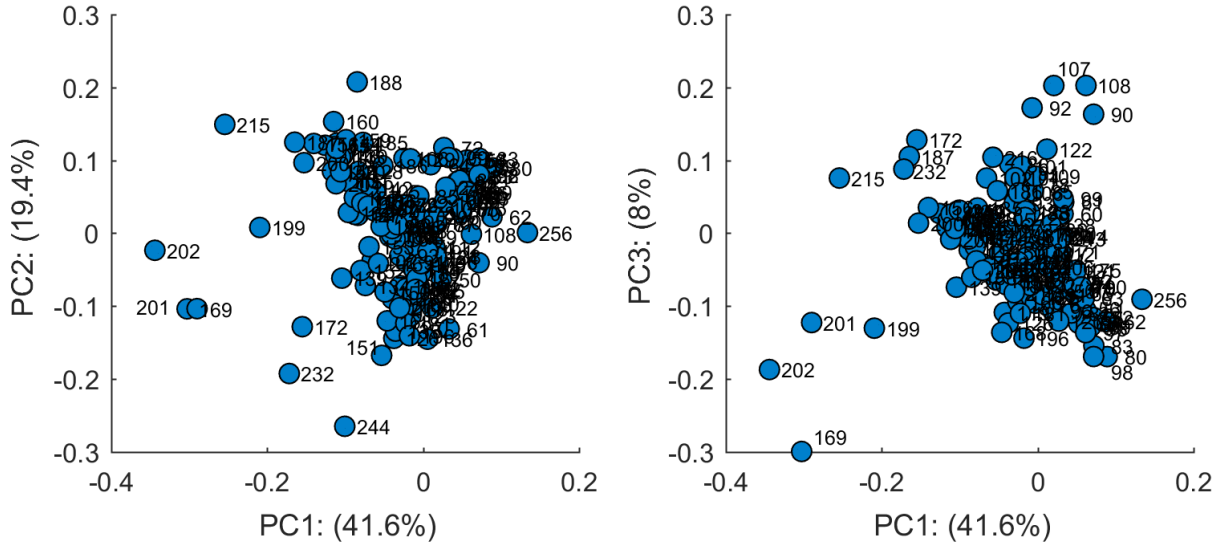


Figure S9: PLS-DA loadings plots (PC1-3) of GC/MS grape juice data obtained from individual inoculated Chardonnay berries 2015.

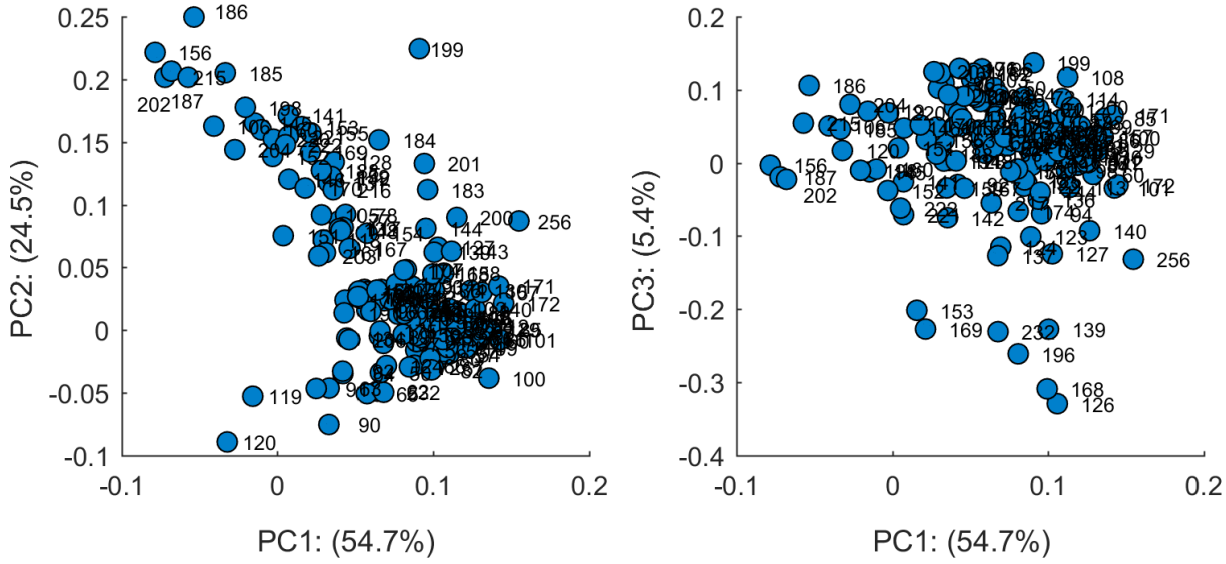


Figure S10: PLS-DA loadings plots (PC1-3) of GC/MS grape juice data obtained from 10 % infected Chardonnay bunches, vintage 2016.

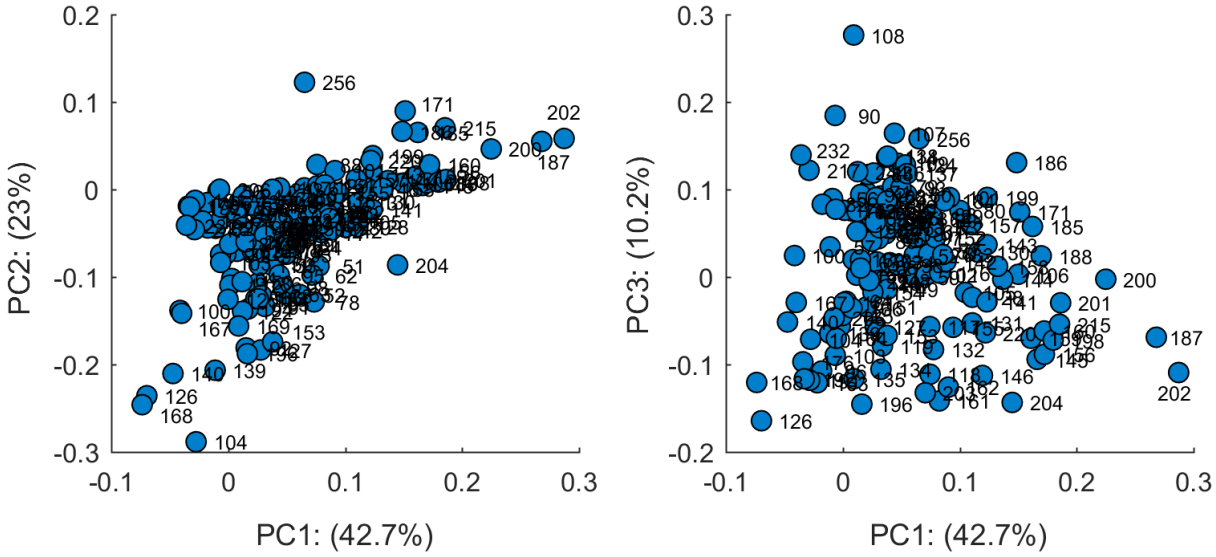


Figure S11: PLS-DA loadings plots (PC1-3) of GC/MS grape juice data obtained from 10 % infected Chardonnay bunches, vintage 2017.